Napolitano and Gardner
EURASIP Journal on Advances in Signal Processing (2025) 2025:13
https://doi.org/10.1186/s13634-025-01207-w

EURASIP Journal on Advances in Signal Processing

SURVEY Open Access

Discovering and modeling hidden periodicities in science data

Antonio Napolitano[1*] and William A. Gardner[2]

*Correspondence:
antonio.napolitano@uniparthenope.it

[1] Department of Engineering, University of Napoli "Parthenope", Centro Direzionale, Isola C4, 80143 Napoli, Italy
[2] Department of Electrical and Computer Engineering, University of California at Davis, 1 Shields Ave, Davis, CA 95616, USA

Abstract

Hidden periodicities in science data have long been a popular topic of investigation. The popularity stems from the fact that detecting and characterizing periodicities can provide a means for extracting information from science data—information that might not otherwise be accessible. In other words, periodicities in data can be exploited for the purposes of statistical inference and decision making. The long history of this topic is briefly reviewed with heavy reference to a historical essay on the topic by H.O.A. Wold, written more than half a century ago, following which the treatise focuses on a paradigm shifting advance in theory and methodology for characterizing hidden periodicities that was initiated by the second author in the mid-1980s and further advanced by both authors since then, including a plethora of algorithms for performing the needed computations in applications. The data models this theory is based on are generally called cyclostationary but include variations that are labeled with modifiers like *wide-sense, strict sense, n-th order for n = 1, 2, 3,..., almost, poly, and irregular*. The theory is probabilistic, but is intentionally not based on stochastic processes which, it is argued, are inappropriate for many, if not most, applications. The basis used is *Fraction-of-Time (FOT) Probability*. The concept, theory, and methodology of FOT Probability is itself a major paradigm shift, also initiated by the second Author more than half a century ago, and it is an integral part of the (preferred) non-stochastic theory of cyclostationarity. Since the birth of this topic, both authors have continued to advance these paradigm shifts, including further development of theory, associated methodology, and computational algorithms. The most advanced of the concepts described (viz., irregular poly-cyclostationarity) is illustrated with an application of the associated algorithms to science data consisting of time series of Sunspot numbers containing approximately 75,000 daily measurements representing a period of about 200 years. The results include the first methodical characterization of the irregularity of the poly-periodicity hidden in the data.

Keywords: Cyclostationarity, Hidden periodicities, Fraction-of-time probability, Irregular periodicity, Sunspot number

1 Introduction and historical perspective

The following introduction to the topic of this essay was written by Herman O. A. Wold more than half a century ago, as the opening paragraph in his survey contribution to the topic "Cycles" in the *International Encyclopedia of the Social Sciences* (1968) [122].

"Cycles, waves, pulsations, rhythmic phenomena, regularity in (investment) return, periodicity—these notions reflect a broad category of natural, human, and social phenomena where cycles are the dominating feature. The daily and yearly cycles in sunlight, temperature, and other geophysical phenomena are among the simplest and most obvious instances. Regular periodicity provides a basis for prediction and for extracting other useful information about the observed phenomena. Nautical almanacs with their tidal forecasts are a typical example. Medical examples are pulse rate as an indicator of cardiovascular status and the electrocardiograph as a basis for analysis of the condition of the heart. The study of cyclic phenomena dates from prehistoric times, and so does the experience that the area has dangerous pitfalls. From the dawn of Chinese history comes the story that the astronomers Hi and Ho lost their heads because they failed to forecast a solar eclipse (perhaps 2137 B.C.). In 1929, after some twelve years of promising existence, the Harvard Business Barometer (or Business Index) disappeared because it failed to predict the precipitous drop in the New York stock market."

The historical essay presented at the University of California, Davis, educational website [42, page 4.1] puts into perspective the breakthrough made in the mid-1980 s in modeling and statistical inference for time-series data exhibiting cyclic behavior, often referred to as *hidden periodicities*. Up until this breakthrough, statistical models for cycles—as a complement to nonstatistical cycles modeled, for example, by differential equations—had been studied analytically using crude mathematical models for more than a century but had not moved beyond the following two models: 1) the sum of one or more periodic time series and a featureless (randomly fluctuating, erratic, unpredictable, stationary) times series, often referred to as noise, which sum is amenable to more than just temporally local prediction, and 2) the response of a linear time-invariant resonant dynamical system, mathematically modeled as a convolution or a corresponding differential equation, driven by a featureless time series, which response is amenable to only local prediction, because the apparent cycles are not true cycles. In a hypothesis testing setting, the null hypothesis (the alternative to models 1) or 2)) is an unpredictable nonstationary time series that may appear from time to time to exhibit cyclicity but that, upon closer inspection, is found to exhibit no true cycles and no substantive predictability. However, model 2) can be considered to be included in the null hypothesis since the disturbed harmonics produced by this model do not represent true cycles, and predictability is relatively limited. For an illustrative discussion of the general problem of cycles from a historical perspective, the reader is referred to Appendices 1-3 in the above-cited historical essay, which consist of excerpts from Wold's article, "Cycles" [122].

The first method that emerged for analysis of data according to model 1), at the turn of the nineteenth century, is the periodogram (the squared magnitude of the Fourier transform of a finite-length times series of data, normalized by the length of the data segment) [33, 35, 105], and this method was followed by a variety of what were termed high-resolution and super-resolution model fitting methods beginning around mid-20th Century [17–19, 62, 63, 100, 116]. The periodogram was proven to be the set of sufficient

statistics for maximum likelihood (ML) estimation of the period of a cycle due to a single sinewave in additive white Gaussian noise (AWGN), and the amplitude and phase of the Fourier component at the detected period produce ML estimates of a sinusoid with that period. The complexity of the generalization to ML estimation for multiple sinusoids in AWGN, especially those with cycle periods that are not substantially different from each other, led to a wide variety of alternative model fitting method, which are surveyed in [39, Chap. 9], where Gardner introduces the use of the fraction-of-time (FOT) probability model to circumvent the unnecessary abstraction of the stochastic process model (cf. [44]) which dominated the literature on this topic essentially to the extent of complete exclusion of the FOT probability model (the focus in this paper) once the stochastic process had been introduced. Data following model 2) were referred to as disturbed harmonics [124] and were analyzed primarily by methods developed specifically for autoregressive (AR) models and AR-moving average (ARMA) models [12, 32, 53, 73, 117, 118]. See [2] for a comparison of these methods. These models were initially implicitly based on the FOT model (i.e., on time averages of lag products, not probabilistic expected values) but soon transitioned to the stochastic process model.

Coarse chronological outline of the development of key concepts in the study of cycles:

- *2000 BC* Interest in the General Notion of Cycles (see excerpt from Wold [122] in the second paragraph of the present essay)
- *1700 s AD* Hidden Periodicities (Euler, Lagrange [68, 69]; see [39, p. 13])
- *1898* Periodogram (Schuster [105])
- *1914* Irregular Fluctuations (Einstein [33])
- *1927* Disturbed Harmonics (Yule [124]; see [39, p. 13])
- *1930* Generalized Harmonic Analysis (Wiener [120])
- *1958* Power spectra measurement (Blackman and Tukey [13])
- *1975–1978* Precursor to Regular (Almost) Cyclostationarity (Gardner; see [36, 46])
- *1985–1987* Regular (Almost) Cyclostationarity (first in-depth treatises: Gardner; [37, Chap. 12], [39, Part II])
- *1998–2012* Generalization of Cyclostationarity (Napolitano [81])
- *2015–2019* Irregular Cyclostationarity (see Gardner and Napolitano [43, 83, 87, 84, Chap. 14])

In 1985 and 1987, two analytical books by Gardner [37, 39] appeared and introduced the first comprehensive theoretical investigations of two new classes of models which he termed 3) cyclostationary time series exhibiting a single periodicity and its generalization to 4) almost cyclostationary time series exhibiting multiple incommensurate periodicities, that is, multiple incommensurate periods of statistical cyclicity. Book [37] introduced these models in terms of stochastic processes and briefly explained their duals defined in terms of time averages instead of expected values and the book [39] maintained close ties to empirical data by developing for the first time a comprehensive theory based on times averages alone or, equivalently, Fraction-of-Time (FOT) probabilities. The term *statistical cyclicity* means that precise cycles appear only in carefully prescribed time averages performed on nonlinear transformations of the data, generally not in the raw data itself, which may or may not exhibit imprecise cycles. For the stochastic

process model, these averages are expected values of functions of the data, which can be approximated with averages over statistical samples from a population of data sets. For the alternative non-stochastic model, these averages are ideally infinitely-long time averages of functions of the data, which can be approximated by finite-time averages. The two models are mathematical duals, and, in addition, they are essentially equivalent for a very special subclass of stochastic processes that satisfy the ergodic hypothesis [39, Chap. 8].

The original models 1) and 2) were first described prior to the advent of the concept of a stochastic process and later were replaced with stochastic-process alternatives. The two new models 3) and 4), which generalize models 1) and 2), were first treated comprehensively almost simultaneously in both forms, stochastic and non-stochastic, in [37], and the non-stochastic alternative was greatly expanded on in [39], because of its parsimony and more direct relevance to most applications—those for which only a single time series of measurements is available instead of a set of multiple statistical samples of time series from a population which is the situation originally motivating the stochastic process model. There were a few isolated journal papers prior to (and cited in) [37, 39, 47] which briefly treated the stochastic process model, but there had been no attempt to develop a comprehensive theory of these stochastic processes, and not even a mention of the alternative theory of non-stochastic models for non-population time series first proposed in [37, 39] (cf. [44, 60, 61, 72, 88]) let alone non-stochastic models for periodically and almost periodically time varying higher-than second-order moments, cumulants, and probability density functions. A few papers and books [7, 8, 55, 70, 99] follow up the non-stochastic approach for generalized harmonic analysis originally adopted by Wiener [76, 120] with reference to a stationary (i.e., not periodically or almost-periodically time variant) statistical model for signals. The almost-periodically time-variant model is considered for mechanical applications in [1]. Cyclostationary and almost-cyclostationary processes have also been referred to as periodically and almost periodically correlated processes, respectively [50, 51, 56].

The fundamental concept underlying (almost) cyclostationarity does not require the concept or mathematical model of a population of time series and a corresponding stochastic process. Rather (almost) cyclostationarity can be defined directly in terms a single instance of a time series by introducing time-series models consisting of (almost) periodically time-varying FOT probability density functions defined independently of the probability space notion upon which the stochastic process is defined. The earliest work on the underlying measure theory foundation for FOT probability is presented in [72], and further discussion is presented in [29, 30, 44, 88] on the key mathematical differences between FOT probability, which is constructed from a single time series, and Kolmogorov's abstract axiomatically defined probability theory [65], which is defined in terms of what is called a probability space. Periodically (and almost periodically) time-varying moments and cumulants can be characterized in terms of FOT probability. The breadth of this class of models and the phenomena to which they apply dwarfs the earlier models of cycles of type 1) referred to above. In fact, the model 1) is the most elementary example of a cyclostationary time series—so elementary that it does not need the mathematical machinery of FOT probability to analyze. More specifically, in the model of type 1) a true cycle corresponds to a periodic mean and a residual (the centered time

series) that is *purely stationary* (defined in this paper) and, in the model of type 2), an apparent but not true cycle corresponds to damped oscillation in the lag parameter of the autocorrelation function of the process. In cyclostationary (or almost-cyclostationary) processes, any order moment or cumulant can be periodic (or almost periodic with multiple incommensurate periods). For example, a cyclostationary process or time series can have a constant (time-invariant) mean and constant variance, but a periodic covariance producing cycles in coherence time; or it can have first- and second-order moments all of which are constant, but higher-order moments or cumulants that are periodic. In general, (almost) cyclostationary processes have (almost) periodic joint probability density functions. Gardner's more general FOT probability model of cycles does not rely on a hypothetical deterministic model (a periodic function or a convolution) mixed with or driven by a featureless noise. Rather, it constructs the model from time averages of functions of the time series. This model can consist of FOT probability density functions, joint moments of multiple time samples with any time separations, corresponding joint cumulants, etc. Nevertheless, the FOT probability model can be derived from a mathematical model of deterministic dynamics driven by featureless noise, in terms of the FOT model of such noise, which is typically chosen to be a series of statistically independent identically distributed (in the FOT probability sense) variables. In this case, the statistical cyclicity arises from periodic or almost-periodic time variation of the dynamical system being driven by stationary noise.

It is worthwhile to underline that the advantage of the FOT probability framework is mainly conceptual and/or methodological, when a population of signals does not exist. In some cases, calculations and proofs are similar to their counterparts in the stochastic process approach. However, examples of dichotomies between properties of a stochastic process and those of its sample paths are illustrated in [88], were properties that are valid for stochastic processes are shown to be not valid for their sample paths. Several technicalities and calculations/proofs in the FOT probability framework can be found in [39, 45, 72, Part II], [81, Sec. 6.5], [29, 30, 84, Secs. 2.6, 4.11], [88, Appendix].

Implementation of the time-series analysis methods referred to in this paper is today invariably based on digital signal processing technology, which is derived from the discrete-time probability theory of cyclostationarity. Both authors have carried out their development work for both discrete- and continuous-time theory. But this treatise presents the continuous-time theory because of its closer ties with the physics underlying the science giving rise to the data subjected to the signal processing methods for studying hidden periodicities. The discrete theory is highly analogous and is not treated herein for the sake of brevity and avoidance of redundancy.

Before proceeding to the body of the summary of the theory of cyclostationarity, the method of classification of cyclostationary time series is explained. This exposes the immense degree of generality of this theory of cyclicity in time-series data.

The time-series model 1) can be partitioned into subclasses, which reflect distinct mathematical properties and issues that arise in performing analysis. Using the Fourier-series representation for a sum of periodic signals, these subclasses can be categorized in terms of their spectral content *(spectrum)*, which is characterized in terms of the ordered countable sequence of Fourier frequencies, well known in the theory of Fourier analysis [14, 21, 125]: Class 1a) is a single nonzero frequency, Class 1b) is a finite number of

commensurate (harmonically related) frequencies, and Class 1c) is a countably infinite number of commensurate frequencies. These are all periodic functions. By adding periodic functions with incommensurate periods, we obtain *almost-periodic functions* that are not periodic [11, 23]. The spectrum becomes the ordered union of the sets of Fourier frequencies for the individual periodic functions. By considering numbers of incommensurate periods that are, say, two, or greater than two but finite, or countably infinite, we obtain a hierarchy of quite a large number of almost-periodic functions. For those subclasses that contain between 2 and at most some finite number greater than 2 incommensurate periods, the functions are *poly-periodic*.

By applying this basis for classification to statistical functions derived from a time series according to the methods discussed in the following sections of this paper, when such functions are comprised of sums of periodic FOT moments, or cumulants, or probability distributions, we obtain a hierarchy of models for cyclostationary and almost cyclostationary times series, as discussed below.

It should be clarified that because of the additive noise in Model 1), none of the time series from this model are periodic or poly-periodic, or almost periodic. But they are said to *exhibit periodicity*, and this exhibited periodicity can be measured in terms of the periodic, poly-periodic, or almost-periodic mean function calculated from the time series.

More generally, when the more general statistical functions, such as FOT moments, cumulants, and probability distributions are periodic, or poly-periodic, or almost periodic, we say the time series are *cyclostationary*, or *poly-cyclostationary*, or *almost cyclostationary*. The frequencies in the Fourier spectrum of the time-varying statistical functions are called the *cycle frequencies*. In addition, when any formal subset of the spectrum of cycle frequencies is chosen for a model, and the resultant statistical functions are not all identically zero for nonzero cycle frequencies, the time series is said to *exhibit* cyclostationarity or poly-cyclostationarity or almost cyclostationarity. Therefore, a time series can, for example, exhibit cyclostationarity without being cyclostationary. A cyclostationary statistical function for such a model is only one additive periodic component of the almost cyclostationary statistical function. More discussion of the hierarchy of cyclostationarity is provided in [41].

Most of the existing literature on cyclostationarity, poly-cyclostationarity, and almost cyclostationarity focuses on periodicity, poly-periodicity, and almost periodicity of second- and higher-order moments and cumulants of time series. This paper reviews these results, but emphasis is given to the periodic, poly-periodic, and almost-periodic cumulative distribution function (CDF) and probability density function (PDF) of time series [39, Chap. 15], [84, Chap. 2] that only recently have been applied for signal detection [31].

The paper is organized as follows: First-order hidden periodicities are characterized in Sect. 2. Second-order cyclostationarity is treated in Sect. 3, and extension to higher-order cyclostationarity is treated in Sect. 4. Models and methods for dealing with irregular cyclicities are treated in Sect. 5. As an example of application, hidden periodicities present in the well-known Sunspot number time series are analyzed in Sect. 6. Conclusions are drawn in Sect. 7.

2 First-order hidden periodicity

2.1 Decomposition into almost-periodic component and residual term

Every signal $z(t)$ such that the sinusoidally weighted infinite time average

$$\left\langle z(t)\, e^{-j2\pi\eta t}\right\rangle_t \triangleq \lim_{T\to\infty} \frac{1}{T}\int_{t_0-T/2}^{t_0+T/2} z(t)\, e^{-j2\pi\eta t}\, \mathrm{d}t \tag{2.1}$$

exists for every $\eta \in \mathbb{R}$ (independent of t_0) can be expressed as the sum of a (possibly zero) almost-periodic (AP) component $z_{\mathrm{ap}}(t)$ and a residual term $z_{\mathrm{r}}(t)$ not containing any finite-strength sine wave component. That is,

$$z(t) = z_{\mathrm{ap}}(t) + z_{\mathrm{r}}(t) \tag{2.2}$$

where

$$\left\langle z_{\mathrm{r}}(t)\, e^{-j2\pi\eta t}\right\rangle_t = 0 \qquad \forall \eta \in \mathbb{R}\,. \tag{2.3}$$

The almost-periodic term is given by the superposition of complex sine waves

$$z_{\mathrm{ap}}(t) = \sum_{\eta\in\mathcal{E}^{(1)}} z_\eta\, e^{j2\pi\eta t} \tag{2.4}$$

where $\mathcal{E}^{(1)}$ is a countable set of possibly incommensurate frequencies and the Fourier coefficients z_η are given by

$$z_\eta \triangleq \left\langle z_{\mathrm{ap}}(t)\, e^{-j2\pi\eta t}\right\rangle_t = \left\langle z(t)\, e^{-j2\pi\eta t}\right\rangle_t. \tag{2.5}$$

In particular, if $\mathcal{E}^{(1)}$ contains frequencies that are all integer multiples of a fundamental one, say $\eta_0 = 1/T_0$, then $z_{\mathrm{ap}}(t)$ is a periodic function with period T_0. If $z_{\mathrm{ap}}(t)$ is the superposition of a finite number of periodic functions with incommensurate periods, then it is dubbed *poly-periodic*. Under the condition

$$\sum_{\eta\in\mathcal{E}^{(1)}} |z_\eta| < \infty \tag{2.6}$$

the convergence in (2.4) is uniform and the function $z_{\mathrm{ap}}(t)$ is referred to as uniformly almost periodic [11]. Generalized forms of almost periodicity can be defined considering weaker forms of convergence for the Fourier series (2.4) [11, Chap. 2], [23, 81, Secs. 1.2.2−1.2.5], [84, Sec. B.4].

Let $\mathrm{E}^{\{\alpha\}}\{\cdot\}$ denote the almost-periodic component extraction operator. That is, the operator that extracts all the additive finite-strength sine-wave components of its argument [45]. It results

$$\mathrm{E}^{\{\alpha\}}\{z(t)\} = z_{\mathrm{ap}}(t)\,. \tag{2.7}$$

The power spectral density (PSD) of the signal $z(t)$, defined in a generalized sense, contains spectral lines (Dirac deltas) at frequencies $\eta \in \mathcal{E}^{(1)}$ and $z(t)$ is said to exhibit first-order periodicities. If the almost-periodic component is weak relative to the residual

term, then the first-order periodicities might not be evident and the signal is said to contain hidden periodicities. However, because of the associated spectral lines at frequencies $\eta \in \mathcal{E}^{(1)}$, the hidden periodicities can be detected through techniques of spectral analysis.

In general, signals may contain more subtle kinds of hidden periodicities. Spectral lines might not be present in the PSD but could be generated, that is, converted from higher-order periodicities into first-order periodicities, by transforming the signal with a bounded-input bounded-output (BIBO) stable time-invariant nonlinear transformation. That is, the signal $z(t)$ in (2.2) can be such a kind of transformation of a finite average-power original signal $x(t)$

$$\left\langle |x(t)|^2 \right\rangle_t < \infty \,. \tag{2.8}$$

When a transformation that generates a sinewave is homogeneous quadratic, the signals are said to exhibit *second-order cyclostationarity* [38, 39, Part II], (Sec. 3). When a higher-than-second-order homogeneous transformation generates spectral lines, then the signal is said to exhibit *higher-order cyclostationarity* [49, 112], (Sec. 4).

Let us assume that the time series $z(t)$ contains an additive periodic component with period T_0. Such a component can be extracted by *synchronized averaging* [37, Chap. 12], [39, Sec. 10.B.2], [84, Sec. B.5]:

$$\mathrm{E}^{T_0}\{z(t)\} = \lim_{N\to\infty} \frac{1}{2N+1} \sum_{n=-N}^{N} z(t - nT_0) \,. \tag{2.9}$$

This is simply the discrete average over all nT_0-translates, $\{z(t - nT_0) : \ n \in \mathbb{Z}\}$.

Note that two different notations are used in the superscript of the periodic or almost-periodic component extraction operator: If a periodic component is extracted, then the period is indicated in the superscript (see (2.9)). If the almost-periodic component is extracted, then the generic $\{\alpha\}$ is indicated in the superscript (see (2.7)).

2.2 Almost-periodic FOT probability

Only real-valued signals are treated in this paper for the sake of simplicity. In this paper, the properties of the first-order CDF are analyzed in detail. A first-order characterization of a complex-valued almost cyclostationary signal must be made by considering the second-order joint CDF of its real and imaginary parts making the presentation unnecessarily more complicated.

A characterization of the real-valued signal $x(t)$ can be obtained by considering, for every fixed $\xi \in \mathbb{R}$, the nonlinear transformation $z(t) = \mathrm{u}(\xi - x(t))$, where $\mathrm{u}(\cdot)$ is the unit-step function, that is, $\mathrm{u}(\xi) = 1$ for $\xi \geqslant 0$ and $\mathrm{u}(\xi) = 0$ for $\xi < 0$. We have the following decomposition

$$\mathrm{u}(\xi - x(t)) = \sum_{\gamma\in\Gamma_\xi} F_x^\gamma(\xi)\, e^{j2\pi\gamma t} + \nu(t;\xi) \,. \tag{2.10}$$

In (2.10), Γ_ξ is a countable set of possibly incommensurate frequencies, the Fourier coefficients $F_x^\gamma(\xi)$ are given by

$$F_x^{\gamma}(\xi) = \left\langle \mathrm{u}(\xi - x(t))\, e^{-j2\pi\gamma t} \right\rangle_t \tag{2.11}$$

provided that the time average exists $\forall \gamma \in \mathbb{R}$, and

$$\left\langle \nu(t;\xi)\, e^{-j2\pi\gamma t} \right\rangle_t \equiv 0 \quad \forall \gamma \in \mathbb{R}\,. \tag{2.12}$$

The almost-periodic component in (2.10), when not identically zero, not only reveals the presence of hidden periodicities in the signal $x(t)$, but also provides a probabilistic characterization of the signal $x(t)$. In fact, it can be shown that the almost-periodic function of t,

$$F_x(t;\xi) \triangleq \sum_{\gamma\in\Gamma_\xi} F_x^{\gamma}(\xi)\, e^{j2\pi\gamma t} \tag{2.13}$$

for every fixed t, as a function of ξ , is a valid CDF except for the right-continuity property. That is, the function $\xi \mapsto F_x(t;\xi)$ is nondecreasing and takes on values only in the interval [0, 1] [45, 84, Sec. 2.3.1]. The Fourier coefficients $F_x^{\gamma}(\xi)$ are referred to as *cyclic CDF*s.

From (2.10) and (2.13), it follows that

$$F_x(t;\xi) = \mathrm{E}^{\{\alpha\}}\{\mathrm{u}(\xi - x(t))\}\,. \tag{2.14}$$

Therefore, by analogy with the stochastic counterpart of (2.14), we have that the almost-periodic component extraction operator $\mathrm{E}^{\{\alpha\}}\{\cdot\}$ is the expectation operator in almost-periodic FOT probability theory with respect to the distribution (2.13).

If the set

$$\Gamma^{(1)} \triangleq \bigcup_{\xi\in\mathbb{R}} \Gamma_\xi \tag{2.15}$$

is countable, then the sum in (2.10) can be taken over $\Gamma^{(1)}$ [81, Sec. 2.2.1], [84, Sec. 2.3.1].

From this point forward, we shall consider the case for which $\Gamma^{(1)}$ is countable.

If $\Gamma^{(1)}$ contains incommensurate frequencies, then $x(t)$ is said to be first-order almost cyclostationary in the strict sense; if the frequencies are all integer multiples of a same fundamental frequency, then $x(t)$ is said to be first-order cyclostationary in the strict sense; if $\Gamma^{(1)}$ contains only the frequency $\gamma = 0$, then $x(t)$ is said to be first-order stationary in the strict sense.

Let $T_1, \ldots, T_P$ be the incommensurate periods of the additive periodic components of $\mathrm{u}(\xi - x(t))$. Thus, the CDF is poly-periodic and the following decomposition holds [39, Chap. 15]

$$F_x(t;\xi) = F_x^0(\xi) + \sum_{p=1}^{P} \left[F_x^{T_p}(t;\xi) - F_x^0(\xi) \right] \tag{2.16}$$

where each

$$F_x^{T_p}(t;\xi) \triangleq \mathrm{E}^{T_p}\{\mathrm{u}(\xi - x(t))\} \qquad p = 1, \ldots, P \tag{2.17}$$

is a valid periodic CDF with period T_p.

An almost-periodically time-variant probability density function (PDF) can be defined as the limit (provided that it exists) as $\Delta\xi$ goes to zero of the ratio of the FOT probability that $x(t)$ is contained within an interval of length $\Delta\xi$ about the point ξ to $\Delta\xi$. That is, if the function $F_x(t;\xi)$ is differentiable with respect to ξ, the PDF is given by:

$$f_x(t;\xi) \triangleq \frac{\mathrm{d}}{\mathrm{d}\xi} F_x(t;\xi) \tag{2.18a}$$

$$= \sum_{\gamma\in\Gamma^{(1)}} f_x^{\gamma}(\xi)\, e^{j2\pi\gamma t} \tag{2.18b}$$

where the Fourier coefficients, referred to as *cyclic PDF*s, are given by:

$$f_x^{\gamma}(\xi) = \frac{\mathrm{d}}{\mathrm{d}\xi} F_x^{\gamma}(\xi)\,. \tag{2.19}$$

The cyclic CDFs and PDFs with $\gamma \neq 0$ are complex valued in general. And because of this they are not cumulative probability distributions and probability density functions. The following properties of the cyclic CDFs and PDFs hold.

1) $F_x^{\gamma}(-\infty) = 0 \quad \forall\gamma \in \mathbb{R}$
2) $F_x^{\gamma}(+\infty) = \begin{cases} 1 & \gamma = 0 \\ 0 & \gamma \neq 0 \end{cases}$
3) $|F_x^{\gamma}(\xi)| \leqslant F_x^0(\xi)$
4) For $\xi_2 > \xi_1, |F_x^{\gamma}(\xi_2) - F_x^{\gamma}(\xi_1)| \leqslant F_x^0(\xi_2) - F_x^0(\xi_1)$
5) $\displaystyle\int_{\mathbb{R}} f_x^{\gamma}(\xi)\,\mathrm{d}\xi = \begin{cases} 1 & \gamma = 0 \\ 0 & \gamma \neq 0 \end{cases}$
6) $\displaystyle\left|\int_{\xi_1}^{\xi_2} f_x^{\gamma}(\xi)\,\mathrm{d}\xi\right| \leqslant \int_{\xi_1}^{\xi_2} f_x^0(\xi)\,\mathrm{d}\xi$

where property 5 follows from 1 and 2 and 6 follows from 4, provided that the PDF exists.

For the signal $x(t)$, we have the decomposition

$$x(t) = x_{\mathrm{ap}}(t) + x_{\mathrm{r}}(t) \tag{2.20}$$

and it results that

$$\mathrm{E}^{\{\alpha\}}\{x(t)\} = x_{\mathrm{ap}}(t) \tag{2.21a}$$

$$= \int_{\mathbb{R}} \xi\, \mathrm{d}F_x(t;\xi) \tag{2.21b}$$

$$= \sum_{\eta \in \mathcal{E}^{(1)}} x_\eta \, e^{j2\pi\eta t} \tag{2.21c}$$

with $\mathcal{E}^{(1)} \subseteq \Gamma^{(1)}$ and

$$x_\eta = \left\langle x(t)\, e^{-j2\pi\eta t} \right\rangle_t \tag{2.22a}$$

$$= \int_{\mathbb{R}} \xi \, \mathrm{d}F_x^\eta(\xi)\,. \tag{2.22b}$$

See [44] for a generalization of this result when the almost-periodic component extraction operator is replaced by a generic orthogonal projection operator.

The Fourier coefficients $F_x^\gamma(\xi)$ and x_η can be estimated by replacing in (2.11) and (2.22a) the infinite time average by finite time averages taken on the observation interval. In [31], kernel-based estimators are proposed for $f_x^\gamma(\xi)$ and $F_x^\gamma(\xi)$. These estimators generalize to almost-periodically time-variant CDFs and PDFs the estimators for the time-invariant CDFs and PDFs originally proposed at discrete time in [96, 104], and then considered at continuous time in [20].

2.3 Example 1: Sine wave with additive noise

Let us consider a sine wave

$$c(t) = A_0 \cos(2\pi f_0 t + \phi_0) \tag{2.23}$$

embedded in additive zero-mean strictly-sense stationary Gaussian noise $n(t)$

$$x(t) = c(t) + n(t) \tag{2.24}$$

with

$$f_n(t;\xi) = f_n(\xi) = \frac{1}{\sqrt{2\pi}\sigma_n} e^{-\xi^2/(2\sigma_n^2)} \tag{2.25}$$

The sine wave is a deterministic signal in the FOT sense. Thus, its probability density function is

$$f_c(t;\xi) = \delta(\xi - c(t)) = \delta(\xi - A_0 \cos(2\pi f_0 t + \phi_0)) \tag{2.26}$$

and it is FOT independent of any other signal [45, 88]. Therefore,

$$f_x(t;\xi) = f_c(t;\xi) \otimes f_n(\xi) \tag{2.27a}$$

$$= \delta(\xi - A_0 \cos(2\pi f_0 t + \phi_0)) \otimes \frac{1}{\sqrt{2\pi}\sigma_n} e^{-\xi^2/(2\sigma_n^2)} \tag{2.27b}$$

$$= \frac{1}{\sqrt{2\pi}\sigma_n} e^{-(\xi - A_0 \cos(2\pi f_0 t + \phi_0))^2/(2\sigma_n^2)} \tag{2.27c}$$

which is Gaussian with a sinusoidal mean, where $\otimes$ denotes convolution. The Fourier coefficients $f_x^{\gamma}(\xi)$ for $\gamma = kf_0$, $k \in \mathbb{Z}$, of this periodic PDF are given by (see Appendix A)

$$\begin{aligned} f_x^{kf_0}(\xi) &\triangleq \left\langle f_x(t;\xi)\, e^{-j2\pi kf_0 t} \right\rangle_t \\ &= \frac{1}{\sqrt{2\pi}\sigma_n}\, e^{-\xi^2/(2\sigma_n^2)}\, e^{-A_0^2/(4\sigma_n^2)}\, e^{jk\phi_0} \\ &\quad \sum_{m=-\infty}^{\infty} j^{(k-m)}\, J_{k-2m}(-j\xi A_0/\sigma_n^2)\, J_m(jA_0^2/(4\sigma_n^2))\,. \end{aligned} \tag{2.28}$$

In (2.28), the Bessel function of the first kind of order n with imaginary argument $J_n(jx)$ can be replaced by $j^n I_n(x)$ [92, Eq. 10.27.6], where $I_n(x)$ is the modified Bessel function of the first kind of order n with real argument x.

Since $n(t)$ has zero mean, then it does not contain any finite-strength additive sine-wave component. Therefore, from (2.24) it follows that the almost-periodic FOT expected value of $x(t)$ is given by:

$$\mathrm{E}^{\{\alpha\}}\{x(t)\} = c(t) = A_0\, \cos(2\pi f_0 t + \phi_0)\,. \tag{2.29}$$

In the stochastic approach, the time-invariant PDF is derived in [103] and the frequency estimation problem is addressed in [102]. The FOT cyclic PDFs for a single sine wave are derived in [108].

In the following, an illustrative numerical experiment is carried out. $N = 2^{18}$ samples of the signal (2.24) are taken with sampling frequency $f_s = 1/T_s$. The signal $n(t)$ is stationary colored Gaussian noise obtained filtering white Gaussian noise with a linear time-invariant (LTI) filter with harmonic response $H(f) = (1 + j2\pi(f/2B))^{-1}$, with $B = 0.005 f_s$. The sine wave $c(t)$ has $f_0 = 0.0251 f_s$, $\phi_0 = 0$, and A_0 is such that SNR = –10 dB (Fig. 1 (Top)) or SNR = 10 dB (Fig. 1 (Bottom)). Only the first 3000 samples are reported in Fig. 1.

The magnitude of the estimate of (Top) the cyclic CDF and (Bottom) the cyclic PDF, as functions of the cycle frequency γ and the parameter ξ, are reported in Fig. 2 for SNR = –10 dB and in Fig. 3 for SNR = 10 dB.

In Fig. 2 (SNR = –10 dB), the slice for $\gamma = 0$ is practically coincident with a Normal CDF (Top) and PDF (Bottom). In Fig. 3 (SNR = 10 dB), the slice for $\gamma = 0$ is a smoothed version of the stationary CDF (Top) and PDF (Bottom) of a sinusoidal function [88, Eq. (42), Fig. 6].

2.4 Example 2: Sine wave with multiplicative noise

Let us consider the product waveform

$$x(t) = n(t)\, c(t) \tag{2.30}$$

where $n(t)$ and $c(t)$ are the same as those in Example 1 (Sec. 2.3).

Since $c(t)$ is periodic, it is a deterministic signal (in the FOT probability sense), and hence, it is independent of every other signal [45, 88]. The PDF of the product of two FOT independent functions can be expressed by the classical formula [3, Chap. 2, Problem 14]

$$f_x(t;\xi) = \int_{\mathbb{R}} f_c(t;s) f_n(\xi/s)\, \frac{1}{|s|}\, \mathrm{d}s \tag{2.31a}$$

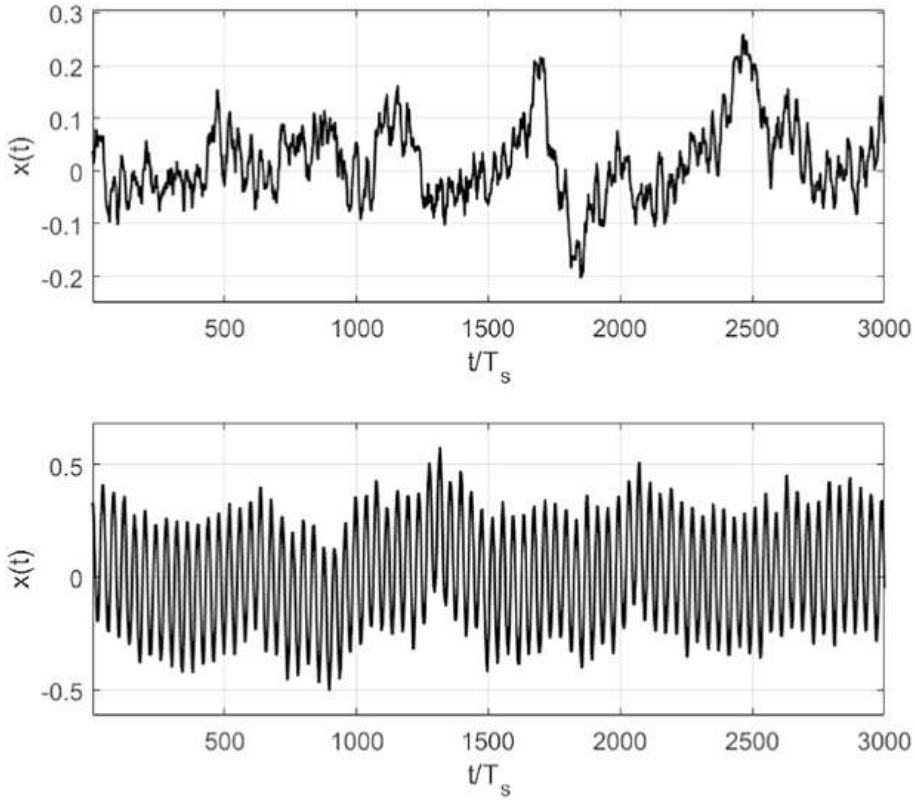

Fig. 1 Sine wave in additive colored Gaussian noise. (Top) SNR = −10 dB; (Bottom) SNR = 10 dB

$$= \int_{\mathbb{R}} \delta(s - A_0 \cos(2\pi f_0 t + \phi_0)) \frac{1}{\sqrt{2\pi}\sigma_n} e^{-(\xi/s)^2/(2\sigma_n^2)} \frac{1}{|s|} \, \mathrm{d}s \tag{2.31b}$$

$$= \frac{1}{\sqrt{2\pi}\sigma_n |A_0 \cos(2\pi f_0 t + \phi_0)|} e^{-\xi^2/(2\sigma_n^2 A_0^2 \cos^2(2\pi f_0 t + \phi_0))} \tag{2.31c}$$

Since $|\cos(2\pi f_0 t + \phi_0)|$ and $\cos^2(2\pi f_0 t + \phi_0)$ are both periodic with period $1/(2f_0)$, then $f_x(t;\xi)$ is periodic with period $1/(2f_0)$. Since $f_x(t;\xi)$ is an even function of ξ, then the signal $x(t)$ has zero mean:

$$\mathrm{E}^{\{\alpha\}}\{x(t)\} = \int_{\mathbb{R}} \xi f_x(t;\xi) \, \mathrm{d}\xi = 0 \,. \tag{2.32}$$

That is, $f_x(t;\xi)$ is a zero-mean Gaussian PDF with periodically time-variant variance.

The obtained results are in agreement with those of the example in [88, Sec. VI.B]. Note that for $\xi \neq 0$ and $2\pi f_0 t \to \pi/2 + k\pi - \phi_0$, we have $f_x(t;\xi) \to 0$. For $\xi = 0$ and $2\pi f_0 t = \pi/2 + k\pi - \phi_0$, one has the impulsive PDF $\delta(\xi)$ obtained by (2.31c) in the limit as the variance approaches zero. This behavior corresponds to the jump in the degenerate CDF u(ξ) (see [88, Fig. 9]).

In the following, an illustrative numerical experiment is carried out. The first 3000 samples of $x(t)$ are reported in Fig. 4. The signals $n(t)$ and $c(t)$ are the same as those of Sect. 2.3.

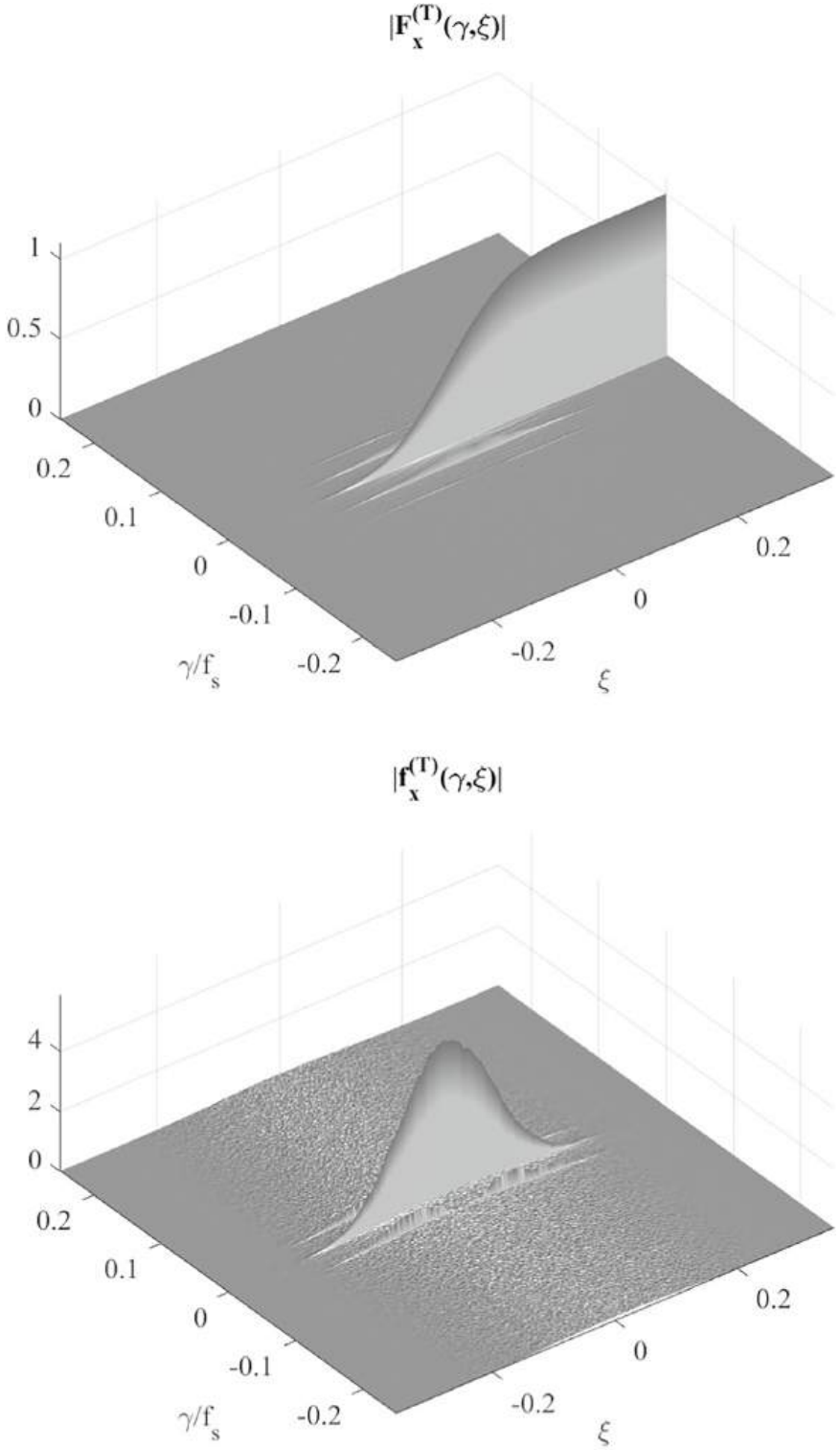

Fig. 2 Sine wave in additive colored Gaussian noise (SNR = –10 dB). Magnitude of the estimate of (Top) the cyclic CDF and (Bottom) the cyclic PDF, as functions of the cycle frequency γ and the parameter ξ

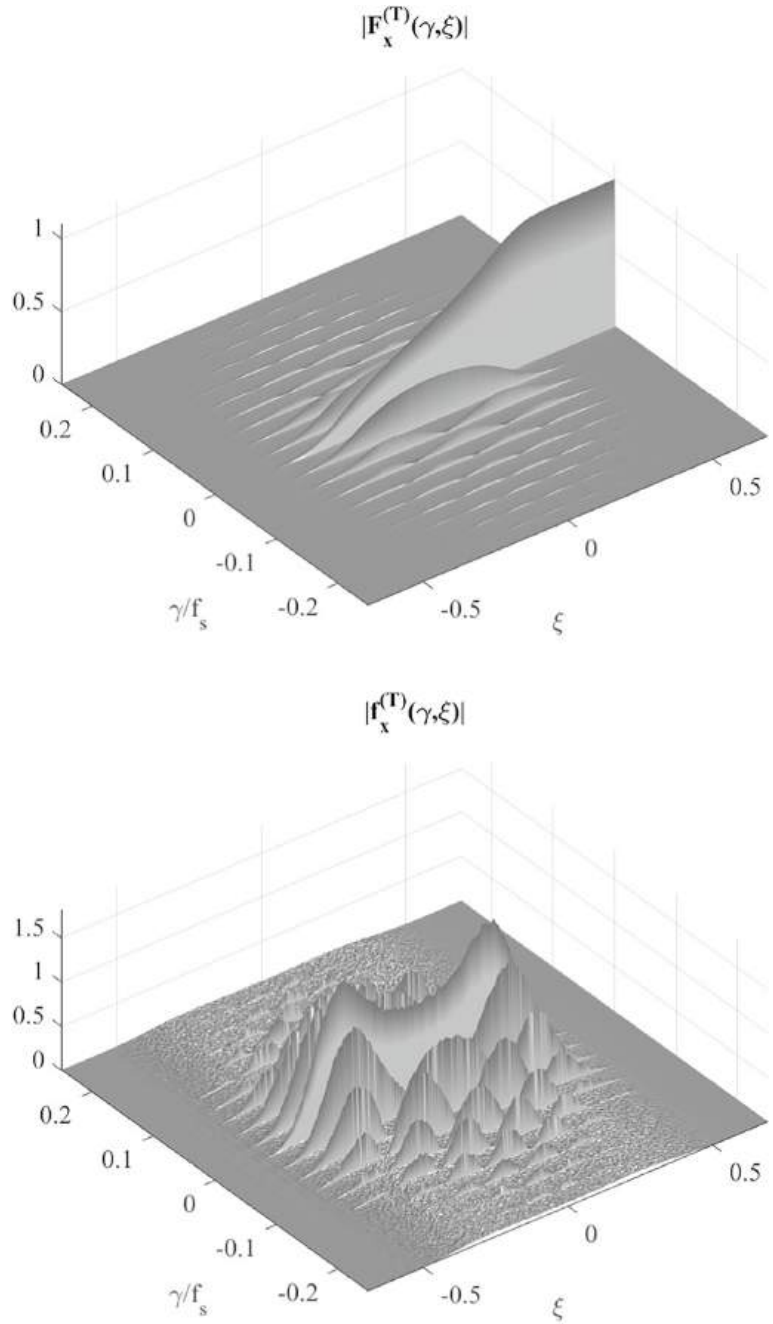

Fig. 3 Sine wave in additive colored Gaussian noise (SNR = 10 dB). Magnitude of the estimate of (Top) the cyclic CDF and (Bottom) the cyclic PDF, as functions of the cycle frequency γ and the parameter ξ

It could be said that the periodicity in Example 2 is more well hidden than that in Example 1, because a nonlinear transformation of that data is required to produce a finite-strength additive periodic component in the data. In subsequent sections, examples of increasingly well hidden periodicities are given. It is seen that the higher the order of the nonlinearity required to reveal periodicity, the more well hidden the periodicity is. In practice, the higher the order required, the longer the required

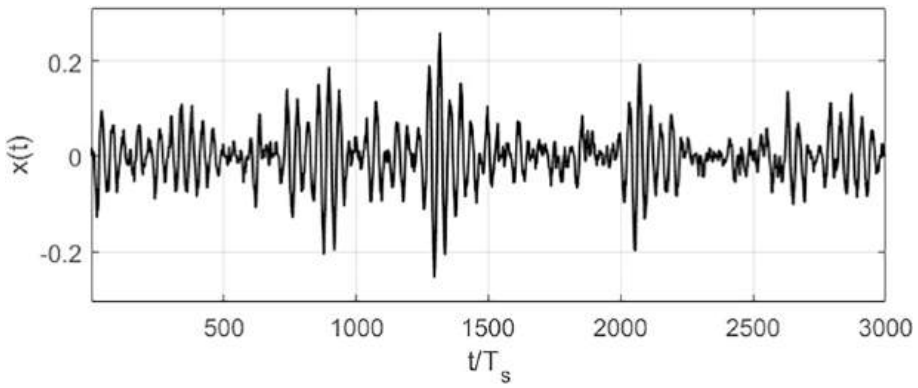

Fig. 4 Sine wave in multiplicative colored Gaussian noise

integration time in the computation of the Fourier integral needed to extract an almost-periodic component or just a single sine wave.

In Fig. 5, the magnitude of the estimate of (Top) the cyclic CDF and (Bottom) the cyclic PDF, as functions of the cycle frequency γ and the parameter ξ, are reported. For every fixed t, the PDF in (2.31c) is a Gaussian PDF. In contrast, the stationary PDF corresponding to the slice for $\gamma = 0$ in Fig. 5 is non Gaussian. Such a result is discussed in [88, Sec. IV.B] to motivate the advantage of using the FOT approach for signal analysis with respect to classical stochastic approach.

3 Second-order cyclostationarity

In this section, the second-order characterization of cyclostationary and almost-cyclostationary time series in the FOT probability framework is presented [38, 39, 45, Part II], [84, Chap. 2].

3.1 FOT characterization

A second-order characterization of the real-valued signal $x(t)$ can be obtained by considering, for every pair $(\xi_1, \xi_2) \in \mathbb{R}^2$, the nonlinear transformation $z(t) = \mathrm{u}(\xi_1 - x(t+\tau_1))\,\mathrm{u}(\xi_2 - x(t+\tau_2))$. By reasoning as in the first-order case, it can be shown that the almost-periodic function

$$F_x(t, \tau_1, \tau_2; \xi_1, \xi_2) \triangleq \mathrm{E}^{\{\alpha\}}\{\mathrm{u}(\xi_1 - x(t+\tau_1))\,\mathrm{u}(\xi_2 - x(t+\tau_2))\} \tag{3.1a}$$

$$= \sum_{\gamma \in \Gamma^{(2)}} F_x^{\gamma}(\tau_1, \tau_2; \xi_1, \xi_2)\, e^{j2\pi\gamma t} \tag{3.1b}$$

for every t is a valid second-order joint CDF in the variables (ξ_1, ξ_2), except for the right-continuity property with respect to each variable ξ_1 and ξ_2. In (3.1b), $\Gamma^{(2)}$ is a countable set of possibly incommensurate cycle frequencies and the Fourier coefficients

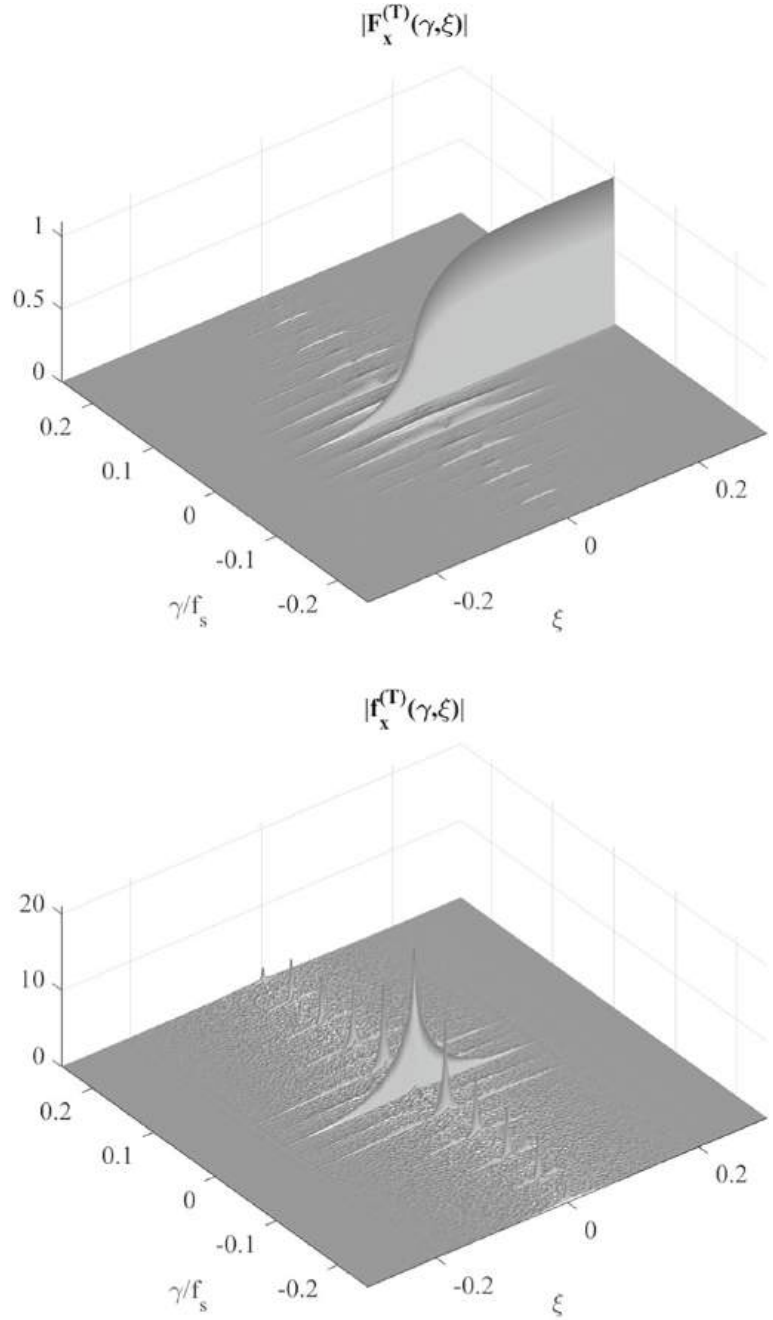

Fig. 5 Sine wave with multiplicative colored Gaussian noise. Magnitude of the estimate of (Top) the cyclic CDF and (Bottom) the cyclic PDF, as functions of the cycle frequency γ and the parameter ξ

$$F_x^{\gamma}(\tau_1,\tau_2;\xi_1,\xi_2) \triangleq \left\langle \mathrm{u}(\xi_1 - x(t+\tau_1))\,\mathrm{u}(\xi_2 - x(t+\tau_2))\,e^{-j2\pi\gamma t}\right\rangle_t \tag{3.2}$$

are referred to as second-order cyclic CDFs.

From this joint CDF, a valid almost-periodically time-variant autocorrelation function can be constructed, which can be shown to be equal to the almost-periodic component of the second-order lag product waveform

$$\mathrm{E}^{\{\alpha\}}\{x(t+\tau_1)\,x(t+\tau_2)\} = \int_{\mathbb{R}^2} \xi_1\,\xi_2\,\mathrm{d}F_x(t,\tau_1,\tau_2;\xi_1,\xi_2)\,. \tag{3.3}$$

Let $x(t)$ be a finite average-power signal (see (2.8)) and let us consider, for every fixed τ, the decomposition of the lag-product waveform $y_\tau(t) \triangleq x(t+\tau)\,x(t)$ into an almost-periodic component and a residual term not containing any finite-strength sine-wave component

$$x(t+\tau)\,x(t) = \sum_{\alpha\in\mathcal{A}_\tau} R_x^\alpha(\tau)\,e^{j2\pi\alpha t} + \ell_x(t,\tau)\,. \tag{3.4}$$

In (3.4), $\mathcal{A}_\tau$ is a countable set of possibly incommensurate frequencies, referred to as *second-order cycle frequencies*, the Fourier coefficients

$$R_x^\alpha(\tau) = \left\langle x(t+\tau)\,x(t)\,e^{-j2\pi\alpha t}\right\rangle_t \tag{3.5}$$

are referred to as *cyclic autocorrelation functions*, and

$$\left\langle \ell_x(t,\tau)\,e^{-j2\pi\alpha t}\right\rangle_t \equiv 0 \quad \forall\alpha\in\mathbb{R}\,. \tag{3.6}$$

The cyclic autocorrelation function (3.5) at cycle frequency α can be expressed in terms of the cyclic CDF at the same cycle frequency as

$$R_x^\alpha(\tau) = \int_{\mathbb{R}^2} \xi_1\,\xi_2\,\mathrm{d}F_x^\alpha(\tau,0;\xi_1,\xi_2) \tag{3.7}$$

which is in agreement with (3.3).

The countability of the set $\mathcal{A}_\tau$ is an immediate consequence of the finite-power assumption (2.8) [16, Secs. 1.2, 2.1], [121]. If the set

$$\mathcal{A} \triangleq \bigcup_{\tau\in\mathbb{R}} \mathcal{A}_\tau \tag{3.8}$$

is countable, then the sum in (3.4) can be over the set $\mathcal{A}$ and the signal $x(t)$ is said to be *second-order almost-cyclostationary* [38, 39, Part II]. If the set $\mathcal{A}$ contains only the integer multiples of a fundamental frequency, say $\alpha_0 = 1/T_0$, then the almost-periodic component reduces to a periodic function with period T_0 and the signal is referred to as *second-order cyclostationary*. If $\mathcal{A}$ is the union of a finite number of sets $\{k/T_p,\ k\in\mathbb{Z}\}$ with incommensurate periods T_p, then the almost-periodic component is poly-periodic and the signal is called *second-order poly-cyclostationary*. If the set $\mathcal{A}$ is uncountable, then the signal $x(t)$ is said to be *second-order generalized almost-cyclostationary* (GACS) [57, 81, Chap. 2]. See also [79].

Let us consider in the following, unless otherwise specified, the case of ACS time series. That is, $\mathcal{A}$ defined in (3.8) is countable.

It can be easily shown that the almost-periodic autocorrelation function is definite non negative. In fact, for every function $h(\tau)\in L^1(\mathbb{R})$ it results

$$\int_{\mathbb{R}^2} h(\tau_1)\, h(\tau_2)\, x(t+\tau_1)\, x(t+\tau_2)\, \mathrm{d}\tau_1 \mathrm{d}\tau_2 = \left| \int_{\mathbb{R}} h(\tau)\; x(t+\tau)\, \mathrm{d}\tau \right|^2 \geqslant 0 \tag{3.9}$$

and, consequently,

$$\int_{\mathbb{R}^2} h(\tau_1) h(\tau_2) \mathrm{E}^{\{\alpha\}}\{x(t+\tau_1)x(t+\tau_2)\}\mathrm{d}\tau_1\mathrm{d}\tau_2 \;= \mathrm{E}^{\{\alpha\}}\left\{ \int_{\mathbb{R}^2} h(\tau_1)h(\tau_2)x(t+\tau_1)x(t+\tau_2)\mathrm{d}\tau_1\mathrm{d}\tau_2 \right\} \geqslant 0. \tag{3.10}$$

In (3.10), the right-hand term is nonnegative since the almost-periodic component of a nonnegative function is nonnegative [84, Lemma 2.18] and the order of integral and almost-periodic component extraction operator can be inverted according to [84, Theorem 2.32].

Finally, note that a first-order characterization of a complex-valued almost cyclostationary signal can be made considering the second-order joint CDF of its real and imaginary parts. Similarly, the second-order characterization is made by considering the fourth-order joint CDF of the real and imaginary parts of the signal and its time-shifted version [16, 84, Secs. 1.3, A.2]. In such a case, both cyclic autocorrelation function (where the second term in (3.5) is conjugated) and conjugate cyclic autocorrelation function (where the second term in (3.5) is not conjugated) must be considered for a complete characterization of the second-order cyclostationarity of the complex-valued signal [112]. The exploitation of both functions finds application, for example, in the minimum mean-squared error (MMSE) linear almost-periodically time-variant filtering (cyclic Wiener filtering) of the complex envelope of communications signals [40].

3.2 Second-order spectral line generation

Let us consider the decomposition (2.2) for the signal $x(t)$

$$x(t) = x_{\mathrm{ap}}(t) + x_{\mathrm{r}}(t) \tag{3.11}$$

where, according to (2.2) and (2.7),

$$\mathrm{E}^{\{\alpha\}}\{x(t)\} = x_{\mathrm{ap}}(t) \tag{3.12}$$

and the residual term $x_r(t)$ does not contain any finite-strength additive sine-wave components and possibly has finite power.

The second-order lag-product waveform is given by

$$\begin{aligned} x(t+\tau_1)\, x(t+\tau_2) &= [x_{\mathrm{ap}}(t+\tau_1) + x_{\mathrm{r}}(t+\tau_1)][x_{\mathrm{ap}}(t+\tau_2) + x_{\mathrm{r}}(t+\tau_2)] \\ &= x_{\mathrm{ap}}(t+\tau_1)\, x_{\mathrm{ap}}(t+\tau_2) + x_{\mathrm{r}}(t+\tau_1)\, x_{\mathrm{ap}}(t+\tau_2) \\ &\quad + x_{\mathrm{ap}}(t+\tau_1)\, x_{\mathrm{r}}(t+\tau_2) + x_{\mathrm{r}}(t+\tau_1)\, x_{\mathrm{r}}(t+\tau_2)\,. \end{aligned} \tag{3.13}$$

In (3.13), since the product of AP functions is an AP function [11, Chap. I, Par. I], [84, Theorem B.9], then the term $x_{\mathrm{ap}}(t+\tau_1)\, x_{\mathrm{ap}}(t+\tau_2)$ is an AP function of t. Since $x_{\mathrm{r}}(t)$ does not contain any finite-strength additive sine-wave components, then the terms $x_{\mathrm{r}}(t+\tau_1)\, x_{\mathrm{ap}}(t+\tau_2)$ and $x_{\mathrm{ap}}(t+\tau_1)\, x_{\mathrm{r}}(t+\tau_2)$ do not contain any finite-strength additive sine-wave components. The term $x_{\mathrm{r}}(t+\tau_1)\, x_{\mathrm{r}}(t+\tau_2)$ can contain additive finite-strength sine-wave components.

Any almost-periodic component contained in $x_r(t+\tau_1)\,x_r(t+\tau_2)$ cannot contain a product of sine waves, since neither factor contains any sine waves. For this reason, the sine waves of the (generalized) Fourier series expansion of such an almost-periodic component are called *pure second-order sine waves* and the corresponding frequencies *pure second-order cycle frequencies*. In contrast, the finite-strength sine waves in $x_{ap}(t+\tau_1)\,x_{ap}(t+\tau_2)$ are due to only the products of first-order finite-strength sine waves and, hence, are called *impure second-order sine waves* and the corresponding frequencies *impure second-order cycle frequencies* [49] (which are called beat frequencies). Note that a second-order sine wave at a given cycle frequency α may contain a portion which is pure and another portion which is impure. The pure second-order sine waves are extracted by the autocovariance function:

$$E^{\{\alpha\}}\left\{\left[x(t+\tau_1)-E^{\{\alpha\}}\{x(t+\tau_1)\}\right]\left[x(t+\tau_2)-E^{\{\alpha\}}\{x(t+\tau_2)\}\right]\right\} \tag{3.14a}$$

$$= \mathrm{E}^{\{\alpha\}}\left\{x(t+\tau_1)\,x(t+\tau_2)\right\} - \mathrm{E}^{\{\alpha\}}\{x(t+\tau_1)\}\,\mathrm{E}^{\{\alpha\}}\{x(t+\tau_2)\} \tag{3.14b}$$

$$= \mathrm{E}^{\{\alpha\}}\left\{x_r(t+\tau_1)\,x_r(t+\tau_2)\right\} \tag{3.14c}$$

$$= \sum_{\beta\in\mathcal{B}} C_x^{\beta}(\tau_1-\tau_2)\,e^{j2\pi\beta(t+\tau_2)} \tag{3.14d}$$

where for (3.14b) and (3.14c), equation (3.13) has been accounted for, and, in (3.14d), $\mathcal{B}\subseteq\mathcal{A}$ denotes the set of pure second-order cycle frequencies and the Fourier coefficients $C_x^{\beta}(\tau)$ are referred to as *cyclic autocovariance functions*.

If $x(t)$ does not contain any additive finite-strength sine-wave component, that is, $x_{ap}(t)\equiv 0$ in (3.11), then the possible AP component in the lag product waveform $x(t+\tau_1)\,x(t+\tau_2)$ is due to the product of only the time-shifted versions $x_r(t+\tau_1)$ and $x_r(t+\tau_2)$ of the residual term. In this case, we have that periodicities that may be hidden at first order are generated in the second-order lag-product waveform, or not. If not, they may be generated in higher-order lag-products as explained in Sect. 4.

Note that, in the case of communication signals, a sine wave or a periodic signal (e.g., a pulse train) is modulated by random data. For this reason, in previous works [49, 84, Secs. 2.3.1.6, 4.2.3] that focus on communication applications, the term "regenerated" is adopted instead of "generated" for sine waves or periodic signals (spectral lines) obtained by nonlinear transformations of the data. More generally, as for example in climate data, there is no underlying sine wave or periodic signal that is modulated. In this case, the term "generated" is more appropriate than "regenerated". The term "generated" is clearly more appropriate for data with irregular cyclicities, like the ECG or other biological signals (Sec. 5) or the Sunspot number time series (Sec. 6).

Let us consider the decomposition (2.2) when $z(t)$ is the second-order lag-product waveform $x(t+\tau_1)\,x(t+\tau_2)$:

$$x(t+\tau_1)\,x(t+\tau_2) = \mathrm{E}^{\{\alpha\}}\{x(t+\tau_1)\,x(t+\tau_2)\} + \ell_x(t,\tau_1,\tau_2) \tag{3.15a}$$

$$= \sum_{\alpha\in\mathcal{A}} R_x^{\alpha}(\tau_1-\tau_2)\,e^{j2\pi\alpha(t+\tau_2)} + \ell_x(t,\tau_1,\tau_2) \tag{3.15b}$$

where $\ell_x(t,\tau_1,\tau_2)$ does not contain any finite-strength additive sine-wave component. In (3.15b), the almost-periodic term is the (generalized) Fourier series expansion of the sum of the first and fourth term in (3.13), and the residual term $\ell_x(t,\tau_1,\tau_2)$ is equal to the sum of the second and third term in (3.13).

If α is an impure second-order cycle frequency, then the cyclic autocorrelation function $R_x^{\alpha}(\tau)$, as a function of τ, oscillates and does not decay to zero as $|\tau|\to\infty$ [49, 81, Sec. 1.4]. In contrast, for finite or practically finite memory time series, $C_x^{\beta}(\tau)\in L^1(\mathbb{R})$, $\forall\beta\in\mathcal{B}$ and therefore the cyclic autocovariance does decay to zero as $|\tau|\to\infty$ [49, 81, Sec. 1.4.1], [84, Sec. 4.2.3.1].

For ACS time series, any homogeneous quadratic time-invariant (QTI) transformation of the signal $x(t)$ has the form

$$\begin{aligned} y(t) &\triangleq \int_{\mathbb{R}^2} k(\tau_1,\tau_2)\,x(t+\tau_1)\,x(t+\tau_2)\,\mathrm{d}\tau_1\,\mathrm{d}\tau_2 \\ &= \sum_{\alpha\in\mathcal{A}} \int_{\mathbb{R}^2} k(\tau_1,\tau_2)\,R_x^{\alpha}(\tau_1-\tau_2)\,e^{j2\pi\alpha\tau_2}\,\mathrm{d}\tau_1\,\mathrm{d}\tau_2\,e^{j2\pi\alpha t} \\ &\quad + \int_{\mathbb{R}^2} k(\tau_1,\tau_2)\,\ell_x(t,\tau_1,\tau_2)\,\mathrm{d}\tau_1\,\mathrm{d}\tau_2 \end{aligned} \tag{3.16}$$

where $k(\tau_1,\tau_2)$ is the kernel of the QTI transformation. That is, finite-strength additive sine-wave components can be generated by homogeneous QTI transformations [39, 41, 45]. In contrast, for stationary time series ($\mathcal{A}$ containing the only element $\alpha=0$), no spectral line at nonzero frequency can be generated in the lag-product or by QTI transformations. In [39, Sec. 10.B.4], the kernel $k(\tau_1,\tau_2)$ of the optimum QTI transformation is derived such that the power in the generated spectral line at a specific frequency α_0 is maximized. The maximization procedure leads to a kernel whose double Fourier transform is proportional to the conjugate of the signal cyclic spectrum at cycle frequency α_0.

More generally, a time series $x(t)$ is said to exhibit *higher-order cyclostationarity* if finite-strength additive sine-wave components can be generated by homogeneous nonlinear time-invariant transformations of $x(t)$ of order greater than two [49, 112], (Sec. 4). In such a case, almost-periodically time-variant higher-order moment and cumulant functions can be defined by the almost-periodic component extraction operator [49, 57, 112]. For communications, ACS signals, cycle frequencies of second- and higher-order statistical functions are related to parameters such as sine-wave carrier frequency, pulse rate, symbol rate, frame rate, sampling frequency. Therefore, spectral line generation by second- or higher-order time-invariant transformations leads to signals suitable for synchronization purposes [39].

In [9, pp. 497-502], conditions are derived such that linear combinations of powers of pseudo-random functions can be decomposed into the sum of a periodic function and a pseudo-random function.

3.3 Spectral correlation

In the case of $\mathcal{A}$ countable, in [39, Chap. 11] it is shown that the presence of a finite-strength additive sine-wave component at cycle frequency α in the second-order lag-product waveform (3.4) is equivalent to the existence of correlation between spectral components of the signal $x(t)$ whose frequency separation is equal to α. That is, denoted by

$$X_{1/\Delta f}(t,f) \triangleq \int_{t-1/(2\Delta f)}^{t+1/(2\Delta f)} x(s)\, e^{-j2\pi fs}\, \mathrm{d}s \tag{3.17}$$

the spectral component of $x(t)$ at frequency f with finite bandwidth Δf, the function

$$S_x^\alpha(f) \triangleq \lim_{\Delta f\to 0} \lim_{T\to\infty} \frac{1}{T} \int_{-T/2}^{T/2} \Delta f\, X_{1/\Delta f}(t,f)\, X_{1/\Delta f}^*(t,f-\alpha)\, \mathrm{d}t \tag{3.18}$$

is not identically zero if the signal $x(t)$ exhibits cyclostationarity at cycle frequency α. The function $S_x^\alpha(f)$ is referred to as the *cyclic spectrum* at cycle frequency α or the *spectral correlation density function*. In fact, it represents the temporal correlation (with zero lag) between the two spectral components $X_{1/\Delta f}(t,f)$ and $X_{1/\Delta f}(t,f-\alpha)$ when the averaging time T becomes infinite and the bandwidth Δf becomes infinitesimal. For $\alpha = 0$, the cyclic spectrum is coincident with the PSD.

The cyclic spectrum is linked to the cyclic autocorrelation function by the Fourier transform relationship

$$S_x^\alpha(f) = \int_{\mathbb{R}} R_x^\alpha(\tau)\, e^{-j2\pi f\tau}\, \mathrm{d}\tau \tag{3.19}$$

originally introduced in [39], which is referred to as the *Gardner relation* [84, Sec. 2.3.1.10]. It is also dubbed *cyclic Wiener relation* since for $\alpha = 0$ it reduces to the Wiener relation that links the time-average autocorrelation function with the PSD [120].

The cyclic spectrum of the residual term

$$x_{\mathrm{r}}(t) = x(t) - \mathrm{E}^{\{\alpha\}}\{x(t)\} \tag{3.20}$$

is referred to as *second-order cyclic polyspectrum* of $x(t)$ and is denoted by $P_x^\beta(f)$. It is linked to the cyclic autocovariance function by the Fourier transform relationship

$$P_x^\beta(f) = \int_{\mathbb{R}} C_x^\beta(\tau)\, e^{-j2\pi f\tau}\, \mathrm{d}\tau\,. \tag{3.21}$$

For finite or practically finite memory signals, $C_x^\beta(\tau) \in L^1(\mathbb{R})$ (Sec. 3.2). Thus, its Fourier transform $P_x^\beta(f)$ exists in the ordinary sense. In particular, it does not contain Dirac impulses. In contrast, if α is an impure second-order sine wave, then $R_x^\alpha(\tau)$ contains sinusoidal terms in τ. Consequently, its Fourier transform is defined in a generalized sense and contains Dirac impulses [49, 84, Sec. 1.4].

3.4 Statistical function measurements

In this section, a brief overview of the estimators of cyclic statistical functions is presented. For extensive treatments, see [39, Chaps. 2, 13], [84, Sec. 5.6].

Let $[t_0, t_0 + T]$ be the observation interval of the time series $x(t)$. The cyclic autocorrelation function can be estimated by the cyclic correlogram

$$R_x^{(T)}(\alpha, \tau; t_0) \triangleq \frac{1}{T} \int_{t_0}^{t_0+T} x(t+\tau)\, x(t)\, e^{-j2\pi\alpha t}\, \mathrm{d}t\,. \tag{3.22}$$

When t_0 ranges in a time interval of length Z, the cyclic correlogram is a mean-square consistent and asymptotically complex normal (as $T \to \infty$ and $Z \to \infty$ with $Z/T \to \infty$) estimator of the cyclic autocorrelation function [30]. The cyclic spectrum can be consistently estimated by the frequency-smoothed cyclic periodogram

$$S_x^{(T,\Delta f)}(\alpha, f; t_0) = \int_{\mathbb{R}} \frac{1}{T} X_T(t_0, \lambda)\, X_T^*(t_0, \lambda - \alpha)\, \frac{1}{\Delta f} W\left(\frac{\lambda - f}{\Delta f}\right) \mathrm{d}\lambda \tag{3.23}$$

where the finite-time Fourier transform $X_T(t_0, \lambda)$ is defined according to (3.17) and $W(f)$ is a unit-area frequency-smoothing window. In the right-hand sides of (3.22) and (3.23), the dependence on t_0 can be omitted if this does not create ambiguity. The frequency-smoothed cyclic periodogram can be shown to have asymptotically the same performance as that of the time-smoothed cyclic periodogram [39, Sec. 11.C]

$$G_x^{(\Delta f,T)}(\alpha, f; t_0) = \frac{1}{T} \int_{t_0-T/2}^{t_0+T/2} X_{1/\Delta f}(t, f)\, X_{1/\Delta f}^*(t, f - \alpha)\, \mathrm{d}t \tag{3.24}$$

when the data-record length T approaches infinity and the spectral resolution Δf approaches zero. For $\alpha = 0$, the time- and frequency-smoothed cyclic periodograms reduce to the classical estimators of the power spectral density [4, 5, 13, 15, 34, 52, 95, 119]. For the advantages of using other-than-rectangular data-tapering and time- or frequency-smoothing windows, see [54, 93] for power spectral densities and [39, Chaps. 2, 13] for both power and cyclic spectral densities.

Estimators for the second-order cyclic polyspectrum and the cyclic covariance when the first-order cycle frequencies are unknown are proposed in [89] and discussed in [84, Sec. 5.2.5]. Estimators for the cyclic CDF and PDF are presented in [31].

3.5 Example 1 (cont'd): Sine wave with additive noise

The second-order lag product of the signal (2.24) is

$$\begin{aligned} x(t+\tau)\, x(t) &= [c(t+\tau) + n(t+\tau)]\, [c(t) + n(t)] \\ &= c(t+\tau)\, c(t) + n(t+\tau)\, c(t) + c(t+\tau)\, n(t) + n(t+\tau)\, n(t) \\ &= A_0^2 \cos(2\pi f_0(t+\tau) + \phi_0) \cos(2\pi f_0 t + \phi_0) \\ &\quad + \ell_{nc}(t,\tau) + \ell_{cn}(t,\tau) + R_n(\tau) + \ell_n(t,\tau) \\ &= \frac{A_0^2}{2} [\cos(2\pi 2 f_0 t + 2\pi f_0 \tau + 2\phi_0) + \cos(2\pi f_0 \tau)] \\ &\quad + \ell_{nc}(t,\tau) + \ell_{cn}(t,\tau) + R_n(\tau) + \ell_n(t,\tau) \end{aligned} \tag{3.25}$$

where $n(t+\tau)\, c(t) = \ell_{nc}(t,\tau)$ and $c(t+\tau)\, n(t) = \ell_{cn}(t,\tau)$ do not contain any finite-strength additive sine-wave component and similarly for $\ell_n(t,\tau)$ in the decomposition $n(t+\tau)\, n(t) = R_n(\tau) + \ell_n(t,\tau)$.

The almost-periodically time-variant autocorrelation is given by:

$$\mathrm{E}^{\{\alpha\}}\{x(t+\tau)\,x(t)\} = R_n(\tau) + \frac{A_0^2}{2}\cos(2\pi f_0\tau) + \frac{A_0^2}{2}\cos(2\pi 2f_0 t + 2\pi f_0\tau + 2\phi_0) \tag{3.26}$$

and the autocovariance is given by:

$$\begin{aligned} & E^{\{\alpha\}}\left\{\left[x(t+\tau) - E^{\{\alpha\}}\{x(t+\tau)\}\right]\left[x(t) - E^{\{\alpha\}}\{x(t)\}\right]\right\} \\ & \quad = E^{\{\alpha\}}\{[x(t+\tau) - c(t+\tau)][x(t) - c(t)]\} \\ & \quad = E^{\{\alpha\}}\{n(t+\tau)n(t)\} = R_n(\tau) \end{aligned} \tag{3.27}$$

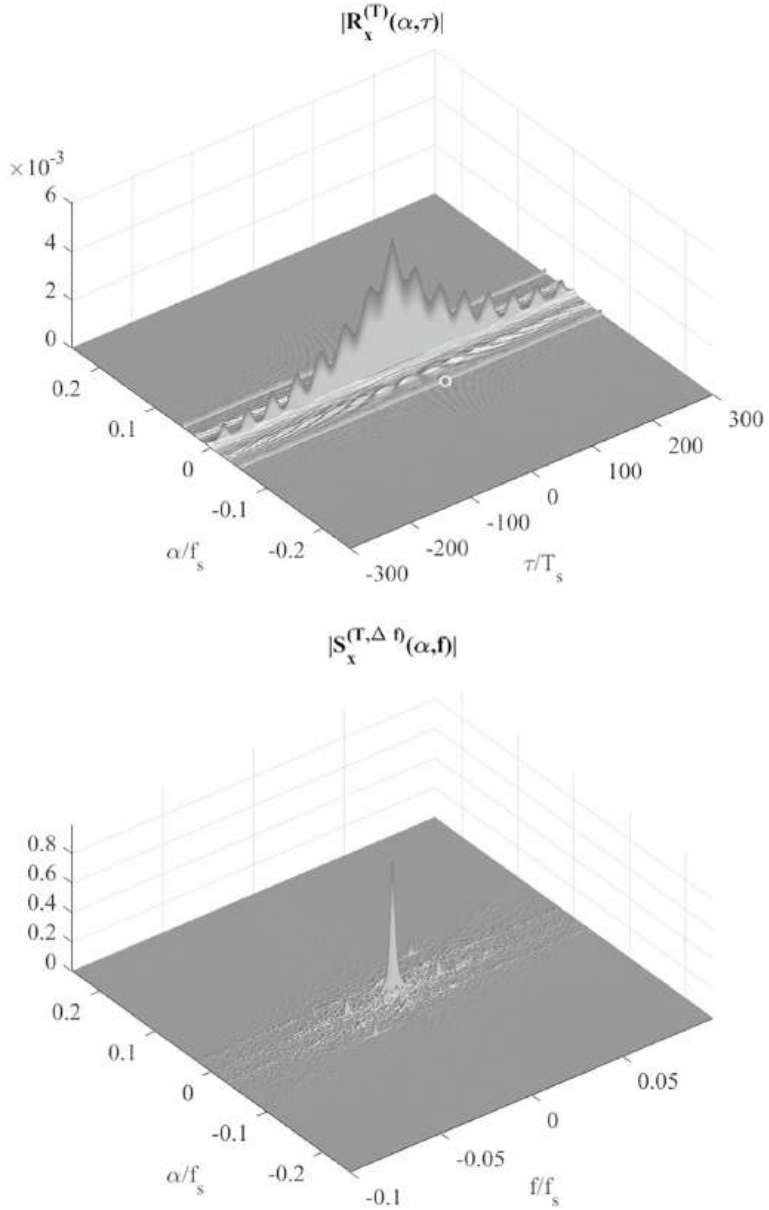

Fig. 6 Sine wave in additive colored Gaussian noise (SNR = −10 dB). (Top) Magnitude of the estimate of the cyclic autocorrelation as a function of the cycle frequency α and the lag parameter τ. (Bottom) Magnitude of the estimate of the cyclic spectrum as a function of the cycle frequency α and the spectral frequency f

Comparison of (3.26) and (3.27) reveals that while the autocorrelation function of the signal (2.24) is a periodic function of time, its autocovariance function does not depend on time. Therefore, for the signal (2.24), the second-order cyclostationarity, that is, the presence of finite-strength additive sine-wave components in the second-order lag-product, is due to only the products of the first-order sine waves present in $x(t)$. When such sine waves are canceled in computing the autocovariance, their effect in the second-order lag product vanishes. All the nonzero second-order cycle frequencies are impure second-order cycle frequencies.

In Fig. 6, (Top) the magnitude of the cyclic correlogram (3.22) as a function of α and τ and (Bottom) the magnitude of the frequency-smoothed cyclic periodogram (3.23) as a function of α and f are reported for the case SNR = −10 dB. The slice for $\alpha = 0$ in Fig. 6 (Top) corresponds to the first two terms in (3.26). A sine wave superimposed to an exponentially decaying shape can be recognized. Due to the low value of SNR, the peak-to-peak oscillation of the sine wave is small if compared with the maximum value of the exponentially decaying term and cyclic features at cycle frequencies $\alpha = \pm 2f_0$ have a small strength compared to that at $\alpha = 0$. Accordingly, four spikes whose magnitude is small compared to that of the low-pass component of the PSD are centered in the four points $(0, \pm f_0)$ and $(\pm 2f_0, 0)$ in the (α, f) plane (Fig. 6 (Bottom)). The shape of the spikes is equal to the shape of the magnitude of the frequency smoothing window.

In Fig. 7, (Top) the magnitude of the estimate of the cyclic autocovariance as a function of α and τ and (Bottom) the magnitude of the estimate of the second-order cyclic polyspectrum as a function of α and f are reported for the case SNR = −10 dB. Since all the nonzero second-order cycle frequencies are impure, no significant cyclic features can be recognized for $\alpha \neq 0$ in Fig. 7 (left and right). In addition, according to (3.27), the cyclic autocovariance at $\alpha = 0$ is constituted by only the exponentially decaying term and there is no added sinusoidal term.

In Fig. 8, (Top) the magnitude of the cyclic correlogram (3.22) as a function of α and τ and (Bottom) the magnitude of the frequency-smoothed cyclic periodogram (3.23) as a function of α and f are reported for the case SNR = 10 dB. In such a case, the strength of the sine wave is much bigger than that of the stationary noise. Therefore, the sinusoidal terms in (3.26) are predominant. As already observed, all the sine waves in the lag product waveform are impure. When the additive sine wave is removed in computing the covariance, the impure sine waves are removed and one obtains the cyclic autocovariance and cyclic second-order polyspectrum estimates in Fig. 9 (left and right) that are coincident with those in Fig. 7 (left and right). There are no cyclic features for $\alpha \neq 0$ since there is no pure second-order cyclostationarity.

The substantial odd-order harmonic content in the cyclic CDF and PDF (Sec. 2.3) is a result of the step discontinuity in the event indicator function of the sine wave plus noise whose sine-wave components are calculated. In contrast, the presence of only low-order harmonic content in the cyclic autocorrelation and cyclic spectrum reflects the smoothness of the nonlinear transformation of the data, the lag product, whose harmonic content is calculated.

3.6 Example 2 (cont'd): Sine wave with multiplicative noise

The second-order lag product of the signal (2.30) is:

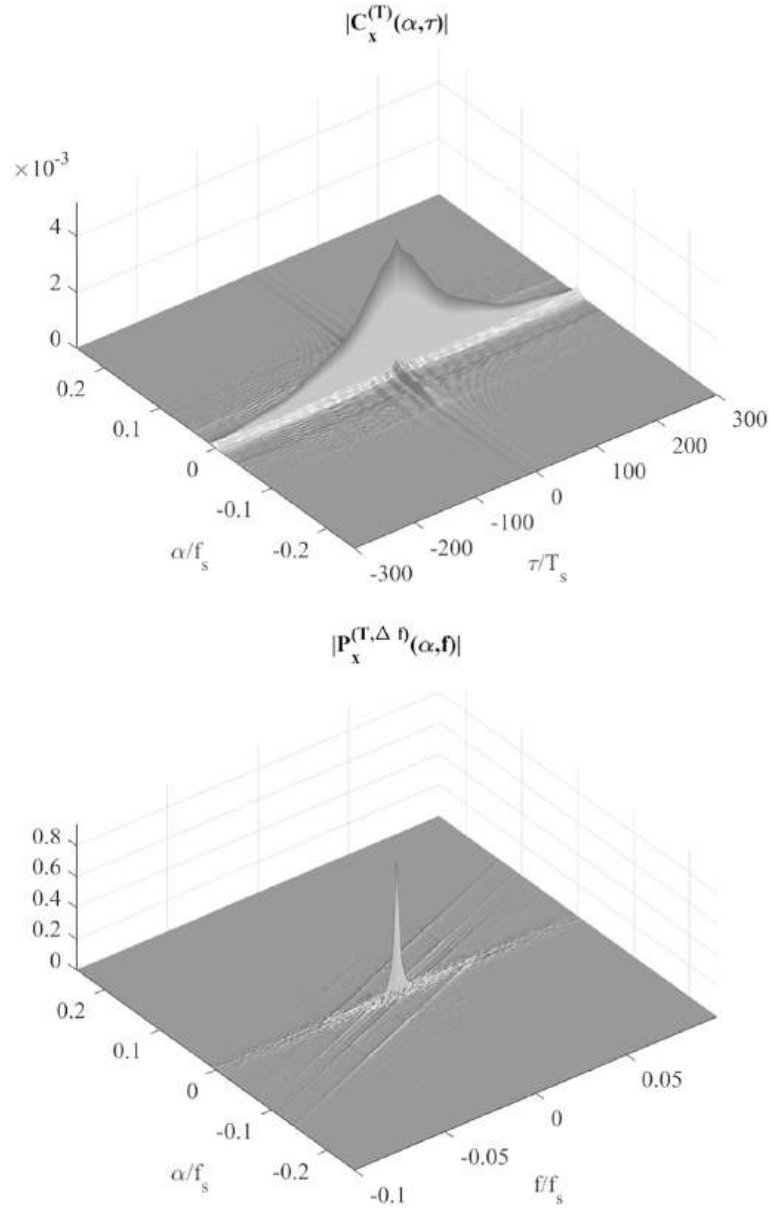

Fig. 7 Sine wave in additive colored Gaussian noise (SNR = −10 dB). (Top) Magnitude of the estimate of the cyclic autocovariance as a function of the cycle frequency α and the lag parameter τ. (Bottom) Magnitude of the estimate of the second-order cyclic polyspectrum as a function of the cycle frequency α and the spectral frequency f

$$\begin{aligned} x(t+\tau)\,x(t) &= c(t+\tau)\,c(t)\,n(t+\tau)\,n(t) \\ &= A_0^2\,\cos(2\pi f_0(t+\tau)+\phi_0)\,\cos(2\pi f_0 t+\phi_0)\,[R_n(\tau)+\ell_n(t,\tau)] \\ &= \frac{A_0^2}{2}\,R_n(\tau)\,[\cos(2\pi 2f_0 t+2\pi f_0\tau+2\phi_0)+\cos(2\pi f_0\tau)] \\ &\quad+\frac{A_0^2}{2}\,\ell_n(t,\tau)\,[\cos(2\pi 2f_0 t+2\pi f_0\tau+2\phi_0)+\cos(2\pi f_0\tau)] \end{aligned} \tag{3.28}$$

and its almost-periodically time-variant autocorrelation is given by:

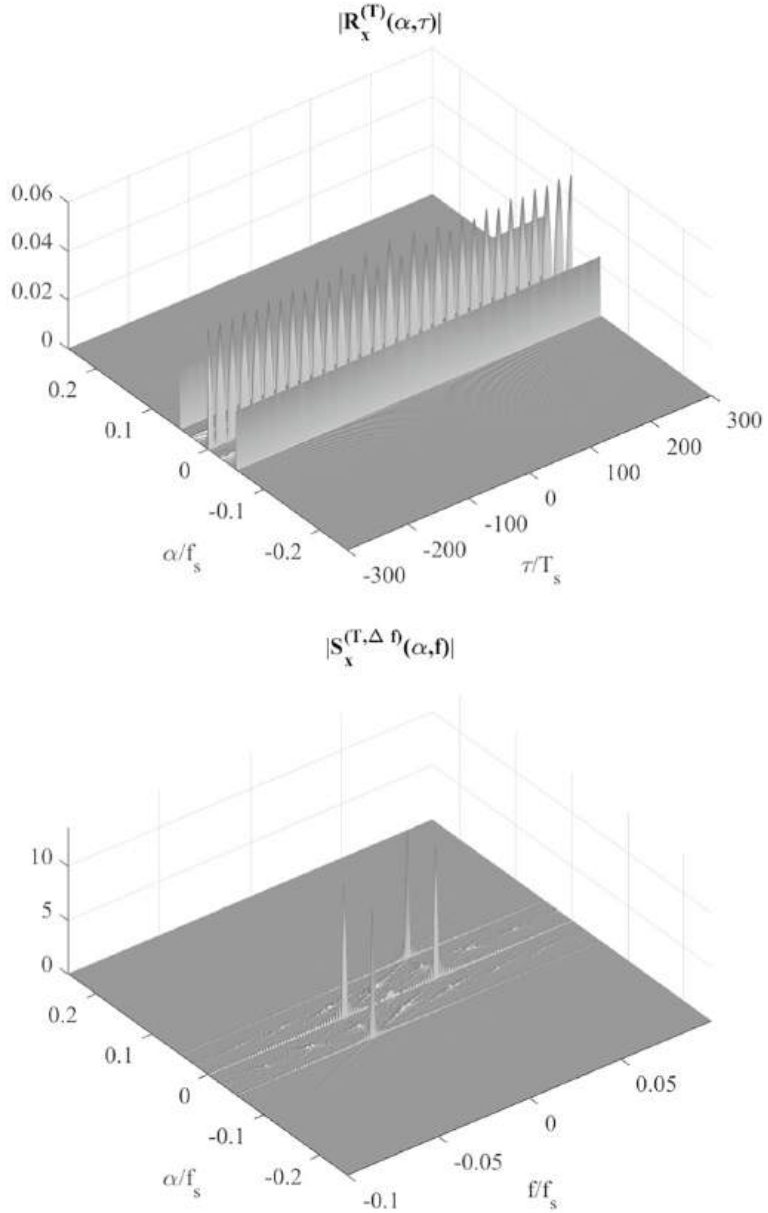

Fig. 8 Sine wave in additive colored Gaussian noise (SNR = 10 dB). (Top) Magnitude of the estimate of the cyclic autocorrelation as a function of the cycle frequency α and the lag parameter τ. (Bottom) Magnitude of the estimate of the cyclic spectrum as a function of the cycle frequency α and the spectral frequency f

$$\mathrm{E}^{\{\alpha\}}\{x(t+\tau)\,x(t)\} = \frac{A_0^2}{2} R_n(\tau)\,[\cos(2\pi 2f_0 t + 2\pi f_0 \tau + 2\phi_0) + \cos(2\pi f_0 \tau)]\,. \quad (3.29)$$

Since $\mathrm{E}^{\{\alpha\}}\{x(t)\} = 0$, the almost-periodically time-variant autocovariance is coincident with the almost-periodically time-variant autocorrelation. Consequently, unlike the case of signal (2.24), for the signal (2.30), the second-order cyclostationarity, that is, the presence of finite-strength additive sine-wave components in the second-order lag-product, is not due to products of the first-order sine waves present in $x(t)$ and is entirely

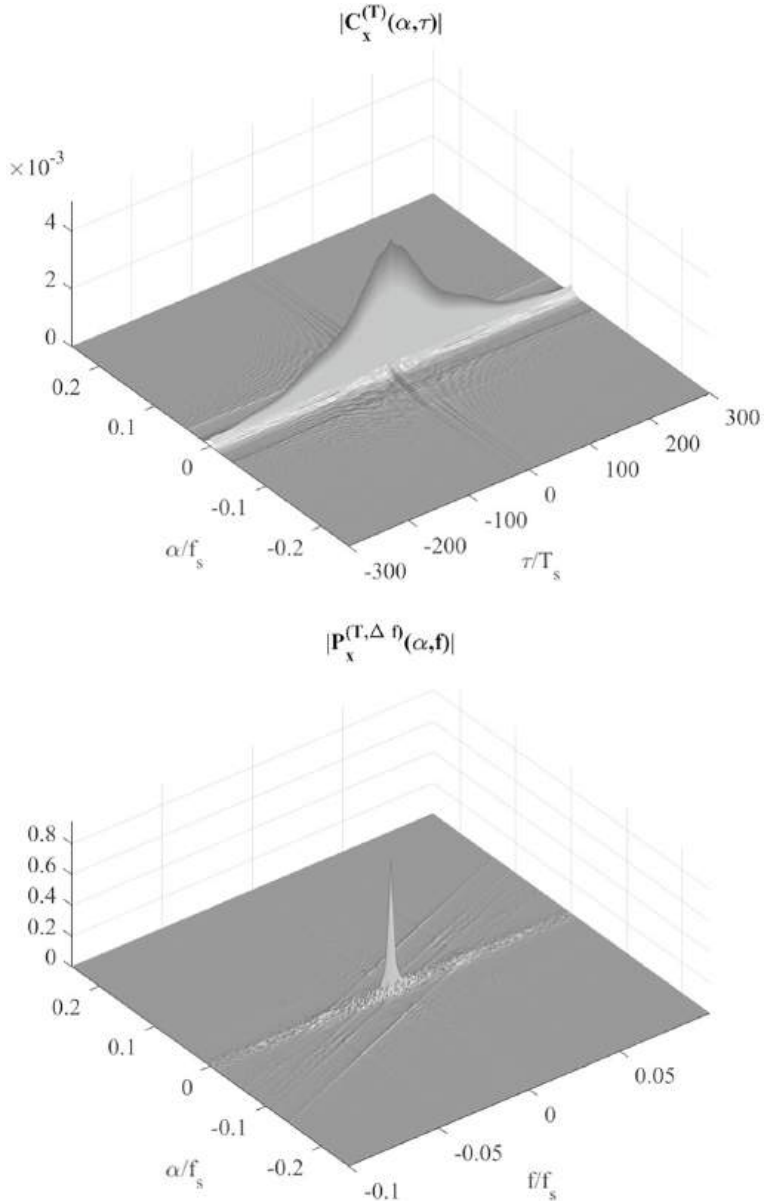

Fig. 9 Sine wave in additive colored Gaussian noise (SNR = 10 dB). (Top) Magnitude of the estimate of the cyclic autocovariance as a function of the cycle frequency α and the lag parameter τ. (Bottom) Magnitude of the estimate of the second-order cyclic polyspectrum as a function of the cycle frequency α and the spectral frequency f

generated by the lag-product of the zero-mean residual term. That is, all the second-order sine waves are pure second-order sine waves.

In Fig. 10, (Top) the magnitude of the estimate of the cyclic correlogram as a function of α and τ and (Bottom) the magnitude of the frequency-smoothed cyclic periodogram as a function of α and f are reported. Since all the second-order sine waves are pure, the estimates of the cyclic autocovariance and the second-order cyclic polyspectrum (Figs. 11) are coincident with those of the cyclic autocorrelation and the cyclic spectrum (Fig. 10), respectively. The slight difference is due to the bias introduced by the median

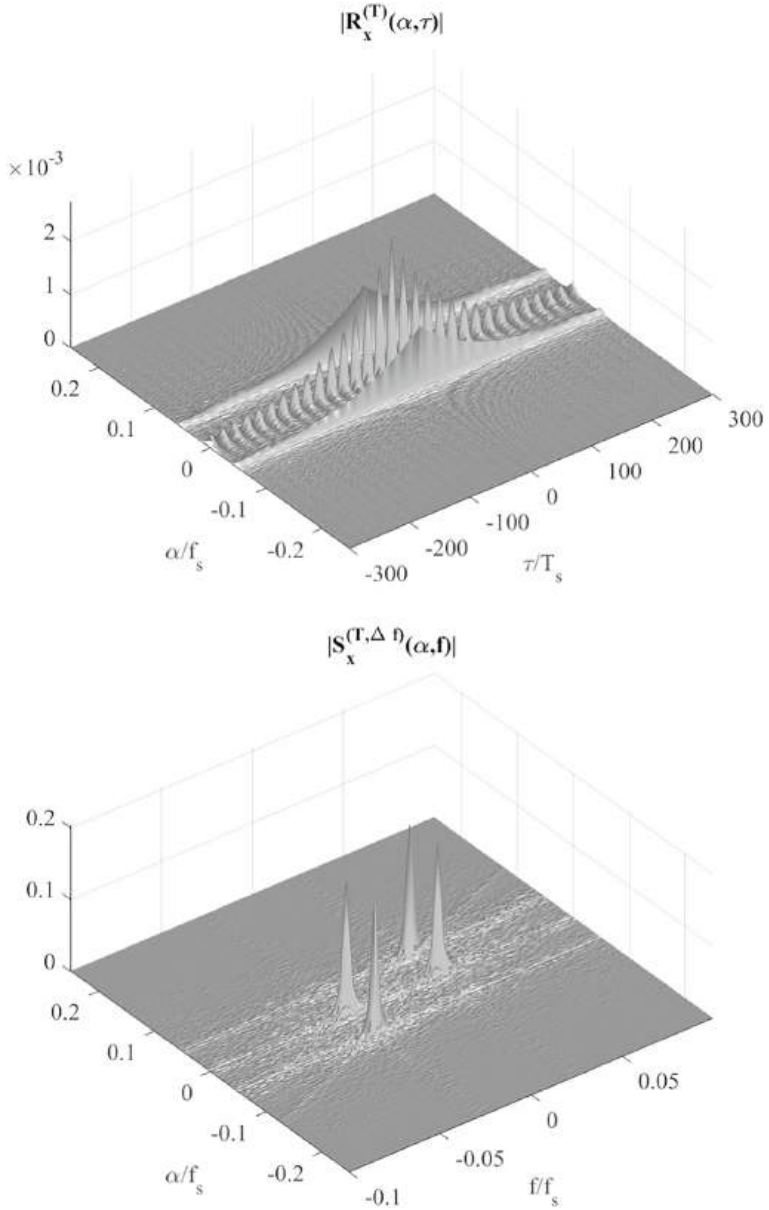

Fig. 10 Sine wave with multiplicative colored Gaussian noise. (Top) Magnitude of the estimate of the cyclic autocorrelation as a function of the cycle frequency α and the lag parameter τ. (Bottom) Magnitude of the estimate of the cyclic spectrum as a function of the cycle frequency α and the spectral frequency f

filtering adopted for the cyclic polyspectrum estimation [89, 84, Sec. 5.2.5]. Since the colored Gaussian noise has practically finite memory, all the cyclic autocorrelations of $x(t)$ decay to zero for large $|\tau|$ and the cyclic spectra do not contain impulses.

As in Example 1, the cyclic CDF contains more harmonics than the cyclic autocorrelation and cyclic spectrum since the lag product is a nonlinear transformation of the data that is smoother than the event indicator function.

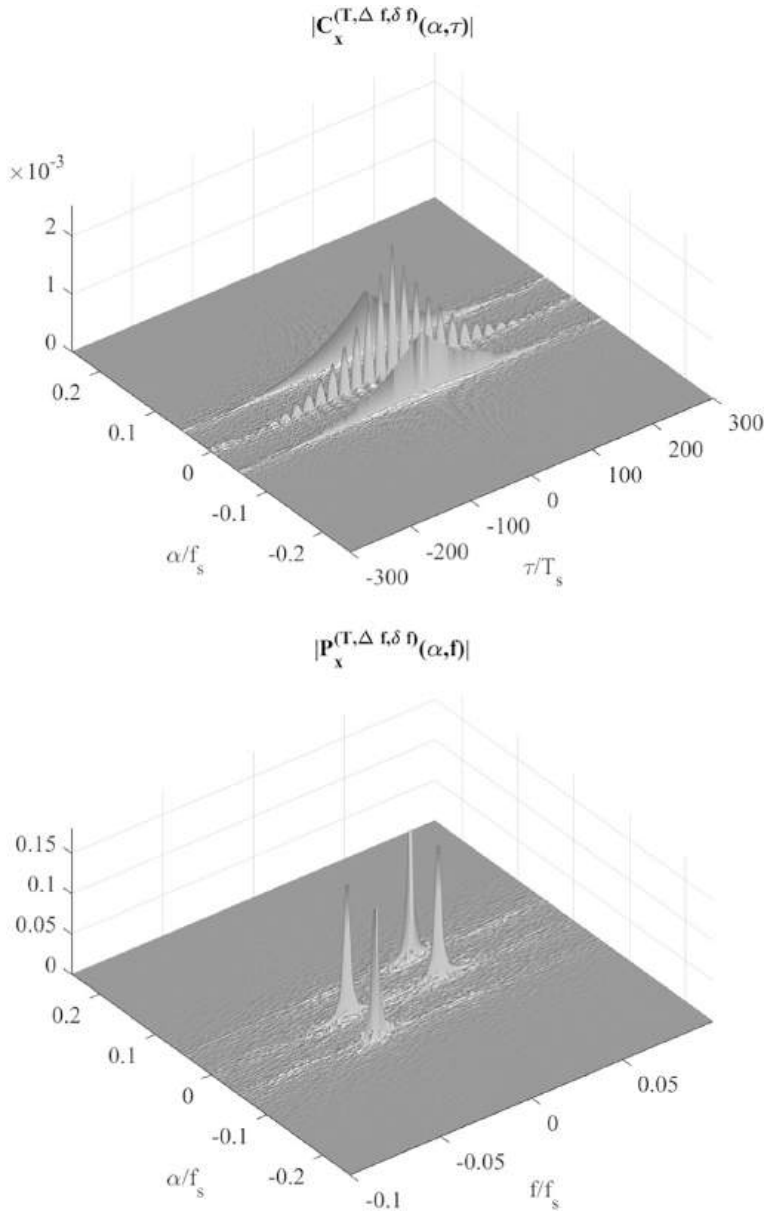

Fig. 11 Sine wave with multiplicative colored Gaussian noise. (Top) Magnitude of the estimate of the cyclic autocovariance as a function of the cycle frequency α and the lag parameter τ. (Bottom) Magnitude of the estimate of the second-order cyclic polyspectrum as a function of the cycle frequency α and the spectral frequency f

3.7 Example 3: The cyclic spectrum is richer than the PSD

Let us consider a band-pass wide-sense stationary signal generated by filtering white Gaussian noise $w(t)$ by a band-pass LTI system (Fig. 12):

$$x(t) = w(t) \otimes h_{\text{bp}}(t) \tag{3.30}$$

where $h_{\text{bp}}(t)$ is the impulse-response function of the band-pass LTI filter with harmonic response $H_{\text{bp}}(f) = [H(f - f_0) + H(f + f_0)]/2$, with $H(f)$ and f_0 the same as in Example 2 (Sec. 2.4).

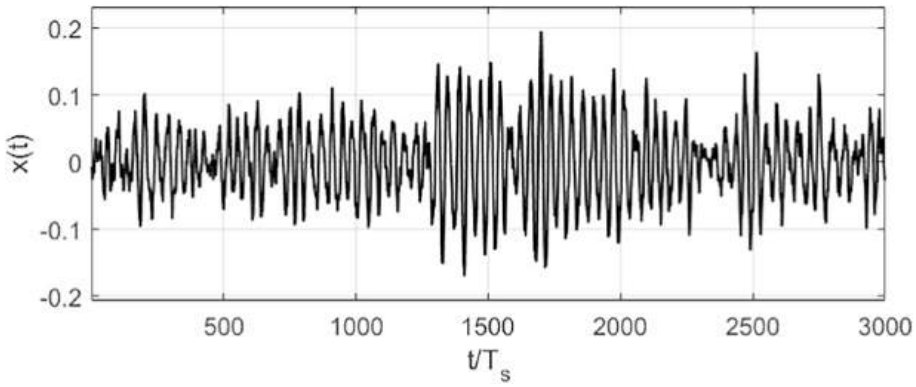

Fig. 12 Band-pass wide-sense stationary Gaussian signal

The signal (3.30) and that in Example 2 have very similar temporal behavior (compare Figs. 4 and 12) and practically the same time-averaged autocorrelation function and PSD (Fig. 13). The two estimated PSDs differ only around $f = 0$ where, however, the PSD level is more than 20 dB below the main peak level.

From the analysis of the temporal behavior and the estimates of the time-averaged autocorrelation function and PSD, one could infer that these two signals have the same statistical characteristics. These signals, however, are generated by two completely different mechanisms. The signal in Example 2 is generated by a linear periodically time-variant filtering (the modulation operation at frequency f_0) of a wide-sense stationary colored noise $n(t)$. Thus, it is second-order cyclostationary with nonzero cycle frequencies $\alpha = \pm 2f_0$. In contrast, the signal (3.30) is obtained by LTI filtering a wide-sense stationary signal and, hence, it is in turn wide-sense stationary. The PSD analysis does not enlighten such a difference and does not allow one to discover, for the signal of Example 2, the existence of a periodic phenomenon in its generation. That is, the PSD analysis does not allow one to discover the hidden periodicity. In contrast, the estimates of the cyclic autocorrelation in the (α, τ) plane and the cyclic spectrum in the (α, f) plane clearly show the difference between the two signals. The sine wave with multiplicative noise (Example 2) is cyclostationary and significant cyclic features are present at $\alpha = \pm 2f_0$ (Fig. 10). The signal (3.30) is wide-sense stationary and significant features are present only at $\alpha = 0$ (Fig. 14).

The parallel straight lines extending between the lower left and upper right quadrants in some of the bottom figures with figure numbers ranging from 6 to 14 and most predominantly in Figs. 7, 8, and 9 are artifacts of the spectral estimation method and are emphasized by the median filtering of the frequency-smoothed cyclic periodogram adopted to estimate the second-order cyclic polyspectrum [89].

3.8 Example 4: Pure and impure second-order sine waves

3.8.1 Case a

Let us consider the signal

$$x(t) = n(t)\ \cos(2\pi f_0 t + \phi_0) + A_1\ \cos(2\pi f_0 t + \phi_1)\,. \tag{3.31}$$

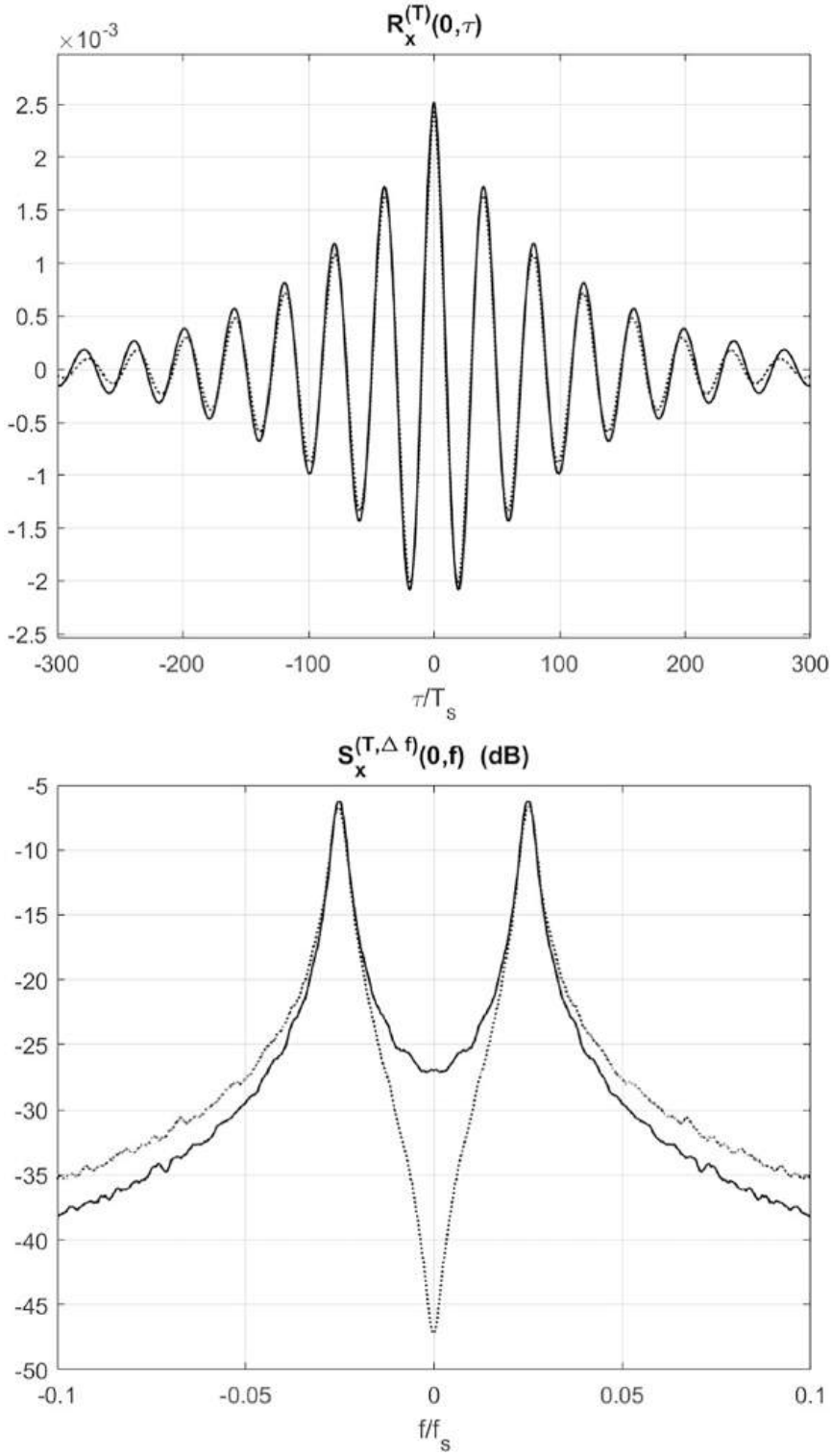

Fig. 13 Sine wave with multiplicative noise (solid line) versus band-pass wide-sense stationary Gaussian signal (dotted line). (Top) Estimate of the autocorrelation function as a function of the lag parameter τ. (Bottom) Estimate of the PSD as a function of the spectral frequency f

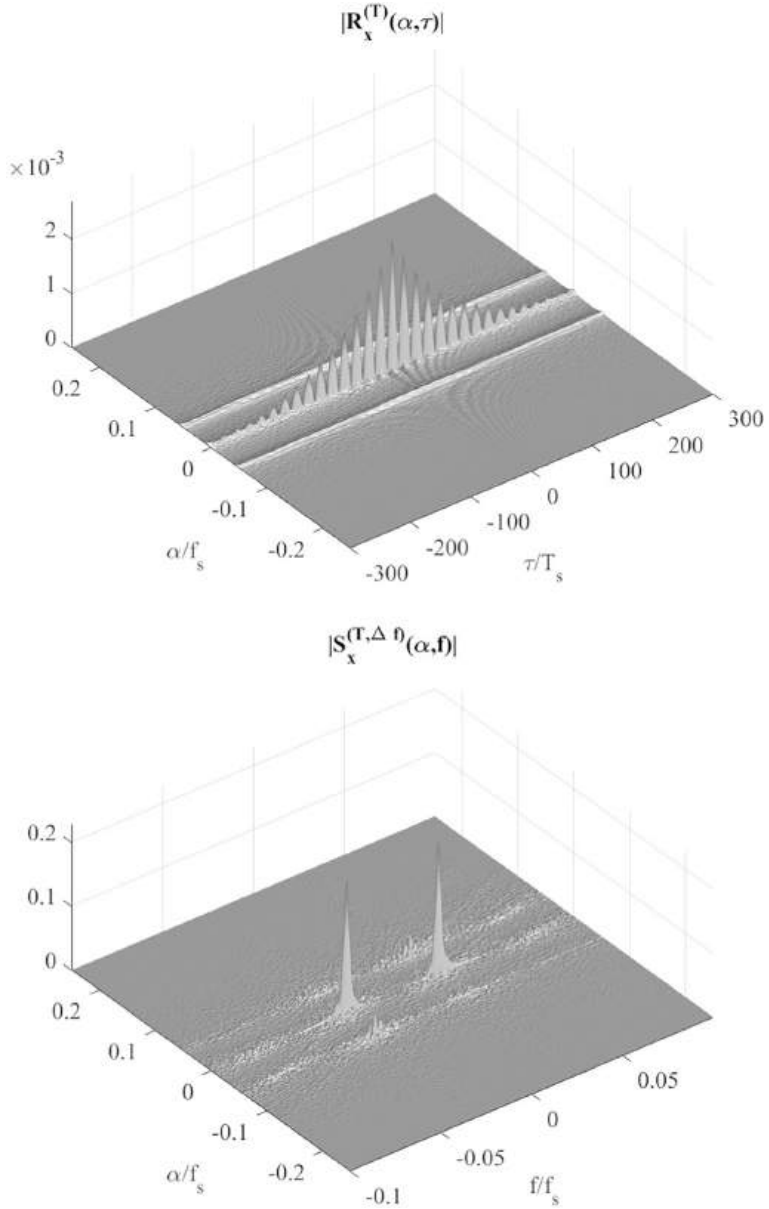

Fig. 14 Band-pass wide-sense stationary Gaussian noise. (Top) Magnitude of the estimate of the cyclic autocorrelation as a function of the cycle frequency α and the lag parameter τ. (Bottom) Magnitude of the estimate of the cyclic spectrum as a function of the cycle frequency α and the spectral frequency f

Sine waves at cycle frequencies $\pm 2f_0$ present in the second-order lag product have a portion which is a pure second-order sine wave and another portion which is an impure second-order sine wave. Such a situation is found in some vibroacoustic signals in mechanics [58, 59] and in the underlying cyclostationary signal in the electrocardiogram (ECG) signal [86].

3.8.2 Case b

Let us consider the signal

$$x(t) = n(t)\ \cos(2\pi f_0 t + \phi_0) + A_1\ \cos(2\pi f_1 t + \phi_1) \tag{3.32}$$

where f_0 and f_1 are incommensurate.

The second-order lag-product waveform contains finite-strength additive sine waves with frequencies $\alpha \in \{\pm 2f_0, \pm 2f_1\}$. Sine waves at frequencies $\alpha = \pm 2f_0$ are pure second-order sine waves. Frequencies $\alpha/2$ are not present at first-order and frequencies α are present in the Fourier series expansion of both autocorrelation and autocovariance. Sine waves at frequencies $\alpha = \pm 2f_1$ are impure second-order cycle frequencies. Frequencies $\alpha/2$ are present at first-order and frequencies α are present in the Fourier series expansion of the autocorrelation but not of the autocovariance.

4 Higher-order cyclostationarity

There are time series for which the hidden periodicity cannot be regenerated by a second-order nonlinear transformation but rather, by a higher-than-second-order transformation. For example, in communications, by a quadratic nonlinearity no cycle frequencies related to the baud rate can be generated for a pulse-amplitude-modulated (PAM) signal with bandwidth equal to the Nyquist rate and no cycle frequencies related to the carrier frequency can be generated for a balanced quadrature-phase-shift-keyed (QPSK) signal. For such signals, cycle frequencies can be generated by adopting a fourth-order nonlinear transformation of the signal [49]. Furthermore, there are signals that exhibit the same second-order cyclic statistical functions but that can be distinguished on the basis of their higher-order cyclostationarity properties [111]. In order to exploit the benefits of the spectral line generation also for this class of signals, the second-order theory of cyclostationary time-series has been extended to higher-orders in [49, 112]. See also [80, 84, Chap. 4].

4.1 Higher-order spectral line generation

The Nth-order temporal moment function is defined as the almost-periodic component of the Nth-order lag product waveform, which is the product of N time-shifted versions of a time series. The Fourier coefficients of its (generalized) Fourier series expansion are referred to as the Nth-order cyclic temporal moment functions. As first shown in [48] and then, in more detail, in [49], the *Nth-order cyclic temporal cumulant function* at cycle frequency α of a time series provides a mathematical characterization of the notion of a *pure Nth-order sine wave*. It is the higher-order generalization of the definition given at second order in Sec. 3.2 and illustrated in the Examples of Secs. 3.5 and 3.8. The pure Nth-order sine wave is that part of the sine wave at frequency α present in the Nth-order lag product waveform that remains after removal of all parts that result from products of sine waves in lower order lag products obtained by factoring the Nth-order product. In contrast, the *impure Nth-order sine wave* is the entire sine wave with frequency α that is contained in the Nth-order lag product. Its amplitude and phase are the magnitude and phase of the *Nth-order cyclic temporal moment function*

$$R_{\boldsymbol{x}}^{\alpha}(\boldsymbol{\tau}) \triangleq \left\langle \prod_{i=1}^{N} x(t+\tau_i)\, e^{-j2\pi\alpha t} \right\rangle_t \tag{4.1}$$

where $\boldsymbol{x}$ denotes the vector of N time-shifted versions of $x(t)$, that is, $\boldsymbol{x} \triangleq [x(t+\tau_1), \ldots, x(t+\tau_N)]^{\mathsf{T}}$, and $\boldsymbol{\tau} \triangleq [\tau_1, \ldots, \tau_N]^{\mathsf{T}}$.

The temporal moments and cumulants of $\boldsymbol{x}$ are linked by the formulas [49]

$$\mathcal{C}_{\boldsymbol{x}}(t, \boldsymbol{\tau}) = \sum_{\mathsf{P}} \left[(-1)^{p-1}(p-1)! \prod_{i=1}^{p} \mathcal{R}_{\boldsymbol{x}_{\mu_i}}(t, \boldsymbol{\tau}_{\mu_i}) \right] \tag{4.2}$$

$$\mathcal{R}_{\boldsymbol{x}}(t, \boldsymbol{\tau}) = \sum_{\mathsf{P}} \left[\prod_{i=1}^{p} \mathcal{C}_{\boldsymbol{x}_{\mu_i}}(t, \boldsymbol{\tau}_{\mu_i}) \right] \tag{4.3}$$

where P is the set of distinct partitions of $\{1, ..., N\}$, each constituted by the subsets $\{\mu_i,\ i = 1, ..., p\}$, $|\mu_i|$ is the number of elements in μ_i, $\boldsymbol{x}_{\mu_i}$ is the $|\mu_i|$-dimensional vector whose components are those of $\boldsymbol{x}$ having indices in μ_i. Equations (4.2) and (4.3) are the FOT counterparts of the Leonov and Shiryaev formulas [71] for stochastic moments and cumulants. That is, (4.2) and (4.3) are the same as the Leonov and Shiryaev formulas obtained by replacing the ensemble average with the almost-periodic component extraction operator. In (4.2) and (4.3), $\mathcal{R}_{\boldsymbol{x}_{\mu_i}}(t, \boldsymbol{\tau}_{\mu_i})$ and $\mathcal{C}_{\boldsymbol{x}_{\mu_i}}(t, \boldsymbol{\tau}_{\mu_i})$ are the temporal moment and cumulant functions, respectively, of the time-shifted time series $x_\ell(t + \tau_\ell)$ with $\ell \in \mu_i$.

Estimators of higher-order cyclic statistical functions are presented and discussed in [112, 84, Sec. 5.7]. Results in the stochastic approach are presented in [25–27]. Estimation in the presence of non-Gaussian noise is addressed in [126].

The extension to complex-valued signals of the above definitions of temporal moment and cumulant functions is obtained by considering an optional complex conjugation for each of the complex-valued time-shifted signals $x(t + \tau_i)$ [112, 84, Chap. 4]. Thus, 2^{N-1} different conjugation configurations can be considered. In general, at a given order, communication signals exhibit different cyclostationarity properties for different conjugation configurations. The strength of the cyclic features at second- and higher-orders for the several conjugation configurations constitutes a kind of finger print of the modulation format and can be suitably exploited for modulation format classification [111].

4.2 Example 5: Spectral-line generation by fourth-order nonlinearity

Let us consider a pulse-amplitude-modulated (PAM) signal $x_{\mathrm{PAM}}(t)$ with binary white modulating sequence, full duty-cycle rectangular pulse, and bit period T_0. Let $x(t)$ be a version of such a PAM signal filtered by a strictly band-limited low-pass filter with monolateral bandwidth equal to $0.45\ \alpha_0$, where $\alpha_0 = 1/T_0$ is the smallest (in magnitude) nonzero cycle frequency of the PAM signal [39, Sec. 12.D], [84, Sec. 7.3].

For a linear time-invariant (LTI) system with input and output signals $x_{\mathrm{PAM}}(t)$ and $x(t)$, respectively, the input/output relationship in terms of cyclic spectra is [39, Sec. 11.D], [84, Sec. 3.2.2]

$$S_x^{\alpha}(f) = S_{x_{\mathrm{PAM}}}^{\alpha}(f)\, H(f)\, H^*(f - \alpha) \tag{4.4}$$

where $H(f)$ is the harmonic-response function of the filter.

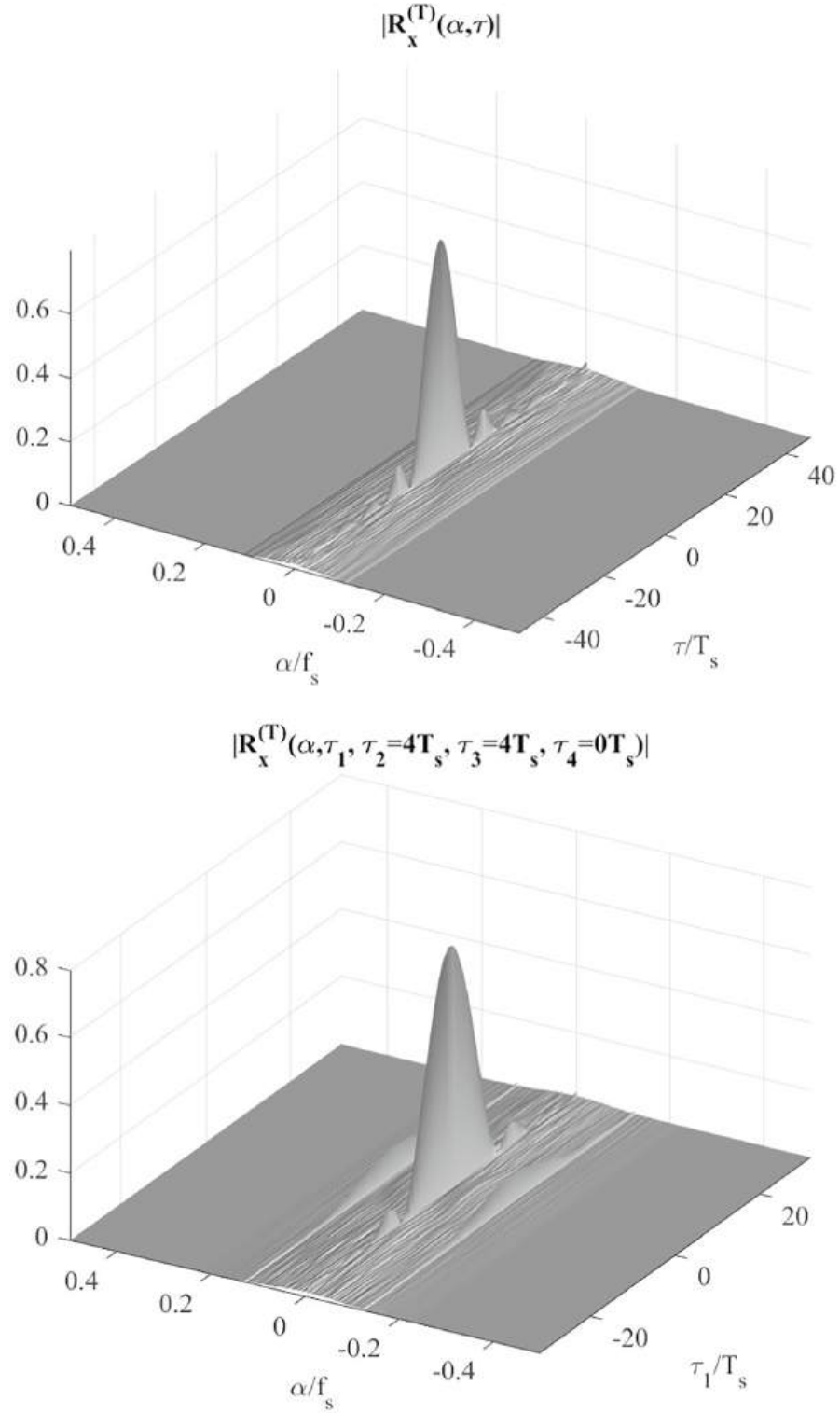

Fig. 15 Filtered PAM signal. (Top) Magnitude of the estimate of the cyclic autocorrelation as a function of the cycle frequency α and the lag parameter τ. (Bottom) Magnitude of the estimate of a slice of the the fourth-order cyclic temporal moment function as a function of the cycle frequency α and the lag parameter τ_1

Since the bilateral bandwidth of the considered filter is less than the smallest (in magnitude) nonzero cycle frequency of the input signal $x_{\mathrm{PAM}}(t)$, the supports of $H(f)$ and its frequency-shifted version $H^*(f-\alpha)$ in (4.4) do not overlap for $\alpha \neq 0$. That is, the output signal $x(t)$ does not exhibit second-order cyclostationarity (Fig. 15 (Top)). In contrast, the hidden periodicity can be generated by considering the fourth-order lag product. That is, the signal $x(t)$ exhibits fourth-order cyclostationarity (Fig. 15 (Bottom)).

5 Irregular cyclicity

In contrast to the examples given up to this point, there are other ways that periodicity can become hidden in a time series. That is, instead of, or in addition to, the mixing of random fluctuations with periodicity, there are situations in which time variation of a quantity is non-periodic because otherwise periodic behavior has been subjected to time warping. Yet, it is possible in some situations to perform de-warping, thereby uncovering otherwise hidden periodicity.

Let

$$y(t) = x(\psi(t)) \tag{5.1}$$

be a time-warped version of the ACS signal $x(t)$, where $\psi(t)$ is an invertible time-warping function with inverse $\varphi(t) = \psi^{-1}(t)$. Starting from the decomposition (3.4) for the lag product of the underlying ACS signal $x(t)$, one obtains the following decomposition for the lag product of $y(t)$

$$y(t+\tau)\, y(t) = x(\psi(t+\tau))\, x(\psi(t)) \tag{5.2a}$$

$$= \sum_{\alpha \in \mathcal{A}} R_x^{\alpha}(\psi(t+\tau) - \psi(t)) e^{j2\pi\alpha\psi(t)} + \ell_x(\psi(t), \psi(t+\tau) - \psi(t)) \tag{5.2b}$$

The ACS signal $x(t)$ presents hidden periodicities that can be generated by appropriate nonlinear transformations (Secs. 2, 3, 4). However, the time-warping transforms regular paces into irregular ones. The analysis and characterization of time-warped ACS time series is made in [43, 83, 87]. Other approaches are proposed in [74, 75]. Models with irregular cyclicities have been considered for the electrocardiogram (ECG) signal [86], the electroencephalogram (EEG) signal [94], signals of mechanical machinery [113], astrophysics signals [28], signals reflected by accelerating targets [77, 78], underwater communication signals [110], and heavy-tailed data [90]. The modifications of the almost-cyclostationarity properties of the transmitted signal due to relative motion (with general motion law) between transmitter and receiver are analyzed in [81, Chap. 7].

5.1 Cyclostationarity restoral

Let us assume that $x(t)$ exhibits cyclostationarity with at least one cycle frequency α_0. In [43], estimates $\widehat{\psi}$ or $\widehat{\varphi} = \widehat{\psi}^{-1}$ of ψ or ψ^{-1} are determined such that, for the recovered signal $x_\varphi(t) = y(\widehat{\varphi}(t))$, the amplitude of the complex sine wave at frequency α_0 contained in the second-order lag-product $x_\varphi(t+\tau)\, x_\varphi^{(*)}(t)$ is maximized.

Let $\{c_k(t)\}_{k=1,\ldots,K}$ be a set of (not necessarily orthonormal) functions. Two procedures are proposed in [43]:

Procedure a) Consider the expansion

$$\widehat{\varphi}(t) = \widehat{\psi}^{-1}(t) = \mathbf{a}^{\mathsf{T}}\mathbf{c}(t) \tag{5.3}$$

where $\mathbf{c}(t) = [c_1(t), \ldots, c_K(t)]^{\mathsf{T}}$ and $\mathbf{a} = [a_1, \ldots, a_K]^{\mathsf{T}}$ and maximize with respect to $\mathbf{a}$ the objective function

$$J_a(\mathbf{a}) = \left|\widehat{R}^{\alpha_0}_{x_\varphi}(\tau; \mathbf{a})\right|^2 \tag{5.4}$$

with $\widehat{R}^{\alpha_0}_{x_\varphi}(\tau; \mathbf{a})$ an estimate of the cyclic autocorrelation of the de-warped signal $x_\varphi(t) = y(\mathbf{a}^{\mathsf{T}}\mathbf{c}(t))$

$$\hat{R}^{\alpha_0}_{x_\varphi}(\tau; \mathbf{a}) \triangleq \frac{1}{T}\int_{t_0}^{t_0+T} x_\varphi(t+\tau)x_\varphi^{(*)}(t)e^{-j2\pi\alpha_0 t}\,\mathrm{d}t \tag{5.5a}$$

$$= \frac{1}{T}\int_{t_0}^{t_0+T} y(\mathbf{a}^{\mathsf{T}}\mathbf{c}(t+\tau))\, y^{(*)}(\mathbf{a}^{\mathsf{T}}\mathbf{c}(t))\, e^{-j2\pi\alpha_0 t}\,\mathrm{d}t \tag{5.5b}$$

Procedure b) Consider the expansion

$$\widehat{\psi}(t) = \mathbf{b}^{\mathsf{T}}\mathbf{c}(t) \tag{5.6}$$

where $\mathbf{b} = [b_1, \ldots, b_K]^{\mathsf{T}}$ and maximize with respect to $\mathbf{b}$ the objective function

$$J_b(\mathbf{b}) = \left|\widehat{R}^{\alpha_0}_{x_\varphi}(\tau; \mathbf{b})\right|^2 \tag{5.7}$$

with

$$\widehat{R}^{\alpha_0}_{x_\varphi}(\tau; \mathbf{b}) = \frac{1}{T}\int_{\widehat{\varphi}(t_0)}^{\widehat{\varphi}(t_0+T)} y(u + \Delta^{\tau}_{\varphi}[\widehat{\varphi}^{-1}(u)])\, y^{(*)}(u)\, e^{-j2\pi\alpha_0\widehat{\varphi}^{-1}(u)}\, \dot{\widehat{\varphi}}^{-1}(u)\,\mathrm{d}u \tag{5.8a}$$

$$\simeq \frac{1}{T}\int_{t_0}^{t_0+T} y(u + \tau/\mathbf{b}^{\mathsf{T}}\dot{\mathbf{c}}(u))\, y^{(*)}(u)\, e^{-j2\pi\alpha_0\mathbf{b}^{\mathsf{T}}\mathbf{c}(u)}\, \mathbf{b}^{\mathsf{T}}\dot{\mathbf{c}}(u)\,\mathrm{d}u \tag{5.8b}$$

where (5.8a) is obtained from (5.5a) by the variable change $u = \widehat{\varphi}(t)$ and

$$\begin{aligned}\Delta^{\tau}_{\varphi}[\hat{\varphi}^{-1}(u)] &\triangleq \hat{\varphi}[\hat{\varphi}^{-1}(u) + \tau] - \hat{\varphi}[\hat{\varphi}^{-1}(u)] \\ &\simeq \tau[1/\dot{\widehat{\varphi}}^{-1}(u)] = \tau/\mathbf{b}^{\mathsf{T}}\dot{\mathbf{c}}(u)\end{aligned} \tag{5.9}$$

In (5.8b) and (5.9), the dot denotes first-order derivative.

The value of the vector $\mathbf{a}$ or $\mathbf{b}$ that maximizes the corresponding objective function is taken as an estimate of the coefficient vector for the expansion of $\widehat{\varphi}(t) = \widehat{\psi}^{-1}(t)$ or $\widehat{\psi}(t)$. The maximization can be performed by a gradient-ascent algorithm, with starting points throughout a sufficiently fine grid. The Barzilai–Borwein step size sequence [6] is used since it provides fast convergence for many kinds of objective functions. In both cases a) and b), the gradient of the objective function must be computed whose expressions are provided in [43]. Several important design parameters are discussed in [43].

5.2 Warping function compensation and estimation by angle demodulation

Let us consider the warping function

$$\psi(t) = t + \epsilon(t) \tag{5.10}$$

with $\epsilon(t)$ slowly varying, that is,

$$\sup_t \left| \dot{\epsilon}(t) \right| \ll 1 \,. \tag{5.11}$$

In such a case, it can be shown [83] that the lag product is closely approximated by:

$$y(t+\tau)\, y(t) \simeq \sum_{\alpha \in \mathcal{A}} e^{j2\pi\alpha\epsilon(t)}\, R_{\boldsymbol{x}}^{\alpha}(\tau)\, e^{j2\pi\alpha t} + \ell_x(t+\epsilon(t), \tau + \epsilon(t+\tau) - \epsilon(t)) \,. \tag{5.12}$$

That is, $y(t)$ is a modulated cyclical (MC) signal [82, 94, Sec. 6.2.2] with "modulating function" $m_{\boldsymbol{x}}^{\alpha}(t) \equiv m^{\alpha}(t) = e^{j2\pi\alpha\epsilon(t)}$ (independent of $x(t)$).

Two methods are proposed in [83] for estimating the function $\epsilon(t)$.

The first one considers the expansion

$$\widehat{\epsilon}(t) = \mathbf{e}^{\mathsf{T}} \mathbf{c}(t) \tag{5.13}$$

where $\mathbf{e} = [e_1, \ldots, e_K]^{\mathsf{T}}$ and provides estimates of the coefficients e_k by maximizing with respect to $\mathbf{e}$ the objective function

$$J_e(\mathbf{e}) \triangleq \int_{\mathcal{T}} \left| \widehat{R}_y^{(T)}(\alpha_0, \tau; \mathbf{e}) \right|^2 \mathrm{d}\tau \tag{5.14}$$

where

$$\widehat{R}_y^{(T)}(\alpha_0, \tau; \mathbf{e}) \triangleq \frac{1}{T} \int_{-T/2}^{T/2} y(t+\tau)\, y(t)\, e^{-j2\pi\alpha_0 t}\, e^{-j2\pi\alpha_0 \mathbf{e}^{\mathsf{T}}\mathbf{c}(t)} \mathrm{d}t \tag{5.15}$$

and $\mathcal{T}$ is a set of values of τ where $R_{\mathbf{x}}^{\alpha_0}(\tau)$ is significantly nonzero. The maximization can be performed by a gradient ascent algorithm, similarly to the approach in Sec. 5.1. The estimated coefficients are such that the additive-phase factor $e^{j2\pi\alpha_0\epsilon(t)}\, e^{j2\pi\alpha_0 t}$ in the first term of the lag-product of $y(t)$ (5.12) is compensated in (5.14) by using (5.15).

For the second method [83, 84, Sec. 14.3.3], let us define

$$z^{(\alpha_0, W)}(t, \tau) \triangleq \left[y(t+\tau)\, y(t)\, e^{-j2\pi\alpha_0 t} \right] \otimes h_W(t) \tag{5.16}$$

with $h_W(t)$ the impulse-response function of a low-pass filter with monolateral bandwidth W such that

$$B(\alpha_0) < W < \inf_{\substack{\alpha \in \mathcal{A} \\ \alpha \neq \alpha_0}} \left(|\alpha - \alpha_0| - B(\alpha) \right) \tag{5.17}$$

where $B(\alpha)$ is the monolateral bandwidth of $w(t) = e^{j2\pi\alpha\epsilon(t)}$. Thus, for the frequency-shifted waveform $y(t+\tau)\, y(t)\, e^{-j2\pi\alpha_0 t}$, which—by (5.12)—contains spectral content of width $B(\alpha)$ centered at frequency $\alpha - \alpha_0$ for all cycle frequencies α exhibited by $x(t)$, only the spectral content centered at 0 would be passed by the low-pass filter. This implies

that for sufficiently narrow bandwidth W (i.e., sufficiently long integration time), subject to the left inequality in (5.17), the filtered waveform (5.16) also would contain only the spectral content centered at 0: $z^{(\alpha_0,W)}(t,\tau) \simeq R_{\boldsymbol{x}}^{\alpha_0}(\tau)\, e^{j2\pi\alpha_0\epsilon(t)}$. Therefore, $\epsilon(t)$ can be estimated by:

$$\widehat{\epsilon}(t) = \arg_{\text{uw}}\left[z^{(\alpha_0,W)}(t,\tau)\right]/(2\pi\alpha_0) \tag{5.18}$$

to within the unknown constant $\arg_{\text{uw}}[R_x^{\alpha_0}(\tau)]/(2\pi\alpha_0)$, where $\arg_{\text{uw}}$ denotes the unwrapped phase. Therefore, under the above-stated conditions on $\epsilon(t)$, this warping function can be estimated to within an unknown constant, representing a fixed time delay, without the need for any optimization. This method is also extended in [83] to the case where only a rough estimate of α_0 is available and also amplitude modulation is present.

Note that since angle-modulated sine waves have spectral support covering the entire spectral domain, the filtering procedure in (5.16) only approximately extracts the single angle-modulated sine wave $R_{\boldsymbol{x}}^{\alpha_0}(\tau)\, e^{j2\pi\alpha_0\epsilon(t)}$. In fact, a portion of the spectral content of such a desired term is filtered out and tails of the spectral contents of the other modulated sine waves pass through the filter. Consequently, the estimate $\widehat{\epsilon}(t)$ is biased. The bias is negligible provided that the power spectra of the angle-modulated sine waves in (5.12) are concentrated on non-overlapping frequency intervals. Such a condition is verified in several real data sets that fit model (5.12), namely the electrocardiogram [86], the acoustic signal emitted by an aircraft [85], and the Sunspot number time series (Sec. 6).

In [83], a Priestley spectral representation [101] for the signal is adopted and an estimation algorithm for the amplitude-modulation function is also derived and an amplitude-modulation compensation and time de-warping procedure is presented to recover the underlying cyclostationary signal $x(t)$.

5.3 De-warping

Once the warping function $\psi(t)$ or its inverse is estimated, the time-warped signal $y(t)$ can be de-warped in order to obtain an estimate $\widehat{x}(t)$ of the underlying polycyclostationary signal $x(t)$. If this de-warping is sufficiently accurate, it renders $\widehat{x}(t)$ amenable to well-known signal processing techniques that are unique for polycyclostationary signals (e.g., frequency-shift (FRESH) filtering).

If the estimate $\widehat{\psi}^{-1}(t)$ is obtained by the Procedure a) of Sec. 5.1, then the estimate of $x(t)$ is immediately obtained as:

$$\widehat{x}(t) = y(\widehat{\psi}^{-1}(t)) \tag{5.19}$$

which would have already been calculated in (5.5b). In contrast, if the estimate $\widehat{\psi}(t)$ is available by the Procedure b) of Sec. 5.1 or by one of the two methods of Sec. 5.2, the estimate $\widehat{\psi}^{-1}(t)$ should be obtained by inverting $\widehat{\psi}$.

A general procedure for calculating $\widehat{\psi}^{-1}$ is described in [43]. In the case of $\psi(t) = t + \epsilon(t)$, with $\epsilon(t)$ slowly varying (see (5.11)), in [83, 84, Sec. 14.3.4], it is shown that $\psi^{-1}(t) \simeq t - \epsilon(t)$ and a useful estimate of $x(t)$ is

$$\widehat{x}(t) = y(t - \widehat{\epsilon}(t)), \tag{5.20}$$

provided that the estimation error is sufficiently small in the sense that $\sup_t |\widehat{\epsilon}(t) - \epsilon(t - \widehat{\epsilon}(t)| \ll 1/B$ where B is the bandwidth of $x(t)$. This condition reduces to

$$\sup_t |\epsilon(t) - \widehat{\epsilon}(t)| \ll 1/B \tag{5.21}$$

when (5.11) holds. The samples of $y(t - \widehat{\epsilon}(t))$ are obtained from those of $y(t)$ and $\widehat{\epsilon}(t)$ by an interpolation formula as explained in [83].

6 The Sunspot number time series

The Wolf number Sunspot index, or Sunspot number in short, counts the average number of Sunspots and groups of Sunspots during specific time intervals [123]. This is a typical example where the stochastic process model for signals is inappropriate. To our knowledge, the Sun is the only star of essential the same mass, geometrical size, particle content, quantitative plasma characteristics, spatial distribution of planets revolving around it, statistically identical electromagnetic planetary characteristics, and the same galaxy of which this solar system is a member. So, to assume that an infinitely large ensemble of statistically identical Suns exists takes us outside of realistic astrophysics and is therefore a poor starting point for the study of the physical phenomenon we call Sunspots. That is, there is one unique Sun producing one unique Sunspot-number time series (SNTS), which is of interest on Earth. Such a time series describes the solar activity that disturbs radio communications, the orbits of satellites, and power grids. Considering an ensemble of SNTS', generated by a hypothetical ensemble of Suns, is meaningless.

The time series of Sunspot number is known to exhibit approximate periodicity. In the brief study of this time series provided here, the details of the irregularity in the periodicity are exposed by fitting an irregular almost-cyclostationary model to the data, using the method presented in Sect. 5. The way of calculating the Sunspot number is not unique [22]. In the following analysis, Sunspot data are taken from the World Data Center SILSO, Royal Observatory of Belgium, Brussels [109].

Several previous studies have shown that the SNTS presents irregular cyclicities [106, 107]. In particular, a periodicity with approximate period of 26–30 days and a periodicity with approximate period of 11 years can be observed [66, 115]. The SNTS has been analyzed using several techniques. In [24], the singular spectrum analysis is adopted to analyze the quasi-periodic components of the SNTS. In [10], it is observed that classical Fourier techniques are not useful for the analysis since the SNTS is recognized to be a substantially nonstationary process and the minimum cross-entropy method is exploited to improve the maximum entropy spectrum. In [114], the spectrogram is adopted for time–frequency analysis. Several works infer the presence of periodicity from the PSD analysis or exploiting several kinds of time-dependent spectra or wavelet analysis [64, 67, 98].

As shown in Sect. 3.7 (Example 3), PSD analysis alone does not enable discovery of hidden periodicities in the data generation mechanism of the time series, whereas

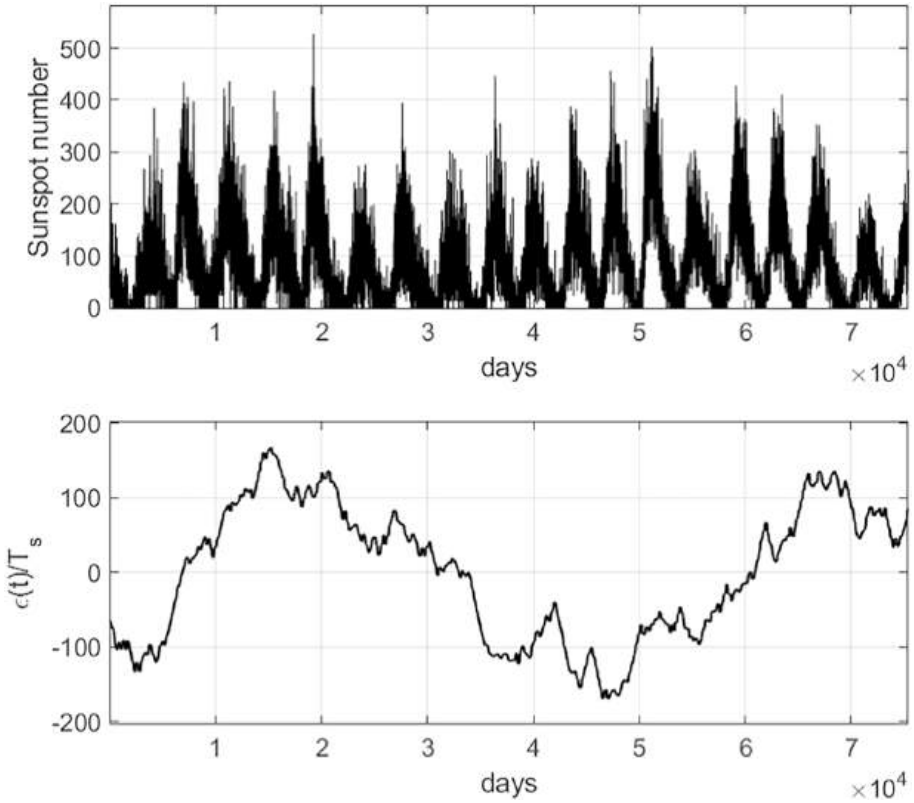

Fig. 16 (Top) daily total Sunspot number in the years 1818–2023. (Bottom) estimated time-warping function ($\widetilde{\alpha}_0 \simeq 0.0365\, f_s, W = 0.003\, f_s, T_s = 1/f_s = 1$ day)

cyclostationarity analysis is designed to reveal such characteristics. Prior to this essay, no cyclostationarity analysis has been conducted on the SNTS. The analysis techniques presented in Sec. 5 are shown here in this section to be ideally suited to the SNTS.

In the following, by two different experiments, it is shown that from the second-order lag product of the SNTS two amplitude- and angle-modulated additive sine-wave components can be extracted. The periods of the non-modulated sinusoids agree with those already observed [10, 24, 66, 114, 115]. Moreover, the time-warping functions in the model provide a mathematical description of the irregularity of the cyclicities observed in the time series, something not previously attempted.

6.1 27.3-Day irregular period

In the first experiment reported here, the daily total Sunspot number in the years 1818–2023 (sampling period $= T_s = 1/f_s = 1$ day) is considered (Fig. 16 (Top)). For this time series, denoted by $y(t)$, the discrete-time counterpart of the cyclic correlogram (3.22) is computed as a function of the lag parameter τ and the cycle frequency α for a data-record length $T = NT_s$ with $N = 75361$. As a measure of the strength of a cyclic component at a cycle frequency α, the integrated squared magnitude of the lag-indexed complex sine waves

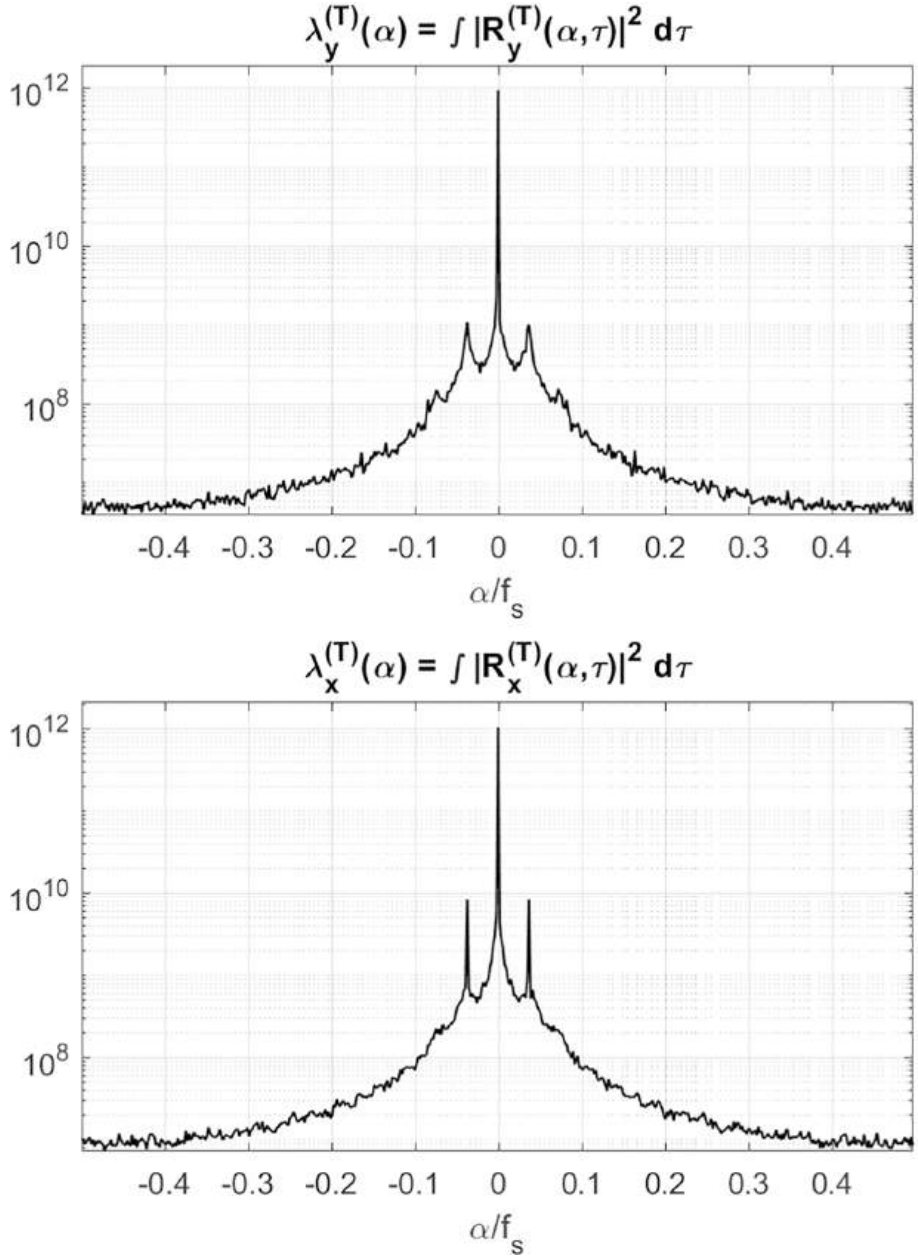

Fig. 17 Strength of the cyclic correlogram as a function of the cycle frequency α. (Top) time series $y(t)$ of the daily total Sunspot number in the years 1818–2023. (Bottom) de-warped time series $x(t)$

$$\lambda_y^{(T)}(\alpha) = \int_{\mathcal{T}} \left| R_y^{(T)}(\alpha,\tau) \right|^2 d\tau \tag{6.1}$$

where $\mathcal{T} = (-512\,T_s, 512\,T_s)$ is reported in Fig. 17 (Top) as a function of α. From Fig. 17 (Top), it appears that cyclic features are spread around a candidate cycle frequency $0.0365 f_s$. The rough estimate $\widetilde{\alpha}_0 \simeq 0.0365 f_s$ and a low-pass filter bandwidth $W = 0.003 f_s$ are adopted for the estimation procedure described in Sec. 5.2. The estimated

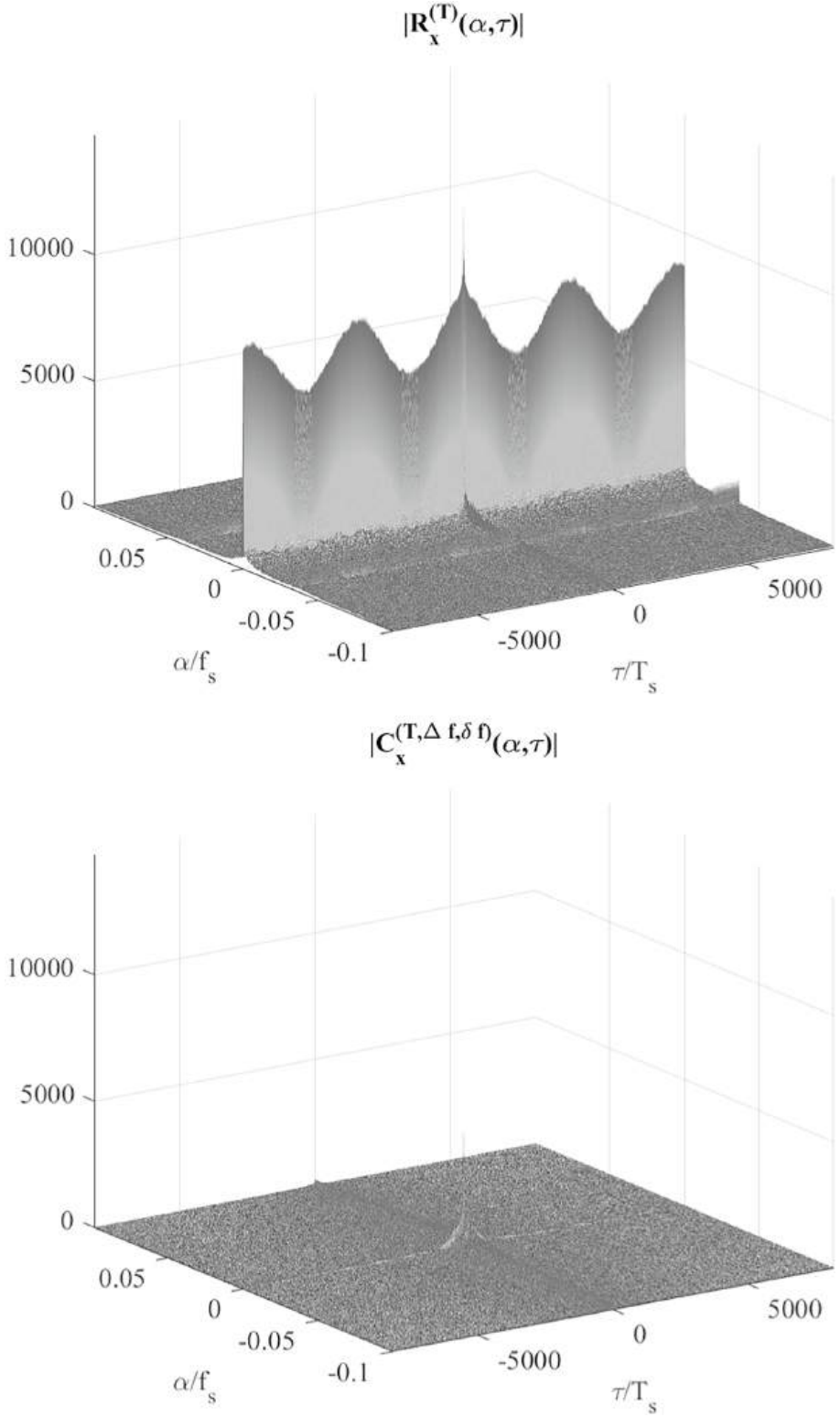

Fig. 18 De-warped time series $x(t)$ of the daily total Sunspot number in the years 1818–2023. (Top) Magnitude of the cyclic correlogram as a function of the cycle frequency α and the lag parameter τ. (Bottom) Magnitude of the estimate of the cyclic autocovariance as a function of α and τ

time-warping function is reported in Fig. 16 (Bottom). The de-warping procedure of Sec. 5.3 (as modified in [83] to also compensate amplitude modulation) is adopted to recover the underlying cyclostationary signal $x(t)$. Its cyclic correlogram, as a function of (α, τ) is computed (Fig. 18 (Top)) and its strength, defined according to (6.1), is reported in Fig. 17 (Bottom). The presence of two sharp peaks at $\alpha = \pm\widehat{\alpha}_0 = \pm 0.0366 f_s$ is evident. It confirms the cyclostationary nature of $x(t)$ and the validity of the conjectured presence of at least a time-warped sine wave in the second-order lag-product of the SNTS. Moreover, from the plot of the magnitude of the cyclic correlogram in Fig. 18 (Top), it is clear that periodic components (in the variable τ) in the cyclic autocorrelation at cycle frequencies $\alpha = \pm\widehat{\alpha}_0 = \pm 0.0366 f_s$ are present. These periodic components in the cyclic autocorrelation are due to an additive periodic term in the underlying cyclostationary time series $x(t)$ (see Sec. 3.5). If the effects of this additive periodic term in $x(t)$ are removed from the second-order lag product, one obtains the pure second-order sinewaves whose amplitudes and phases are the magnitude and phase of the cyclic autocovariance function. In Fig. 18 (Bottom), the magnitude of the estimate of the cyclic autocovariance is reported.

The Sun, in its outer regions at least, is constituted by plasma and, as a result, the Sun's outer regions do not rotate with the same angular speed at every latitude. The poles of the Sun complete a rotation in about 33 days, while the area just above the equator completes a rotation in about 25 days [66]. The detected period $1/\widehat{\alpha}_0 \simeq 27.3$ days corresponds to an average rotation period of the Sun around its axis.

6.2 11-Year irregular period

In the second experiment, a zoom around small cycle frequencies is considered in order to analyze the approximate 11-year periodicity of solar cycles. Solar cycles vary from just under 10 to just over 12 years.

The strength of the cyclic correlogram (6.1) zoomed in the cycle-frequency interval $(-0.0006 f_s, 0.0006 f_s)$ is reported in Fig. 19 (Top).

A new time-warping function is estimated by adopting in the procedure of Sec. 5.2 the parameters $\widetilde{\alpha}_0 \simeq 0.00024906 f_s$ and $W = 0.00010 f_s$. The result is shown in Fig. 20.

The strength of the cyclic correlogram of the de-warped time series is reported in Fig. 19 (Bottom). Peaks corresponding to cycle frequencies are significantly sharper than those in Fig. 19 (Top). Their width is of the order of $1/(NT_s) = 1/(75361\, T_s) \simeq 1.32\, 10^{-5} f_s$ which is the cycle-frequency resolution for an observation-interval length $T = NT_s$ [39, Sec. 11.B], [84, Sec. 5.2.1].

The first peaks of nonzero cycle frequencies are at $\alpha = \pm\widehat{\alpha}_0 \simeq \pm 0.0002496 f_s$ which correspond to a period $T_0 = T_s/0.0002496 \simeq 4006.4$ days $\simeq 10.97$ years. Such a detected period is in agreement with the values already found in [10, 24, 66, 114, 115].

In Fig. 21 (Top), the magnitude of the cyclic correlogram as a function of the cycle frequency α and the lag parameter τ is reported for the de-warped signal $x(t)$. Also in this case $x(t)$ is given by the superposition of a periodic and a zero-mean term. The magnitude of the estimated cyclic autocovariance is reported in Fig. 21 (Bottom).

The approximate period estimated in the second experiment can also be observed by considering the monthly mean total Sunspot number in the years 1749–2023 (sampling period = T_s = 1 month) (Fig. 22 (Top)). This time series has been adopted in previous

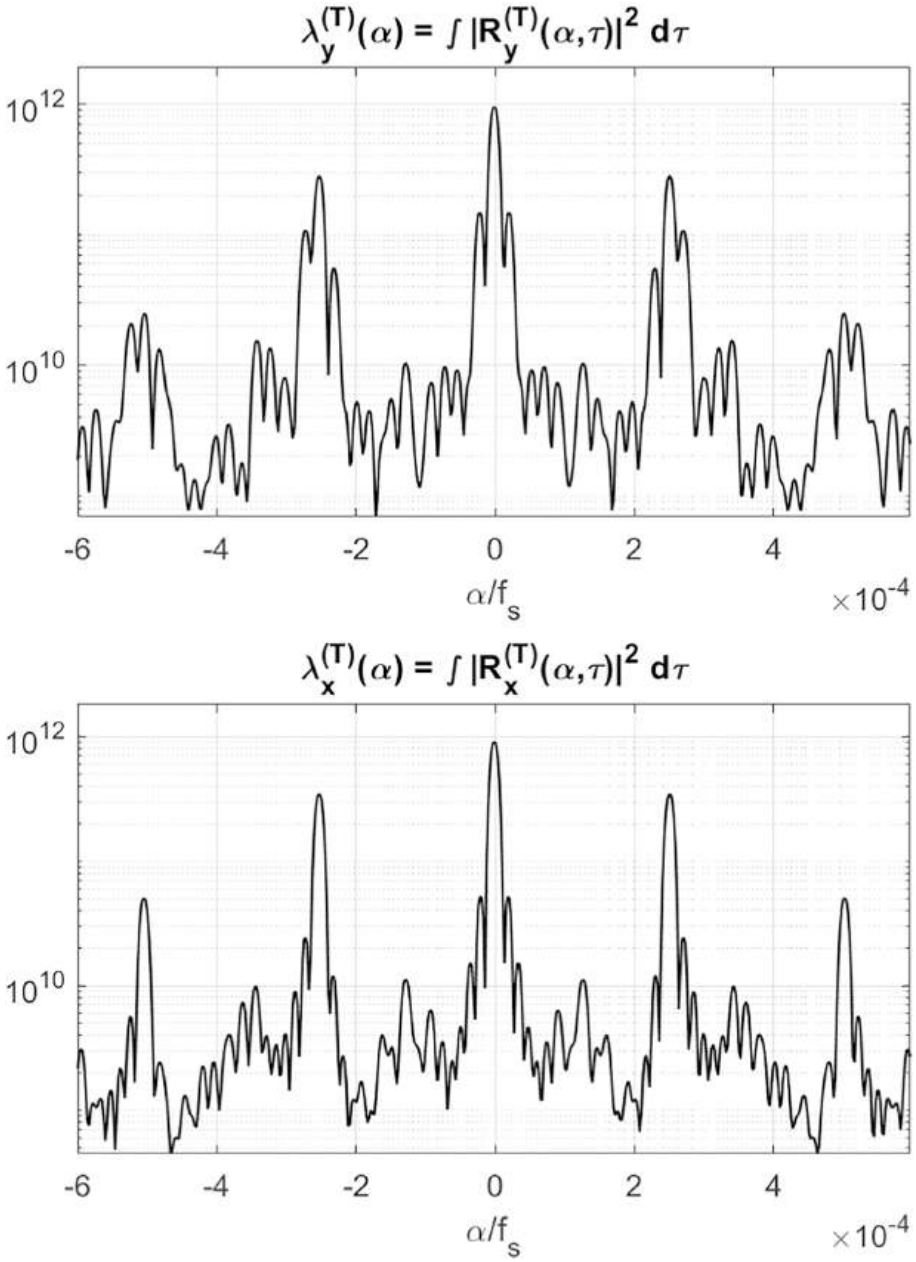

Fig. 19 Strength of the zoom in $\alpha \in (-0.0006\, f_s, 0.0006\, f_s)$ of the cyclic correlogram as a function of the cycle frequency α. (Top) time series $y(t)$ of the daily total Sunspot number in the years 1818–2023. (Bottom) de-warped time series $x(t)$

works [24, 10, 66, 114, 115] to detect the 11-year periodicity. The estimated time-warping function is reported in Fig. 22 (Bottom).

In Fig. 23, the strength of the cyclic correlogram as a function of the cycle frequency α is reported (Top) for the time series $y(t)$ of the monthly mean total Sunspot number in the years 1749–2023 and (Bottom) for the de-warped time series $x(t)$. In Fig. 23 (Bottom), the first peaks of nonzero cycle frequencies are at $\alpha = \pm\widehat{\alpha}_0 \simeq \pm 0.00757\, f_s$ which

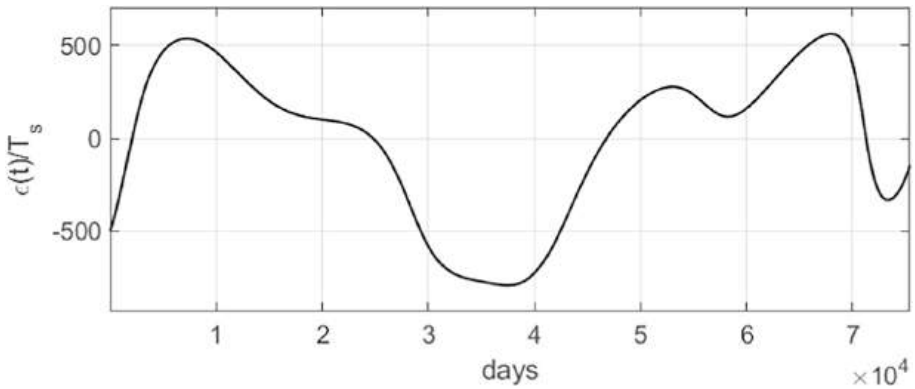

Fig. 20 Daily total Sunspot number in the years 1818–2023. Estimated time-warping function ($\widetilde{\alpha}_0 \simeq 0.00024906\, f_s, W = 0.00010\, f_s, T_s = 1/f_s = 1$ day)

correspond to a period $T_0 = T_s/0.00757 \simeq 132.10$ months $\simeq 11.01$ years, which is in agreement with the previous result.

In Fig. 24, for the de-warped time series $x(t)$, (Top) the magnitude of the cyclic correlogram as a function of α and τ and (Bottom) the magnitude of the estimate of the cyclic autocovariance as a function of α and τ are reported. The periodic term in τ in the cyclic correlogram is a consequence of an additive periodic term in the time series $x(t)$.

6.3 120-200-Year irregular periods

In Figs. 16 (Bottom), 20, and 22 (Bottom), the estimated time-warping function is reported as a function of time (days or months). In all figures, a single cycle of 120-200 years of a (noisy or disturbed) periodic function can be recognized. The period cannot be accurately estimated since the daily total Sunspot number is observed for 205 years and the monthly total Sunspot number for 274 years. However, a crude estimate can be obtained by measuring the distance between the main peaks in the oscillating functions. In Fig. 16 (Bottom), the cycle is approximately $5 \cdot 10^4$ days, which corresponds to 137 years. In Fig. 20, the cycle is approximately $6.5 \cdot 10^4$ days, which corresponds to 178 years. In Fig. 22 (Bottom), the cycle is approximately 2400 months, which corresponds to 200 years.

Long (super-secular) cycles have not been studied using direct SNTS observations, but by means of indirect proxies such as cosmogenic isotopes [115, Sec. 3]. Cycles whose length is comparable with those observed in Figs. 16 (Bottom), 20, and 22 (Bottom), are the Gleissberg cycle which is variable in length from 70 to 130 years and the de Vries or Suess cycle with a period of 205–210 years [115, Sec. 4.1].

7 Conclusion

Hidden periodicities present in science data have been characterized using the fraction-of-time probability framework, which provides a probabilistic model constructed from a single time series. This approach is an alternative to the stochastic-process approach: It does not need to invoke the existence of an ensemble of realizations, that is, of an abstract sample space. Measurement series, such as $x(t+\tau)\,x(t)$, obtained from a given time series $x(t)$, are decomposed into the sum of an almost-periodic component and a

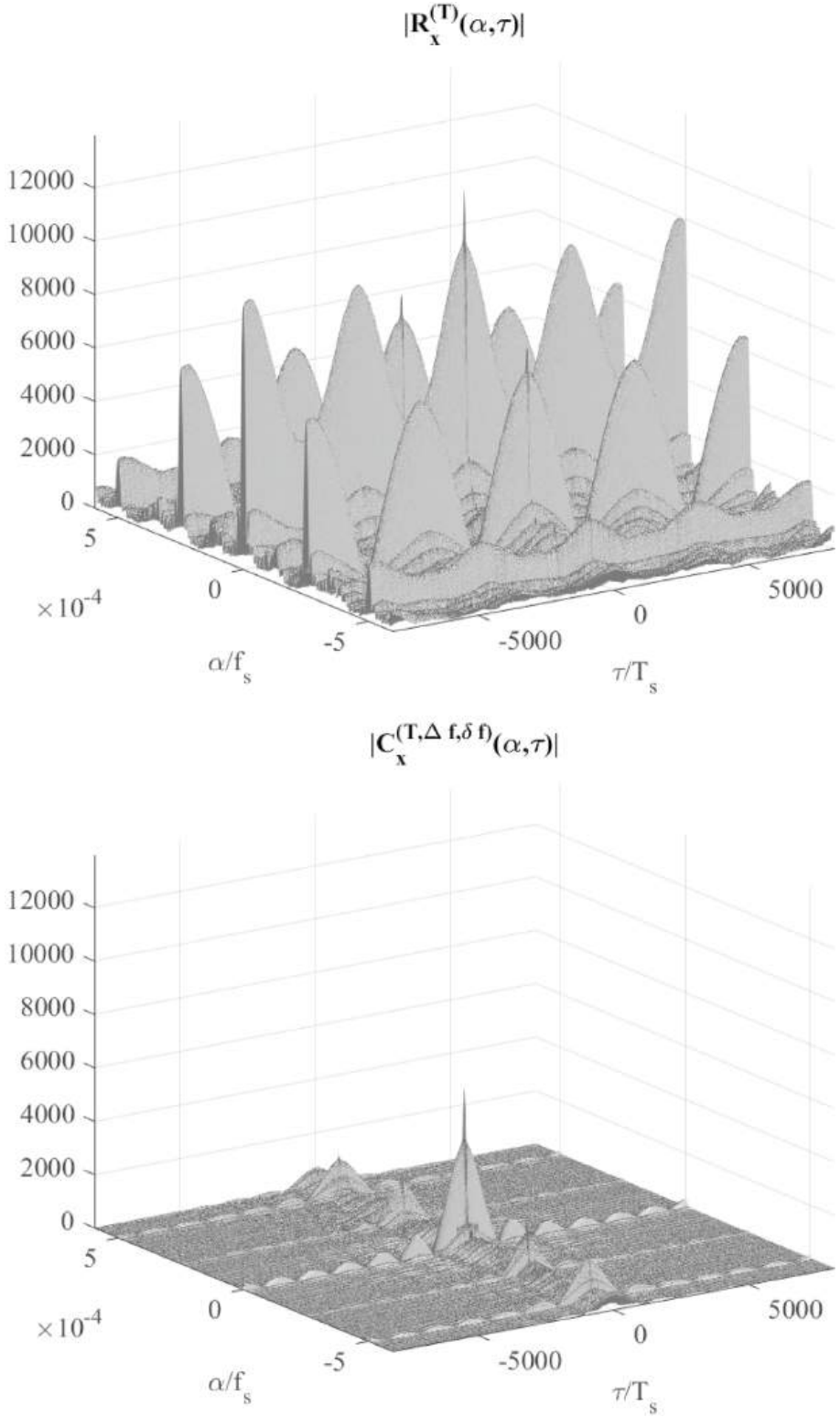

Fig. 21 De-warped time series of the daily total Sunspot number in the years 1818–2023. (Top) Magnitude of the cyclic correlogram as a function of the cycle frequency α and the lag parameter τ. (Bottom) Magnitude of the estimate of the cyclic autocovariance as a function of α and τ. Zoom in $\alpha \in (-0.0006\, f_s, 0.0006\, f_s)$

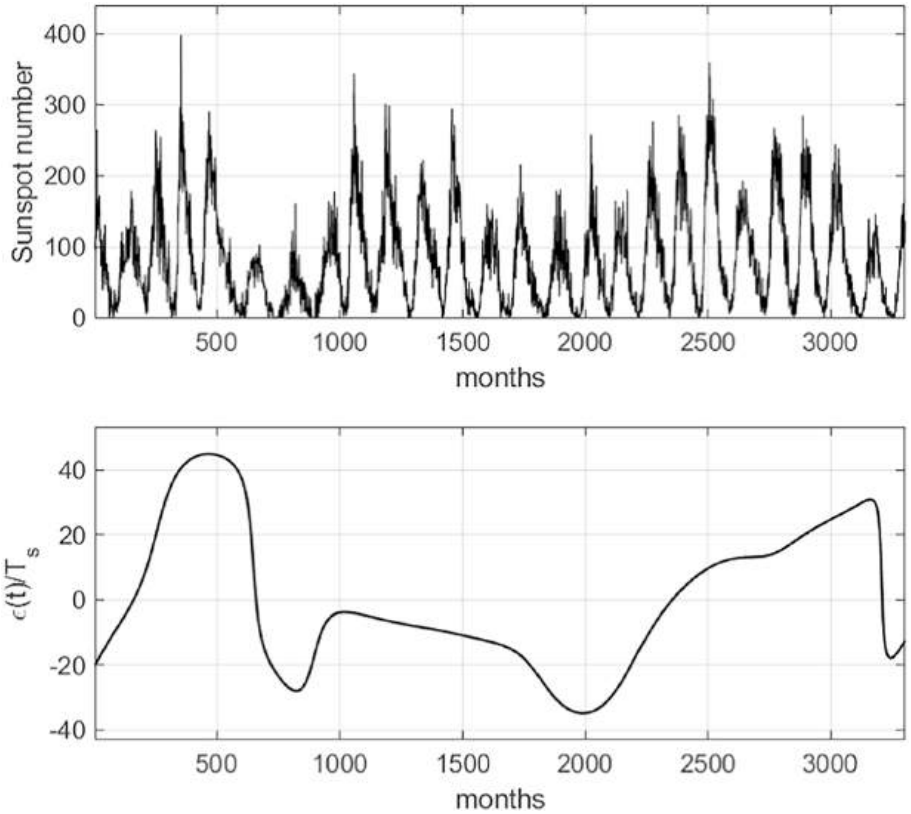

Fig. 22 (Top) monthly mean total Sunspot number in the years 1749–2023. (Bottom) estimated time-warping function. ($\widetilde{\alpha}_0 \simeq 0.00753\, f_s, W = 0.0030\, f_s, T_s = 1/f_s = 1$ month)

residual term not containing any finite-strength additive sine-wave components. The almost-periodic component extraction operator, that is, the operator that extracts all the finite-strength additive sine-wave components of its argument, is recognized to be an expectation operator. Thus, by applying such an operator to nonlinear transformations of a time series and its time-shifted versions, all classical multivariate statistical functions such as cumulative distribution, autocorrelation, autocovariance, moments, and cumulants are constructed. These statistical functions are the building blocks of the fraction-of-time theory of cyclostationarity. A time series is dubbed second-order cyclostationary, poly-cyclostationary, or almost-cyclostationary if its autocorrelation function is periodic, poly-periodic, or almost-periodic, respectively. A similar classification can be made for all other multivariate statistical functions. The *N*th-order cumulative distribution characterizes all hidden *N*th-order periodicities in the time series.

Pure second-order sine waves are defined to be those (portions of) finite-strength sine waves present in the second-order lag product that are not generated by products of first-order sine waves, that is, sine waves of the additive almost-periodic component present in the time series. In contrast, sine waves in the second-order lag product that contain portions due to products of first-order sine waves are referred to as impure second-order sine waves. Pure second-order sine waves characterize periodicities that are hidden in the data, that is, that do not give rise to spectral lines in the Fourier transform

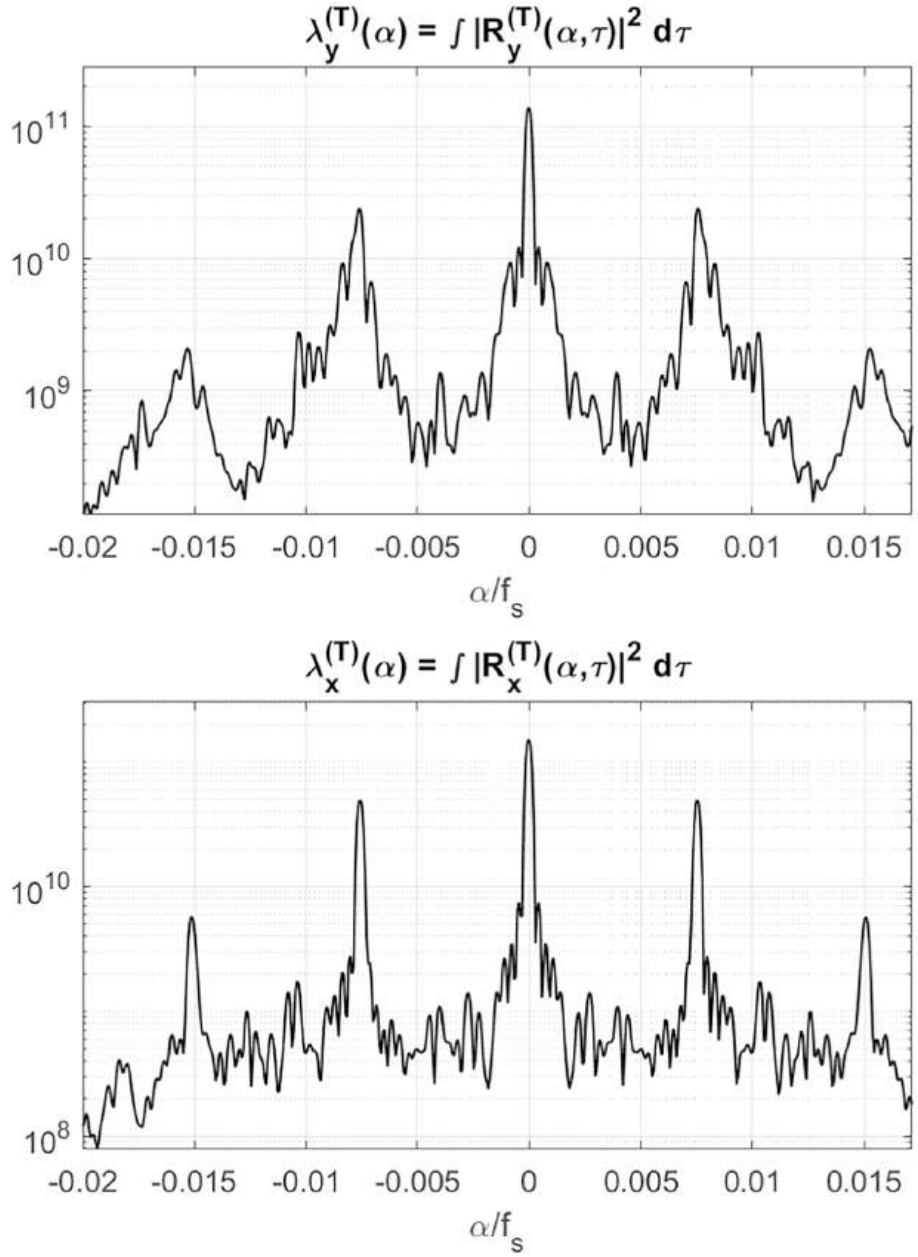

Fig. 23 Strength of the cyclic correlogram as a function of the cycle frequency α. (Top) time series $y(t)$ of the monthly mean total Sunspot number in the years 1749–2023. (Bottom) de-warped time series $x(t)$

of the data. However, they can be generated by a quadratic homogeneous transformation of the data.

As an indication of the suitability of the FOT probability theory of cyclostationarity to the study of hidden periodicities, it is noteworthy that the applied concept of pure Nth-order sine waves gave rise to the definition of the Nth-order cyclic cumulant. This may be the first time in the cumulant's century-plus history that it has been recognized to be the solution to a practical empirical problem.

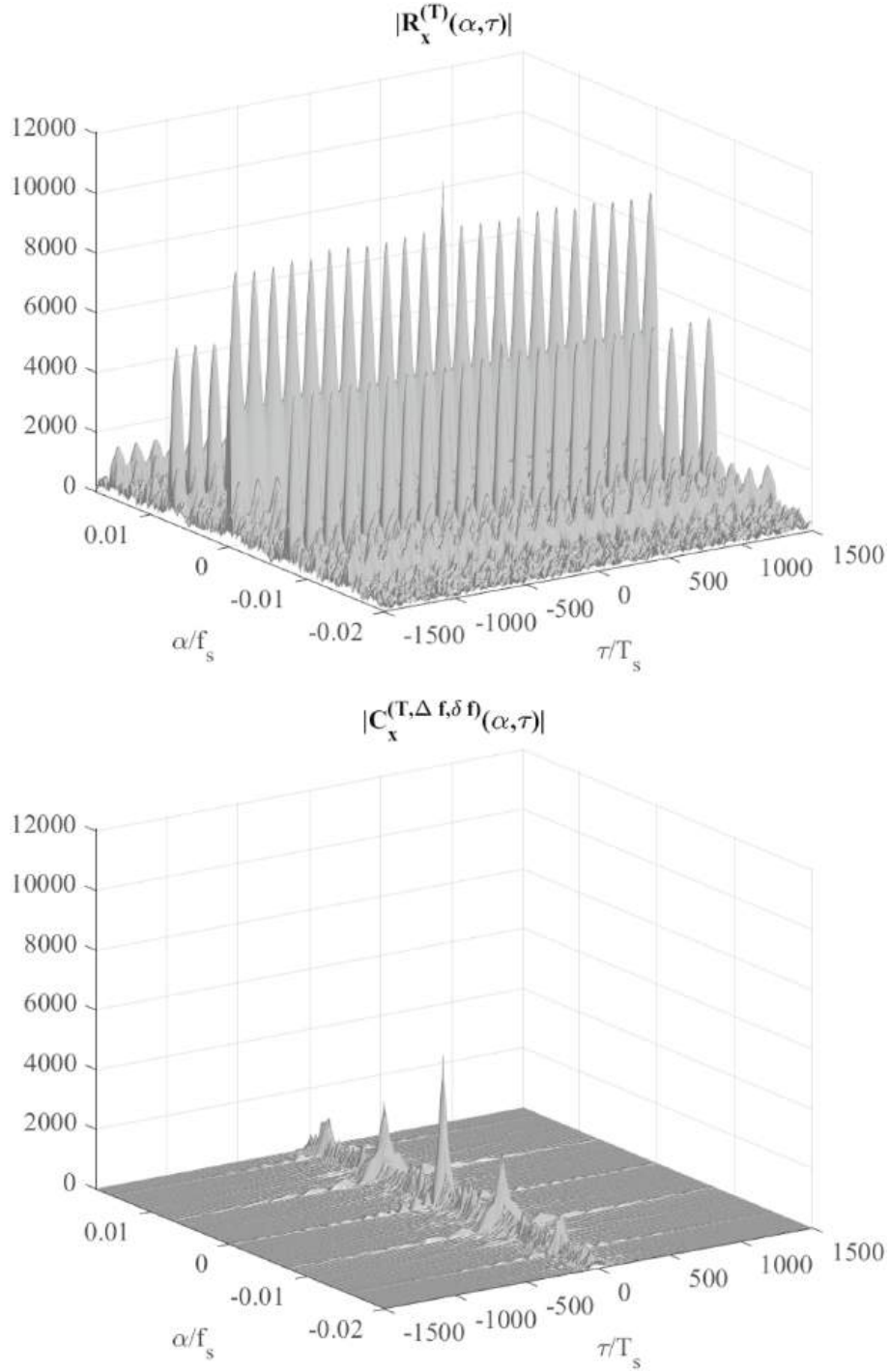

Fig. 24 De-warped time series of the monthly mean total Sunspot number in the years 1749–2023. (Top) Magnitude of the cyclic correlogram as a function of the cycle frequency α and the lag parameter τ. (Bottom) Magnitude of the estimate of the cyclic autocovariance as a function of α and τ

As illustrative examples, a sine wave in additive noise and a sine wave in multiplicative noise are considered. A substantial odd-order harmonic content in the cyclic cumulative distribution, for the case of additive noise, which is not present in the cyclic autocorrelation, is evidenced. It is a consequence of the step discontinuity in the event indicator

function in contrast to the smoothness of the quadratic transformation of the data in the lag product which contains only the second harmonic.

The recently introduced model of time-warped almost-cyclostationary signals is reviewed. It provides a rigorous and accurate model for describing phenomena with irregular cyclicities, that is, phenomena for which the period(s) are time varying. Estimation procedures are presented to restore the regular cyclostationarity by recovering the underlying almost-cyclostationary signal from the original data.

The Sunspot number time series is analyzed. It is shown that at least two hidden irregular periodicities can be identified and modeled as amplitude-modulated time-warped cyclostationary signals. The obtained results are in agreement with several existing results. In particular, the 27.3-day and 11-year irregular periods are detected by estimating the nonzero cycle frequencies of the underlying cyclostationary signals obtained by properly de-warping the original Sunspot number time series. This is the first time that a cyclostationary analysis has been made for this time series, and that amplitude-modulated and time-warped sine waves are extracted from the second-order lag product of the data.

From a historical perspective, we have in this paper reviewed a major paradigm shift that occurred over the preceding 40 years in the field of statistical time series analysis for the specific purpose of detecting and characterizing periodicities (often called cycles) in otherwise randomly fluctuating data. The fraction-of-time probability theory of cyclostationary time series is shown to be a well suited and very effective tool for detecting and analyzing periodicities that are hidden in time-series data by virtue of mixing with random fluctuations and/or distortion due to time warping. The Sunspot number time-series example presented here is one of many published examples from a variety of applications of the fact that the theory of Non-Population Probability of single functions of time is methodologically superior to the standard Population-Probability Theory of ensembles of time functions (stochastic processes) when the time functions are properly modeled as stationary, or cyclostationary, or almost cyclostationary. This is the natural conclusion to the development throughout recorded history of theory and methodology for investigating cyclic phenomena, as last reviewed by H. O. A. Wold over half a century ago, and the Sunspot series example might well represent the first major breakthrough in methodology for analyzing Sunspot series since Sir Arthur Schuster's original application of the periodogram 125 years ago.

The authors propose that progress on hidden periodicities was hindered for many years by a misguided replacement of the budding non-stochastic theory of time-series analysis in the mid-twentieth century with the Kolmogorov theory of stochastic processes for which population data is essential or, at the very least, should not be physically impossible. Readers can find a comprehensive treatise on this theme at the educational website [42]. It is conceivable that adoption of the FOT probability theory of cyclostationarity will facilitate progress in the investigation of periodicities in natural phenomena and that adoption of non-population probability more generally for stationary time series as well as time series exhibiting cyclostationarity of one type or another will facilitate data analysis and statistical inference throughout the field of time-series analysis. As an illustrative example, the field of Signals Intelligence, and Communications Intelligence in particular, was revolutionized by Gardner's initial 1987 revelation of

his non-population theory of cyclostationarity and his demonstration of its applicability to Signal Interception (cf., [42, pp. 6 and 12]). More recently, the nascent movement in Econometrics referred to as Ergodicity Economics is in essence a return from population-probability models and methods to their non-population probability counterpart [97]. The editorial introducing the issue of *Nature Physics*, [91], containing this article is in complete alignment with the editorial remarks on the wisdom of a return to non-population probability the Authors have included throughout many of the publications cited in this summary article. And this is in complete alignment with the remarks from the editor of the Journal of Sound and Vibration cited in the article [44]. Evidence in support of Gardner's 1987 proposal for a paradigm shift in time-series analysis is mounting and suggests that the shift is solidly underway now.

Appendix A: Derivation of (2.28)

The Fourier coefficients of the periodic PDF (2.27c) can be found as follows:

$$f_x(t;\xi) = \frac{1}{\sqrt{2\pi}\sigma_n} e^{-\xi^2/(2\sigma_n^2)} e^{-A_0^2/(4\sigma_n^2)} e^{\xi A_0 \cos(2\pi f_0 t+\phi_0)/\sigma_n^2} e^{-A_0^2 \cos(2\pi 2 f_0 t+2\phi_0)/(4\sigma_n^2)} \tag{A.1}$$

where the identity $\cos^2(\theta) = (1+\cos(2\theta))/2$ is used.

It results that [92, Eq. 10.12.1]

$$e^{\frac{1}{2}z(t-t^{-1})} = \sum_{n=-\infty}^{\infty} t^n J_n(z) \tag{A.2}$$

where $J_n(z)$ is the Bessel function of first kind with index n [92, Eq. 10.9.2]

$$J_n(z) = \frac{j^{-n}}{\pi} \int_0^{\pi} e^{jz\cos\theta} \cos(n\theta)\, \mathrm{d}\theta\,. \tag{A.3}$$

Equation (A.2) with $t = je^{j\theta}$ leads to

$$e^{jz\cos\theta} = \sum_{n=-\infty}^{\infty} j^n J_n(z)\, e^{jn\theta}\,. \tag{A.4}$$

By substituting $z = -j\xi A_0//\sigma_n^2$ and $\theta = 2\pi f_0 t + \phi_0$ into (A.4), one has

$$e^{\xi A_0 \cos(2\pi f_0 t+\phi_0)/\sigma_n^2} = \sum_{n=-\infty}^{\infty} j^n J_n(-j\xi A_0/\sigma_n^2)\, e^{j2\pi n f_0 t + n\phi_0} \tag{A.5}$$

and by substituting $z = jA_0^2/(4\sigma_n^2)$ and $\theta = 2\pi f_0 t + \phi_0$ into (A.4), one has

$$e^{-A_0^2 \cos(2\pi 2 f_0 t+2\phi_0)/(4\sigma_n^2)} = \sum_{n=-\infty}^{\infty} j^n J_n(jA_0^2/(4\sigma_n^2))\, e^{j2\pi 2 n f_0 t + 2n\phi_0} \tag{A.6}$$

Thus, substituting (A.5) and (A.6) into (A.1) one obtains

$$f_x(t;\xi) = \frac{1}{\sqrt{2\pi}\sigma_n} e^{-\xi^2/(2\sigma_n^2)} e^{-A_0^2/(4\sigma_n^2)} \sum_{n=-\infty}^{\infty} \sum_{m=-\infty}^{\infty} j^{(n+m)} J_n(-j\xi A_0/\sigma_n^2) J_m(jA_0^2/(4\sigma_n^2)) e^{j2\pi(n+2m)f_0 t + (n+2m)\phi_0} \tag{A.7}$$

The Fourier coefficients $f_x^{\gamma}(\xi)$ for $\gamma = kf_0, k \in \mathbb{Z}$, are given by:

$$\begin{aligned} f_x^{kf_0}(\xi) &\triangleq \left\langle f_x(t;\xi)\, e^{-j2\pi kf_0 t} \right\rangle_t \\ &= \frac{1}{\sqrt{2\pi}\sigma_n} e^{-\xi^2/(2\sigma_n^2)} e^{-A_0^2/(4\sigma_n^2)} \\ &\quad \sum_{n=-\infty}^{\infty} \sum_{m=-\infty}^{\infty} j^{(n+m)} J_n(-j\xi A_0/\sigma_n^2) J_m(jA_0^2/(4\sigma_n^2)) e^{j(n+2m)\phi_0} \\ &\quad \cdot \underbrace{\left\langle e^{j2\pi(n+2m)f_0 t}\, e^{-j2\pi kf_0 t} \right\rangle_t}_{\delta_{n+2m-k}} \end{aligned} \tag{A.8}$$

from which (2.28) immediately follows.

Author contributions
AN did writing—original draft, review, & editing, validation, visualization, methodology, investigation, formal analysis, software, data curation, and conceptualization. WAG did writing review & editing, validation, methodology, investigation, formal analysis, and conceptualization.

Funding
This work was partially supported by the European Union under the Italian National Recovery and Resilience Plan (PNRR) of NextGenerationEU partnership "Telecommunications of the Future" (PE00000001 - program "RESTART") CUP E63C22002040007 - D.D. n. 1549 of 11/10/2022.

Availability of data and materials
Not applicable.

Declarations

Ethics approval and consent to participate
Not applicable.

Consent for publication
Granted.

Competing interests
The authors declare that they have no Conflict of interest.

Received: 17 November 2024 Accepted: 5 February 2025
Published online: 30 April 2025

References

1. J. Antoni, Cyclostationarity by examples. Mech. Syst. Signal Process. **23**(4), 987–1036 (2009). https://doi.org/10.1016/j.ymssp.2008.10.010
2. M.J. Artis, M. Hoffmann, D.M. Nachane, J. Toro, The detection of hidden periodicities: a comparison of alternative methods. EUI ECO; 2004/10. European University Institute (2004)
3. R.B. Ash, *Basic probability theory* (Wiley, New York, 1970)
4. M. Bartlett, Smoothing periodograms from time-series with continuous spectra. Nature **161**, 686–687 (1948). https://doi.org/10.1038/161686a0
5. M. Bartlett, Periodogram analysis and continuous spectra. Biometrika **37**(1/2), 1–16 (1950). https://doi.org/10.2307/2332141
6. J. Barzilai, J.M. Borwein, Two-point step size gradient methods. IMA J. Numer. Anal. **8**(1), 141–148 (1988). https://doi.org/10.1093/imanum/8.1.141

7. J. Bass, Espaces de Besicovitch, fonctions presque-périodiques, fonctions pseudo-aléatories. Bull. Soc. Math. France **91**, 39–61 (1963)
8. J. Bass, Fonctions stationnaires Fonctions de corrélation. Application à la représentation spatio-temporelle de la turbulence. Annales de l'Inst Henri Poincaré Section B. **5**(2), 135–193 (1969)
9. J. Bass, Stationary functions and their applications to the theory of turbulence: II. Turbulent solutions of the Navier-Stokes equations. J. Math. Anal. Appl. **47**(3), 458–503 (1974). https://doi.org/10.1016/0022-247X(74)90002-X
10. A. Berger, J.L. Melice, I. Van Der Mersch, M. Beran, A. Provenzale, J.L. Stanford, Evolutive spectral analysis of sunspot data over the past 300 years. Philos. Trans. R. Soc. Lond. Ser. A, Math. Phys. Sci. **330**(1615), 529–541 (1990). https://doi.org/10.1098/rsta.1990.0034
11. A.S. Besicovitch, *Almost periodic functions* (Cambridge University Press, London, 1932)
12. R. Bhansali, D. Downhan, Some properties of the order of an autoregressive model selected by a generalization of Akaike's FPE criterion. Biometrika **64**, 547–551 (1977)
13. R.B. Blackman, J.W. Tukey, The measurement of power spectra from the point of view of communications engineering - Part I. Bell Syst. Tech. J. **37**(1), 185–282 (1958). https://doi.org/10.1002/j.1538-7305.1958.tb03874.x
14. P. Bloomfield, *Fourier analysis of time series: an introduction* (Wiley, New York, 1976)
15. D.R. Brillinger, *Time series data analysis and theory* (Holden Day Inc, San Francisco, 1981)
16. W.A. Brown, On the theory of cyclostationary signals. Ph.D. Dissertation, Dept. Elect. Eng. Comp. Sci., Univ. California, Davis, CA (1987)
17. J.P. Burg, *Maximum entropy spectral analysis* (Stanford exploration project. Stanford University, Stanford, CA, 1975)
18. J. Cadzow, High performance spectral estimation: a new ARMA method. IEEE Trans. Acoust. Speech Signal Process. **28**(5), 524–529 (1980). https://doi.org/10.1109/TASSP.1980.1163440
19. J. Capon, High-resolution frequency-wavenumber spectrum analysis. Proc. IEEE **57**(8), 1408–1418 (1969). https://doi.org/10.1109/PROC.1969.7278
20. J.V. Castellana, M.R. Leadbetter, On smoothed probability density estimation for stationary processes. Stoch. Processes Appl. **21**(2), 179–193 (1986). https://doi.org/10.1016/0304-4149(86)90095-5
21. D.C. Champeney, *Fourier transforms and their physical applications* (Academic Press, London, 1973)
22. F. Clette, L. Svalgaard, J. Vaquero, E. Cliver, Revisiting the sunspot number. Space Sci. Rev. **186**, 35–103 (2014). https://doi.org/10.1007/s11214-014-0074-2
23. C. Corduneanu, *Almost periodic functions* (Chelsea Publishing Company, New York, 1989)
24. V. Courtillot, F. Lopes, J.L. Le Mouel, On the prediction of solar cycles. Sol. Phys. **296**(1), 1–23 (2021). https://doi.org/10.1007/s11207-020-01760-7
25. A.V. Dandawaté, G.B. Giannakis, Nonparametric polyspectral estimators for *k*th-order (almost) cyclostationary processes. IEEE Trans. Inf. Theory **40**(1), 67–84 (1994). https://doi.org/10.1109/18.272456
26. A.V. Dandawaté, G.B. Giannakis, Statistical tests for presence of cyclostationarity. IEEE Trans. Signal Process. **42**(9), 2355–2369 (1994). https://doi.org/10.1109/78.317857
27. A.V. Dandawaté, G.B. Giannakis, Asymptotic theory of mixed time averages and *k*th-order cyclic-moment and cumulant statistics. IEEE Trans. Inf. Theory **41**(1), 216–232 (1995). https://doi.org/10.1109/18.370106
28. S. Das, M.G. Genton, Cyclostationary processes with evolving periods and amplitudes. IEEE Trans. Signal Process. **69**, 1579–1590 (2021). https://doi.org/10.1109/TSP.2021.3057268
29. D. Dehay, J. Leśkow, A. Napolitano, Central limit theorem in the functional approach. IEEE Trans. Signal Process. **61**(16), 4025–4037 (2013). https://doi.org/10.1109/TSP.2013.2266324
30. D. Dehay, J. Leśkow, A. Napolitano, Time average estimation in the fraction-of-time probability framework. Signal Process. **153**, 275–290 (2018). https://doi.org/10.1016/j.sigpro.2018.07.005
31. D. Dehay, J. Leskow, A. Napolitano, T. Shevgunov, Cyclic detectors in the fraction-of-time probability framework. Inventions (2023). https://doi.org/10.3390/inventions8060152
32. J. Durbin, The fitting of time-series models. Revue de l'Institut International de Statistique **28**(3), 233–244 (1960). https://doi.org/10.2307/1401322
33. A. Einstein, Method for the determination of the statistical values of observations concerning quantities subject to irregular fluctuations. Archives des Sciences et Naturelles **37**, 254–256 (1914). https://doi.org/10.1109/MASSP.1987.1165595
34. R.M. Fano, Short-time autocorrelation functions and power spectra. J Acoust. Soc. Am. **22**, 546–550 (1950). https://doi.org/10.1121/1.1906647
35. R. Fisher, Tests of significance in harmonic analysis. Proc. R. Soc. A **125**(796), 54–59 (1929). https://doi.org/10.1098/rspa.1929.0151
36. W.A. Gardner, Stationarizable random processes. IEEE Trans. Inf. Theory IT. **24**, 8–22 (1978). https://doi.org/10.1109/TIT.1978.1055820
37. W.A. Gardner, *Introduction to random processes with applications to signals and systems*, 2nd edn (Macmillan, New York, 1990)
38. W.A. Gardner, The spectral correlation theory of cyclostationary time series. Signal Process. **11**, 13–36 (1986). https://doi.org/10.1016/0165-1684(86)90092-7. (**Erratum: Signal Processing, vol. 11, p. 405**)
39. W.A. Gardner, *Statistical spectral analysis: a nonprobabilistic theory* (Prentice-Hall, Englewood Cliffs, 1987)
40. W.A. Gardner, Cyclic Wiener filtering: theory and method. IEEE Trans. Commun. **41**(1), 151–163 (1993). https://doi.org/10.1109/26.212375
41. W.A. Gardner, An introduction to cyclostationary signals, in *Cyclostationarity in communications and signal processing*. ed. by W.A. Gardner (IEEE Press, New York, 1994), pp.1–90
42. W.A. Gardner, Cyclostationarity.com. https://cyclostationarity.com (2018)
43. W.A. Gardner, Statistically inferred time warping: extending the cyclostationarity paradigm from regular to irregular statistical cyclicity in scientific data. EURASIP J. Adv. Signal Process. **2018**(1), 59 (2018). https://doi.org/10.1186/s13634-018-0564-6
44. W.A. Gardner, Transitioning away from stochastic process models. J. Sound Vib (2023). https://doi.org/10.1016/j.jsv.2023.117871

45. W.A. Gardner, W.A. Brown, Fraction-of-time probability for time-series that exhibit cyclostationarity. Signal Process. **23**, 273–292 (1991). https://doi.org/10.1016/0165-1684(91)90005-4
46. W.A. Gardner, L.E. Franks, Characterization of cyclostationary random signal processes. IEEE Trans. Inf. Theory IT. **21**, 4–14 (1975). https://doi.org/10.1109/TIT.1975.1055338
47. W.A. Gardner, A. Napolitano, L. Paura, Cyclostationarity: Half a century of research. Signal Process. **86**(4), 639–697 (2006). https://doi.org/10.1016/j.sigpro.2005.06.016
48. W.A. Gardner, C.M. Spooner, Higher order cyclostationarity, cyclic cumulants, and cyclic polyspectra. In Proceedings of the 1990 International Symposium on Information Theory and Its Applications (ISITA'90), Honolulu, HI, pp. 355–358 (1990)
49. W.A. Gardner, C.M. Spooner, The cumulant theory of cyclostationary time-series, Part I: Foundation. IEEE Trans. Signal Process. **42**, 3387–3408 (1994). https://doi.org/10.1109/78.340775
50. E.G. Gladyshev, Periodically correlated random sequences. Soviet Math. Dokl. **2**, 385–388 (1961). (**Russian**)
51. E.G. Gladyshev, Periodically and almost periodically correlated random processes with continuous time parameter. Theory Prob. Appl. **8**(2), 173–177 (1963). https://doi.org/10.1137/1108016. (**Russian**)
52. U. Grenander, M. Rosenblatt, *Statistical analysis of stationary time series* (Wiley, New York, 1957)
53. E.J. Hannan, B.G. Quinn, The determination of the order of an autoregression. J. R. Stat. Soc.: Ser. B (Methodol.) **41**(2), 190–195 (1979). https://doi.org/10.1111/j.2517-6161.1979.tb01072.x
54. F.J. Harris, On the use of windows for harmonic analysis with the discrete Fourier transform. Proc. IEEE **66**(1), 51–83 (1978). https://doi.org/10.1109/PROC.1978.10837
55. E.M. Hofstetter, Random processes, in *The mathematics of physics and chemistry*, vol. II, ed. by H. Margenau, G.M. Murphy (D. Van Nostrand Co., Princeton, 1964)
56. H.L. Hurd, A.G. Miamee, *Periodically correlated random sequences: spectral theory and practice* (Wiley, New Jersey, 2007)
57. L. Izzo, A. Napolitano, The higher-order theory of generalized almost-cyclostationary time-series. IEEE Trans. Signal Process. **46**(11), 2975–2989 (1998). https://doi.org/10.1109/78.726811
58. I. Javorskyj, R. Yuzefovych, I. Matsko, Z. Zakrzewski, J. Majewski, Coherent covariance analysis of periodically correlated random processes for unknown non-stationarity period. Digit. Signal Process. **65**, 27–51 (2017). https://doi.org/10.1016/j.dsp.2017.02.013
59. I. Javorskyj, R. Yuzefovych, I. Matsko, Z. Zakrzewski, The least square estimation of the basic frequency for periodically non-stationary random signals. Digit. Signal Process. **122**, 103333 (2022). https://doi.org/10.1016/j.dsp.2021.103333
60. M. Kac, *Statistical independence in probability* (Analysis and number theory. The Mathematical Association of America, USA, 1959)
61. M. Kac, H. Steinhaus, Sur les fonctions indépendantes (IV) (Intervalle infini). Stud. Math. **7**, 1–15 (1938)
62. M. Kaveh, High resolution spectral estimation for noisy signals. IEEE Trans. Acoust. Speech Signal Process. **27**(3), 286–287 (1979). https://doi.org/10.1109/TASSP.1979.1163243
63. S.M. Kay, S.L. Marple, Spectrum analysis: A modern perspective. Proc. IEEE **69**(11), 1380–1419 (1981). https://doi.org/10.1109/PROC.1981.12184
64. Z. Kollath, K. Olah, Multiple and changing cycles of active stars - I. Methods of analysis and application to the solar cycles. Astron. Astrophys. **501**(2), 695–702 (2009). https://doi.org/10.1051/0004-6361/200811303
65. A.N. Kolmogorov, *Foundations of the theory of probability* (1933) (Chelsea, New York, 1956)
66. T. Kucera, C.J. Crannell, Solar physics, in *Encyclopedia of physical science and technology*, 3rd edn., ed. by R.A. Meyers (Academic Press, Cambridge, 2001)
67. N.A. Krivova, S.K. Solanki, The 1.3-year and 156-day periodicities in sunspot data: wavelet analysis suggests a common origin. Astron. Astrophys. **394**(2), 701–706 (2002). https://doi.org/10.1051/0004-6361:20021063
68. J.L. Lagrange, Reserches sur la manièrede former des tables des planètes d'apres les seules observations. Oeuvres de Lagrange **6**, 507–627 (1873)
69. J.L. Lagrange, Sur les interpolations. Oeuvres de Lagrange **7**, 535–553 (1877)
70. Y.W. Lee, *Statistical theory of communication* (Wiley, New York, 1960)
71. V.P. Leonov, A.N. Shiryaev, On a method of calculation of semi-invariants. Theory of probability and its applications **4**(3), 319–329 (1959). https://doi.org/10.1137/11040
72. J. Leśkow, A. Napolitano, Foundations of the functional approach for signal analysis. Signal Process. **86**(12), 3796–3825 (2006). https://doi.org/10.1016/j.sigpro.2006.03.028
73. N. Levinson, The Wiener (root mean square) error criterion in filter design and prediction. J. Math. Phys. **25**(1–4), 261–278 (1946). https://doi.org/10.1002/sapm1946251261
74. S. Lupenko, The rhythm-adaptive Fourier series decompositions of cyclic numerical functions and one-dimensional probabilistic characteristics of cyclic random processes. Digit. Signal Process. **140**, 104104 (2023). https://doi.org/10.1016/j.dsp.2023.104104
75. S. Lupenko, Rhythm-adaptive statistical estimation methods of probabilistic characteristics of cyclic random processes. Digit. Signal Process. **151**, 104563 (2024). https://doi.org/10.1016/j.dsp.2024.104563
76. P. Masani, Commentary on the Memorie [30a] on generalized harmonic analysis, in *Wiener, collected works II*. ed. by P. Masani (MIT Press, Cambridge, 1979)
77. H. Miao, F. Zhang, Chirp cyclic moment for chirp cyclostationary processes: definitions and estimators. Digit. Signal Process. **141**, 104185 (2023). https://doi.org/10.1016/j.dsp.2023.104185
78. H. Miao, F. Zhang, R. Tao, New statistics of the second-order chirp cyclostationary signals: definitions, properties and applications. IEEE Trans. Signal Process. **67**(21), 5543–5557 (2019). https://doi.org/10.1109/TSP.2019.2941072
79. H. Miao, F. Zhang, R. Tao, A general fraction-of-time probability framework for chirp cyclostationary signals. Signal Process. **179**, 107820 (2021). https://doi.org/10.1016/j.sigpro.2020.107820
80. A. Napolitano, Cyclic higher-order statistics: input/output relations for discrete- and continuous-time MIMO linear almost-periodically time-variant systems. Signal Process. **42**(2), 147–166 (1995). https://doi.org/10.1016/0165-1684(94)00124-I

81. A. Napolitano, *Generalizations of cyclostationary signal processing: spectral analysis and applications* (Wiley Ltd - IEEE Press, Chichester, 2012) https://doi.org/10.1002/9781118437926
82. A. Napolitano, Cyclostationarity: limits and generalizations. Signal Process **120**, 323–347 (2016). https://doi.org/10.1016/j.sigpro.2015.09.013
83. A. Napolitano, Time-warped almost-cyclostationary signals: characterization and statistical function measurements. IEEE Trans. Signal Process. **65**(20), 5526–5541 (2017). https://doi.org/10.1109/TSP.2017.2728499
84. A. Napolitano, *Cyclostationary processes and time series: theory, applications, and generalizations* (Elsevier, London, 2019). https://doi.org/10.1016/C2017-0-04240-4
85. A. Napolitano, Aircraft acoustic signal modeled as oscillatory almost-cyclostationary process. In: XXVIII European Signal Processing Conference (EUSIPCO 2020), Amsterdam, The Netherlands (2021). https://doi.org/10.23919/Eusipco47968.2020.9287381
86. A. Napolitano, Modeling the electrocardiogram as oscillatory almost-cyclostationary process. IEEE Access **10**, 13193–13209 (2022). https://doi.org/10.1109/ACCESS.2022.3147500
87. A. Napolitano, W.A. Gardner, Algorithms for analysis of signals with time-warped cyclostationarity. In: 50th Asilomar Conference on Signals, Systems, and Computers, Pacific Grove, California (2016). https://doi.org/10.1109/ACSSC.2016.7869099
88. A. Napolitano, W.A. Gardner, Fraction-of-time probability: advancing beyond the need for stationarity and ergodicity assumptions. IEEE Access **10**, 34591–34612 (2022). https://doi.org/10.1109/ACCESS.2022.3162620
89. A. Napolitano, C.M. Spooner, Median-based cyclic polyspectrum estimation. IEEE Trans. Signal Process. **48**(5), 1462–1466 (2000). https://doi.org/10.1109/78.839992
90. A. Napolitano, A. Wylomanska, Characterization of irregular cyclicities in heavy-tailed data. Signal Process. in press (2025)
91. Nature Physics Editorial, Time to move beyond average thinking. Nat. Phys. **15**(12), 1207 (2019). https://doi.org/10.1038/s41567-019-0758-3
92. F.W.J. Olver, D.W. Lozier, R.F. Boisvert, C.W. Clark (eds.), *NIST handbook of mathematical functions* (Cambridge University Press, New York, 2010). https://dlmf.nist.gov
93. A. Nuttall, Some windows with very good sidelobe behavior. IEEE Trans. Acoust. Speech Signal Process. **29**(1), 84–91 (1981). https://doi.org/10.1109/TASSP.1981.1163506
94. S.C. Olhede, H. Ombao, Modeling and estimation of covariance of replicated modulated cyclical time series. IEEE Trans. Signal Process. **61**(8), 1944–1957 (2013). https://doi.org/10.1109/TSP.2012.2237168
95. E. Parzen, On consistent estimates of the spectrum of a stationary time series. Ann. Math. Stat. **28**(2), 329–348 (1957). https://doi.org/10.1214/aoms/1177706962
96. E. Parzen, On estimation of a probability density function and mode. Ann. Math. Stat. **33**(3), 1065–1076 (1962). https://doi.org/10.1214/aoms/1177704472
97. O. Peters, The ergodicity problem in economics. Nat. Phys. **15**(12), 1216–1221 (2019). https://doi.org/10.1038/s41567-019-0732-0
98. K. Petrovay, Solar cycle prediction. Living Rev. Solar Phys. (2010). https://doi.org/10.12942/lrsp-2010-6
99. E. Pfaffelhuber, Generalized harmonic analysis for distributions. IEEE Trans. Inf. Theory IT. **21**, 605–611 (1975). https://doi.org/10.1109/TIT.1975.1055473
100. V.F. Pisarenko, The retrieval of harmonics from a covariance function. Geophys. J. Int. **33**(3), 347–366 (1973). https://doi.org/10.1111/j.1365-246X.1973.tb03424.x
101. M.B. Priestley, Evolutionary spectra and non-stationary processes. J. R. Stat. Soc. Ser. B (Methodol.) **27**(2), 204–237 (1965). https://doi.org/10.1111/j.2517-6161.1965.tb01488.x
102. B. Quinn, P. Thomson, Estimating the frequency of a periodic function. Biometrika **78**(1), 65–74 (1991). https://doi.org/10.2307/2336896
103. S.O. Rice, Statistical properties of a sine wave plus random noise. Bell Syst. Tech. J. **27**(1), 109–157 (1948). https://doi.org/10.1002/j.1538-7305.1948.tb01334.x
104. M. Rosenblatt, Curve estimates. Ann. Math. Stat. **42**(6), 1815–1842 (1971). https://doi.org/10.1214/aoms/1177693050. (**Accessed 2023-01-09**)
105. A. Schuster, On the investigation of hidden periodicities with application to a supposed 26 day period of meteorological phenomena. Terr. Magn. **3**(1), 13–41 (1898). https://doi.org/10.1029/TM003i001p00013
106. A. Schuster, The periodicity of sun-spots. Astrophys. J. **23**, 101 (1906)
107. A. Schuster, On the periodicity of sun-spots. Proc. R. Soc. A **85**, 50–53 (1911). https://doi.org/10.1098/rspa.1911.0020
108. T. Shevgunov, The synthesis of explicit analytical formulae for the probabilistic models of signals using fraction-of-time approach. T-Comm **16**(11), 21–29 (2022). https://doi.org/10.36724/2072-8735-2022-16-11-21-29
109. SILSO World Data Center: The international sunspot number. In: International sunspot number monthly bulletin and online catalogue, royal observatory of Belgium, 1180 Brussels, Belgium (2023). https://www.sidc.be/silso
110. F.-X. Socheleau, Cyclostationarity of communication signals in underwater acoustic channels. IEEE J. Ocean. Eng. (2022). https://doi.org/10.1109/JOE.2022.3218106
111. C.M. Spooner, Classification of co-channel communication signals using cyclic cumulants. In: Twenty-Ninth Asilomar Conference on Signals, Systems and Computers, vol. 1. Pacific Grove, CA, USA, pp. 531–536 (1995). https://doi.org/10.1109/ACSSC.1995.540605
112. C.M. Spooner, W.A. Gardner, The cumulant theory of cyclostationary time-series Part II: Development and applications. IEEE Trans. Signal Process. **42**, 3409–3429 (1994). https://doi.org/10.1109/78.340776
113. R.-B. Sun, F.-P. Du, Z.-B. Yang, X.-F. Chen, K. Gryllias, Cyclostationary analysis of irregular statistical cyclicity and extraction of rotating speed for bearing diagnostics with speed fluctuations. IEEE Trans. Instrum. Meas. **70**, 1–11 (2021). https://doi.org/10.1109/TIM.2021.3069381
114. D.J. Thomson, L.J. Lanzerotti, F.L. Vernon, M.R. Lessard, L.T.P. Smith, Solar modal structure of the engineering environment. Proc. IEEE **95**(5), 1085–1132 (2007). https://doi.org/10.1109/JPROC.2007.894712

115. I.G. Usoskin, A history of solar activity over millennia. Living Rev. Sol. Phys. **20**(2), 1–113 (2023). https://doi.org/10.1007/s41116-023-00036-z
116. A. van den Bos, Alternative interpretation of maximum entropy spectral analysis. IEEE Trans. Inf. Theory **17**(4), 493–494 (1971). https://doi.org/10.1109/TIT.1971.1054660
117. A.M. Walker, Large-sample estimation of parameters for autoregressive processes with moving-average residuals. Biometrika **49**(1/2), 117–131 (1962). https://doi.org/10.2307/2333472
118. A.M. Walker, On the estimation of a harmonic component in a time series with stationary independent residuals. Biometrika **58**(1), 21–36 (1971). https://doi.org/10.1093/biomet/58.1.21
119. P. Welch, The use of fast Fourier transform for the estimation of power spectra: a method based on time averaging over short, modified periodograms. IEEE Trans. Audio Electroacoust. **15**(2), 70–73 (1967). https://doi.org/10.1109/TAU.1967.1161901
120. N. Wiener, Generalized harmonic analysis. Acta Math. **55**, 117–258 (1930). https://doi.org/10.1007/BF02546511
121. A. Wintner, On Fourier averages. Am. J. Math. **63**(4), 698–704 (1941). https://doi.org/10.2307/2371613
122. H.O.A. Wold, Cycles, in *International encyclopedia of the social sciences*, 2nd edn., ed. by D.L. Sills, R.K. Merton (MacMillan, New York, 1968)
123. R. Wolf, Neue Untersuchungen uber die Periode der Sonnenflecken und ihre Bedeutung (new investigations regarding the period of sunspots and its significance). Mittheilungen der Naturforschenden Gesellschaft in Bern **255**, 249–270 (1852). https://doi.org/10.3931/e-rara-62981
124. G.U. Yule, On a method of investigating periodicities in disturbed series, with special reference to Wolfer's sunspot numbers. Philos. Trans. R. Soc. Lond. Ser. A **226**, 267–298 (1927). https://doi.org/10.1098/rsta.1927.0007
125. A.H. Zemanian, *Distribution theory and transform analysis* (Dover, New York, 1987)
126. W. Zulawinski, J. Antoni, R. Zimroz, A. Wylomanska, Robust coherent and incoherent statistics for detection of hidden periodicity in models with non-Gaussian additive noise. EURASIP J. Adv. Signal Process. (2024). https://doi.org/10.1186/s13634-024-01168-6

Publisher's Note